The following pages contain scaled artwork proofs and are intended primarily for your review of figure/illustration sizing and overall quality. The bounding box shows the type area dimensions defined by the design specification for your book. The figures are not necessarily placed as they will appear with the text in page proofs. Design specification and page makeup parameters determine actual figure placement relative to callouts on actual page proofs, which you will review later.

If you are viewing these art proofs as hard-copy printouts rather than as a PDF file, please note the pages were printed at 600 dpi on a laser printer. You should be able to adequately judge if there are any substantial quality problems with the artwork, but also note that the overall quality of the artwork in the finished bound book will be better because of the much higher resolution of the book printing process.

You will be reviewing copyedited manuscript/typescript for your book, so please refrain from marking editorial changes or corrections to the captions on these pages; defer caption corrections until you review copyedited manuscript. The captions here are intended simply to confirm the correct images are present.

Please be as specific as possible in your markup or comments to the artwork proofs.

P1: SBT
cuus984-net CUUS984-Easley 0 521 19533 1 November 30, 2009 16:2

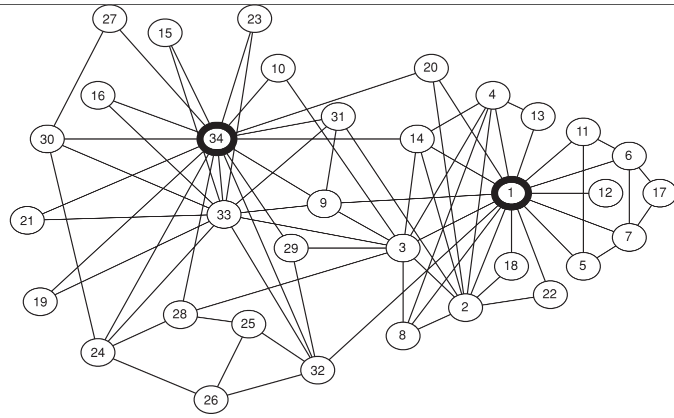

Figure 1.1. The social network of friendships within a 34-person karate club [409].

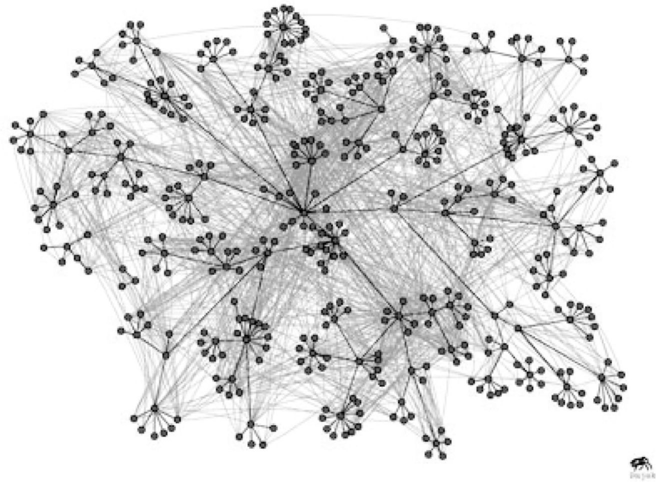

Figure 1.2. Social networks based on communication and interaction can also be constructed from the traces left by on-line data. In this case, the pattern of e-mail communication among 436 employees of Hewlett Packard Research Lab is superimposed on the official organizational hierarchy [6]. (Image from http://www-personal.umich.edu/ ladamic/img/hplabsemailhierarchy.jpg)

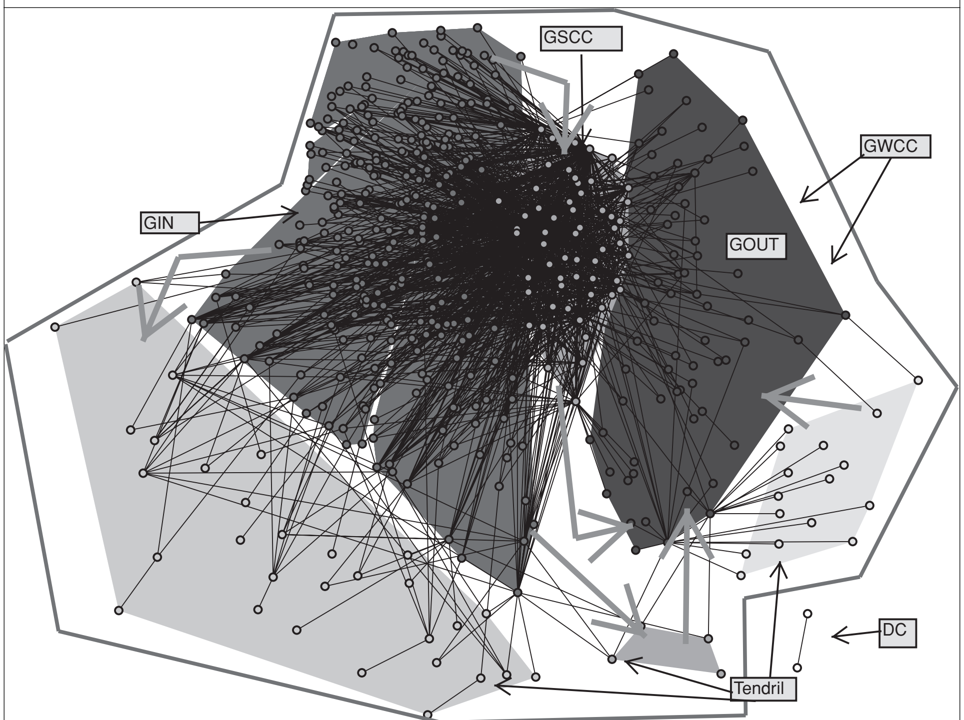

Figure 1.3. The network of loans among financial institutions can be used to analyze the roles that different participants play in the financial system, and how the interactions among these roles affect the health of individual participants and the system as a whole The network here is annotated in a way that reveals its dense core, according to a scheme we will encounter in Chapter 13. (Image from Bech and Atalay [49].)

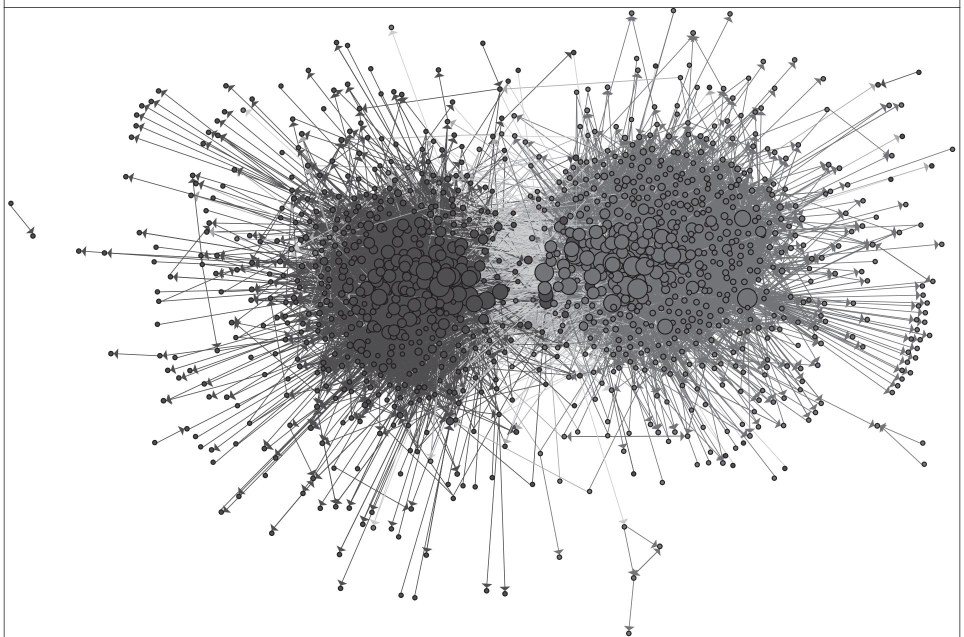

Figure 1.4. The links among Web pages can reveal densely-knit communities and prominent sites. In this case, the network structure of political blogs prior to the 2004 U.S. Presidential election reveals two natural and well-separated clusters [5]. (Image from http://www-personal.umich.edu/ ladamic/img/politicalblogs.jpg)

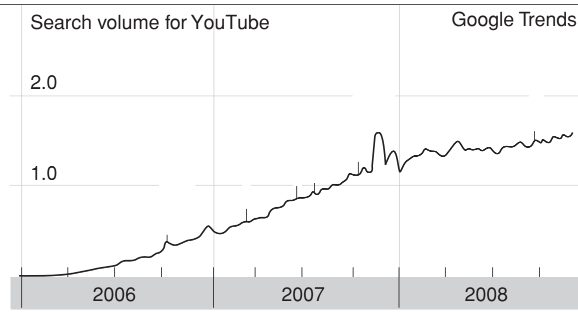

Figure 1.5. The rapidly growing popularity of YouTube is characteristic of the way in which new products, technologies, or innovations rise to prominence, through feedback effects in the behavior of many individuals across a population. The plot depicts the number of Google queries for YouTube over time. The image comes from the site Google Trends (http://www.google.com/trends?q=youtube); by design, the units on the y-axis are suppressed in the output from this site.

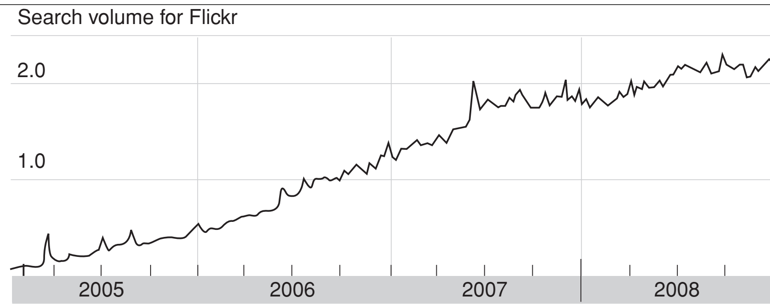

Figure 1.6. This companion to Figure 1.5 shows the rise of the social media site Flickr; the growth in popularity has a very similar pattern to that of other sites including YouTube. (Image from Google Trends, http://www.google.com/trends?q=flickr)

P1: SBT
cuus984-net CUUS984-Easley 0 521 19533 1 November 30, 2009 16:2

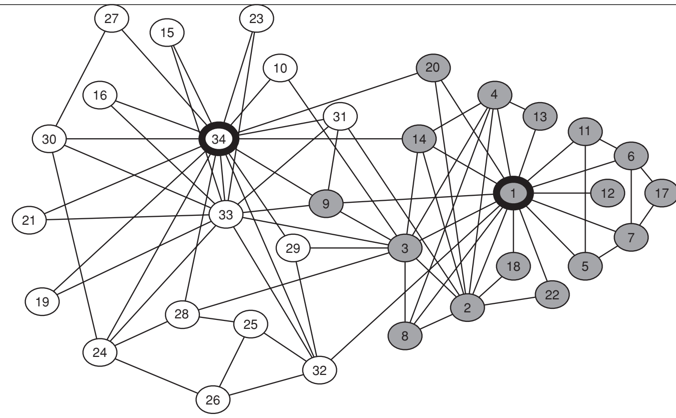

Figure 1.7. From the social network of friendships in the karate club from Figure 1.1, we can find clues to the latent schism that eventually split the group into two separate clubs (indicated by the two different shadings of individuals in the picture).

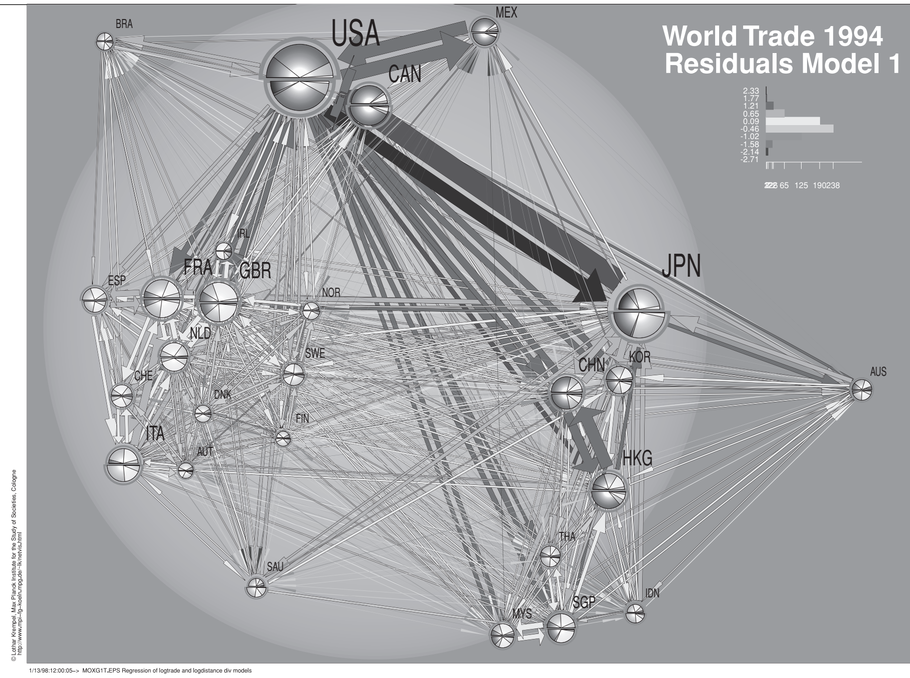

Figure 1.8. In a network representing international trade, one can look for countries that occupy powerful positions and derive economic benefits from these positions [258]. (Image from http://www.cmu.edu/joss/content/articles/volume4/KrempelPlumper.html)

Figure 1.9. In some settings, such as this map of Medieval trade routes, physical networks constrain the patterns of interaction, giving certain participants an intrinsic economic advantage based on their network position. (Image from http://upload.wikimedia.org/wikipedia/commons/e/e1/Late_Medieval_Trade_Routes.jpg.)

Figure 1.10. Cascading adoption of a new technology or service (in this case, the social-networking site MySpace in 2005-2006) can be the result of individual incentives to use the most widespread technology — either based on the informational effects of seeing many other people adopt the technology, or the direct benefits of adopting what many others are already using. (Image from Google Trends, http://www.google.com/trends?q=myspace)

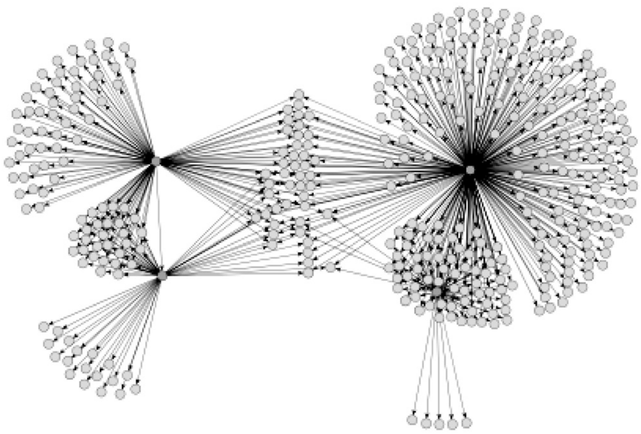

Figure 1.11. When people are influenced by the behaviors their neighbors in the network, the adoption of a new product or innovation can cascade through the network structure. Here, e-mail recommendations for a Japanese graphic novel spread in a kind of informational or social contagion. (Image from Leskovec et al. [267].)

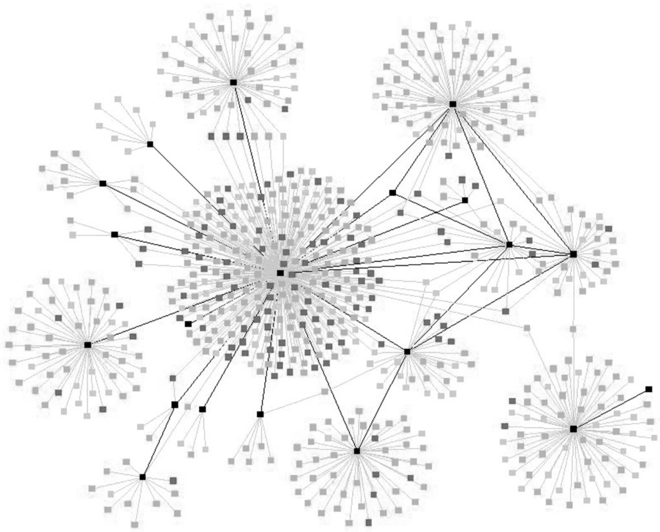

Figure 1.12. The spread of an epidemic disease (such as the tuberculosis outbreak shown here) is another form of cascading behavior in a network. The similarities and contrasts between biological and social contagion lead to interesting research questions. (Image from Andre et al. [17].)

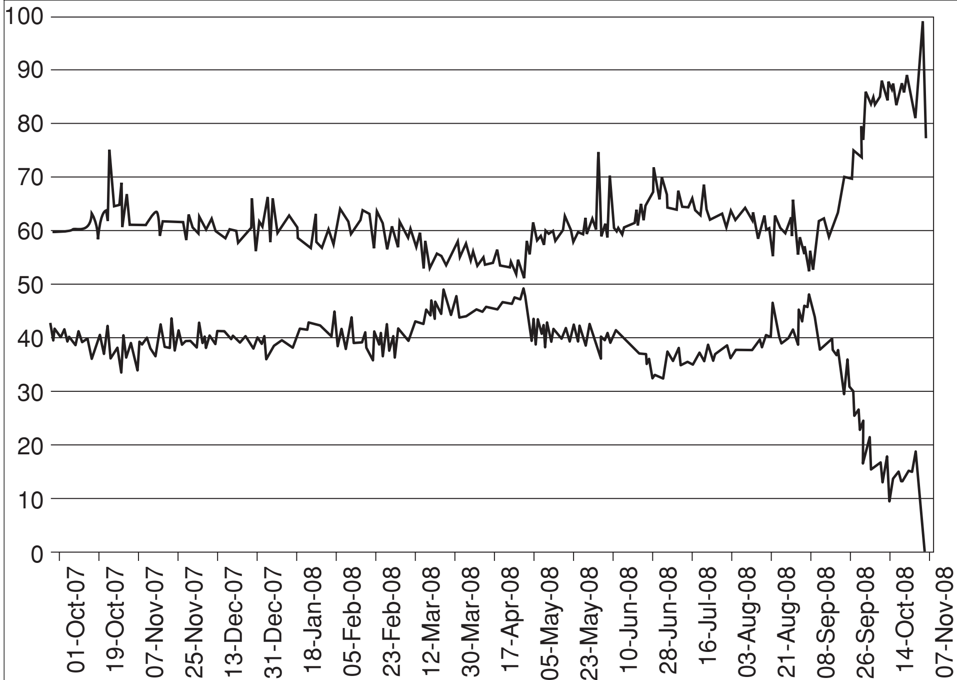

Figure 1.13. Prediction markets, as well as markets for financial assets such as stocks, can synthesize individual beliefs about future events into a price that captures the aggregate of these beliefs. The plot here depicts the varying price over time for two assets that paid $1 in the respective events that the Democratic or Republican nominee won the 2008 U.S. Presidential election. (Image from Iowa Electronic Markets, http://iemweb.biz.uiowa.edu/graphs/graph_PRES08_WTA.cfm.)

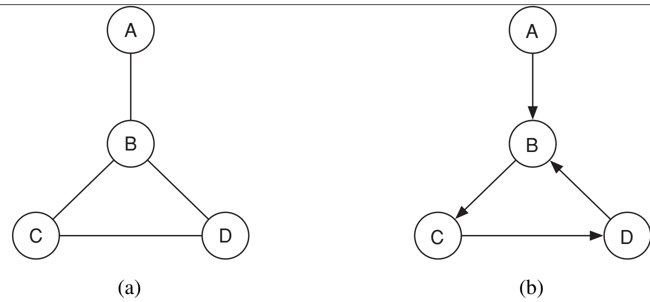

Figure 2.1. Two graphs: (a) an undirected graphs, and (b) a directed graph.

P1: SBT
cuus984-net CUUS984-Easley 0 521 19533 1 November 30, 2009 16:2

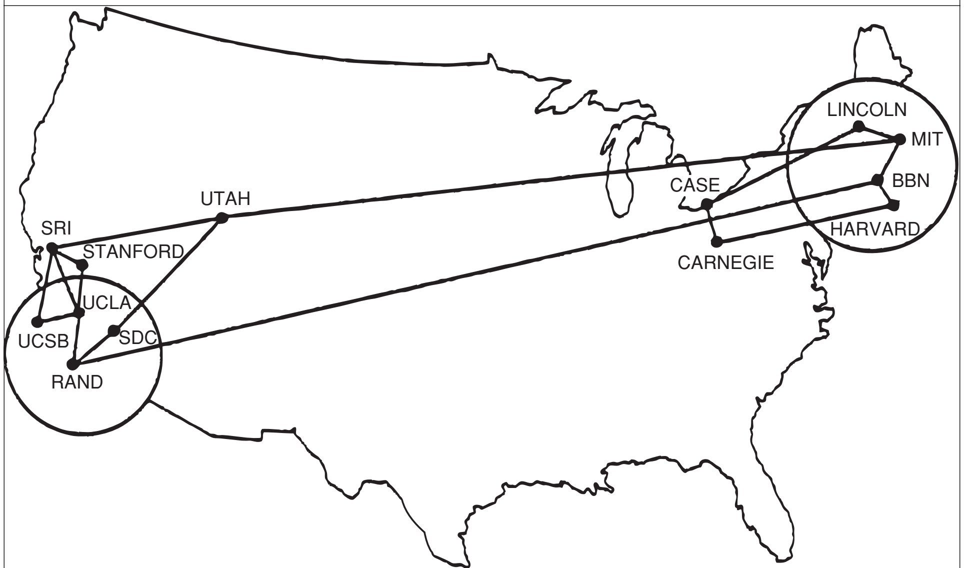

Figure 2.2. A network depicting the sites on the Internet, then known as the Arpanet, in December 1970. (Image from F. Heart, A. McKenzie, J. McQuillian, and D. Walden [212]; on-line at http://som.csudh.edu/cis/lpress/history/arpamaps/.)

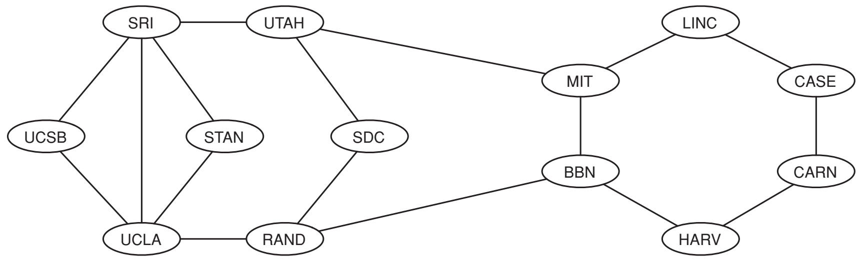

Figure 2.3. An alternate drawing of the 13-node Internet graph from December 1970.

(a)

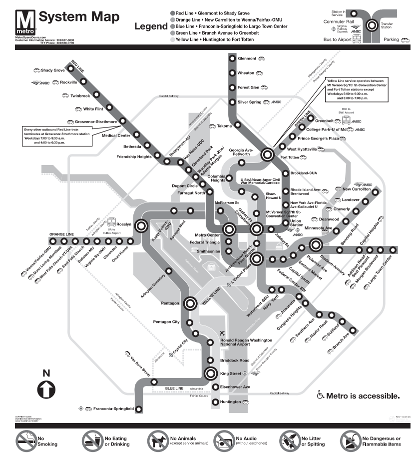

(b)

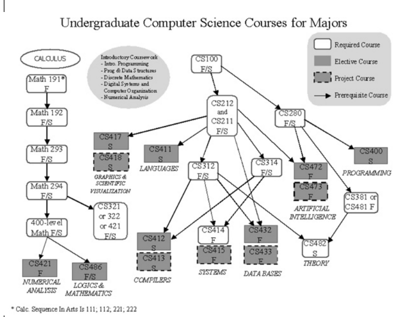

(c)

(d)

Figure 2.4. Images of graphs arising in different domains. The depictions of airline and subway systems in (a) and (b) are examples of *transportation networks*, in which nodes are destinations and edges represent direct connections. Much of the terminology surrounding graphs derives from metaphors based on transportation through a network of roads, rail lines, or airline flights. The prerequisites among college courses in (c) is an example of a *dependency network*, in which nodes are tasks and directed edges indicate that one task must be performed before another. The design of complex software systems and industrial processes often requires the analysis of enormous dependency networks, with important consequences for efficient scheduling in these settings. The sculptural art in (d) is an example of a *structural network*, with joints as nodes and physical linkages as edges. The internal frameworks of mechanical structures such as buildings, vehicles, or human bodies are based on such networks, and the area of *rigidity theory*, at the intersection of geometry and mechanical engineering, studies the stability of such structures from a graph-based perspective [382]. (Images: (a) www.airlineroutemaps.com/USA/Northwest_Airlines_asia_pacific.shtml, (b) www.wmata.com/metrorail/systemmap.cfm, (c) www.cs.cornell.edu/ugrad/flowchart.htm, (d) www.stormking.org/free_ride_home.htm.)

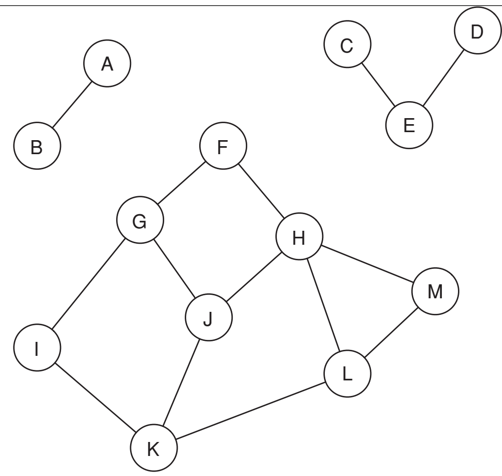

Figure 2.5. A graph with three connected components.

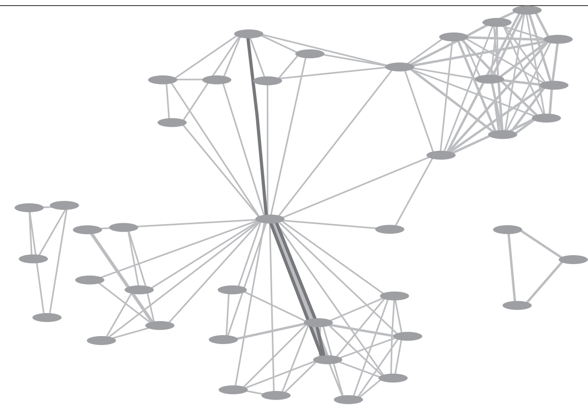

Figure 2.6. The collaboration graph of the biological research center *Structural Genomics of Pathogenic Protozoa (SGPP)* [133], which consists of three distinct connected components. This graph was part of a comparative study of the collaboration patterns graphs of nine research centers supported by NIH's Protein Structure Initiative; SGPP was an intermediate case between centers whose collaboration graph was connected and those for which it was fragmented into many small components.

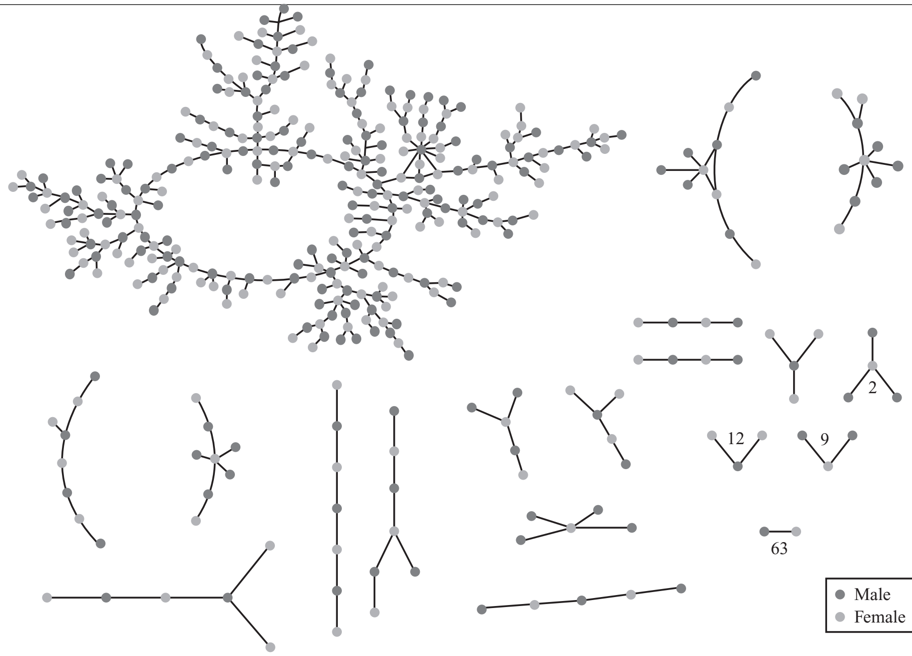

Figure 2.7. A network in which the nodes are students in a large American high school, and an edge joins two who had a romantic relationship at some point during the 18-month period in which the study was conducted [48].

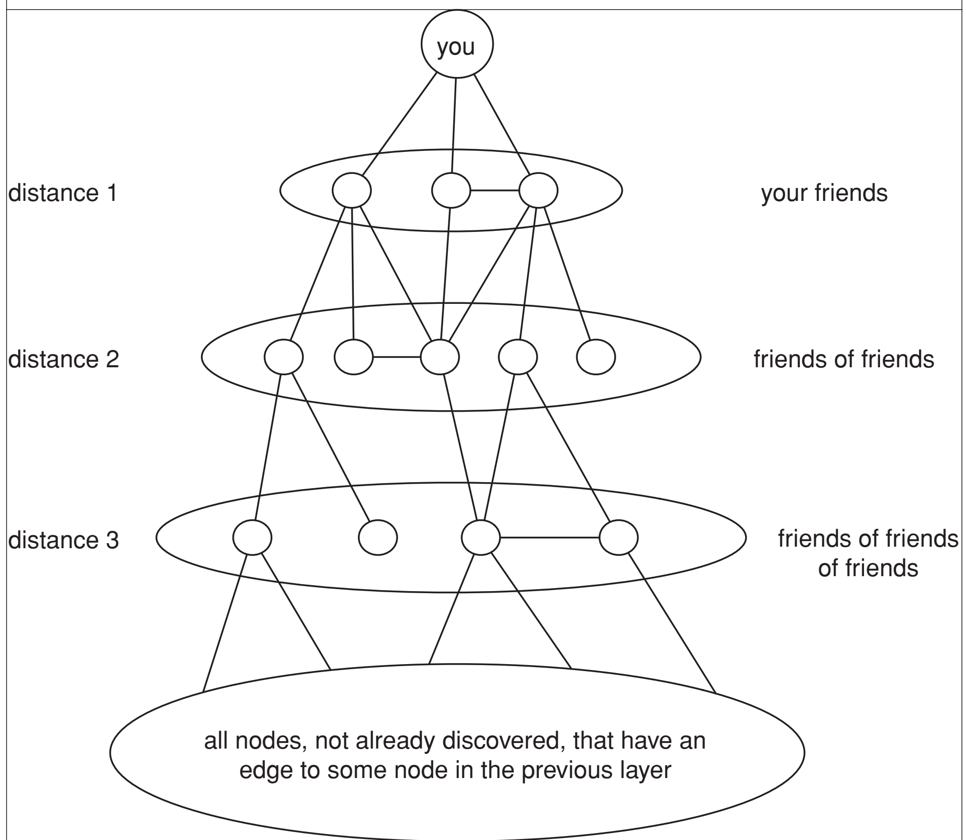

Figure 2.8. Breadth-first search discovers distances to nodes one "layer" at a time; each layer is built of nodes that have an edge to at least one node in the previous layer.

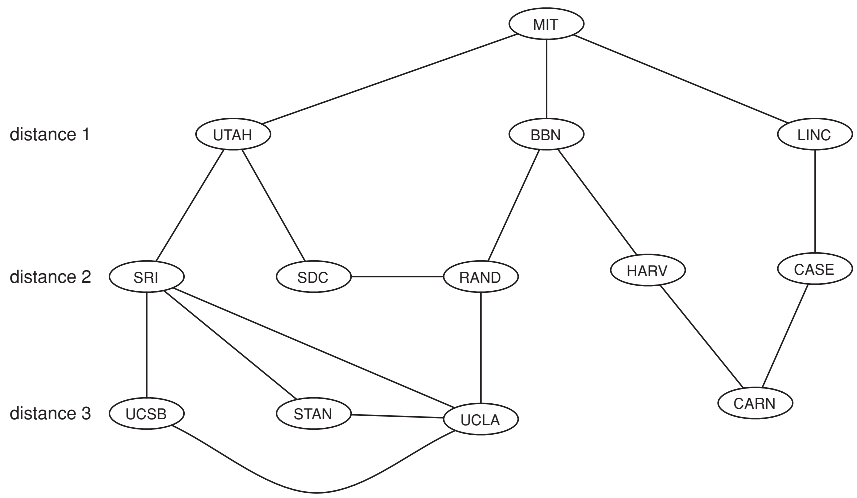

Figure 2.9. The layers arising from a breadth-first of the December 1970 Arpanet, starting at the node MIT.

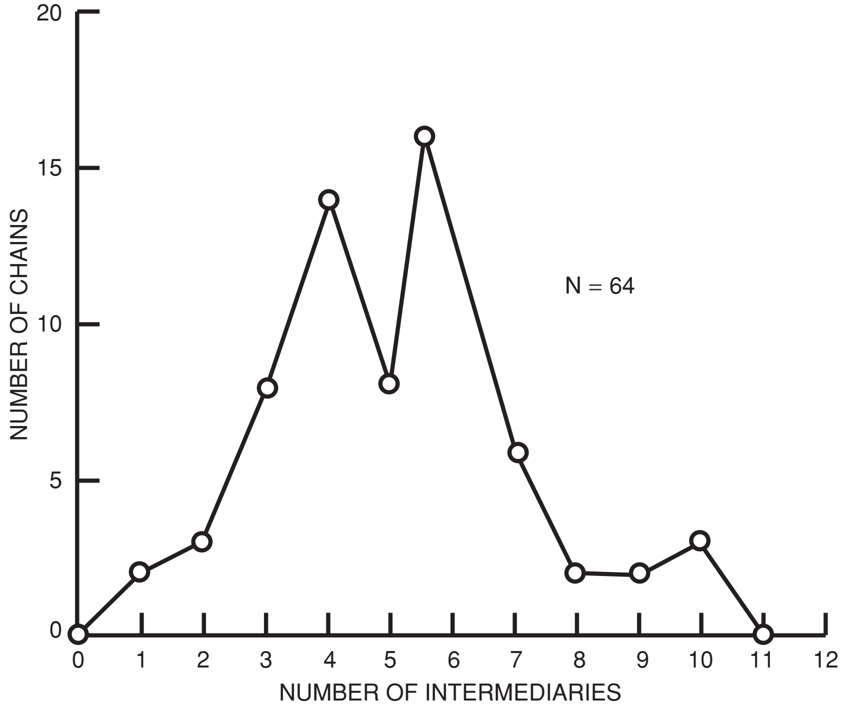

Figure 2.10. A histogram from Travers and Milgram's paper on their small-world experiment [385]. For each possible length (labeled "number of intermediaries" on the *x*-axis), the plot shows the number of successfully completed chains of that length. In total, 64 chains reached the target person, with a median length of six.

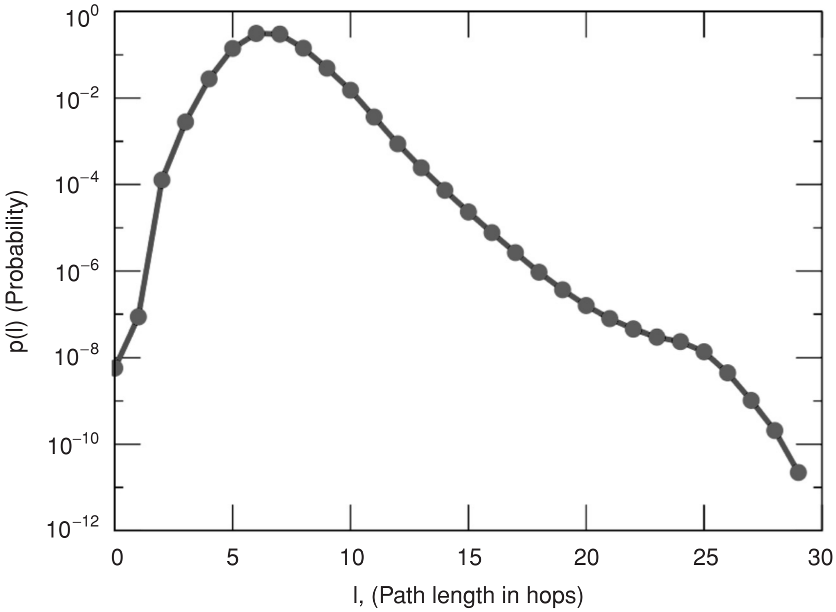

Figure 2.11. The distribution of distances in the graph of all active Microsoft Instant Messenger user accounts, with an edge joining two users if they communicated at least once during a month-long observation period [269].

P1: SBT
cuus984-net CUUS984-Easley 0 521 19533 1 November 30, 2009 16:2

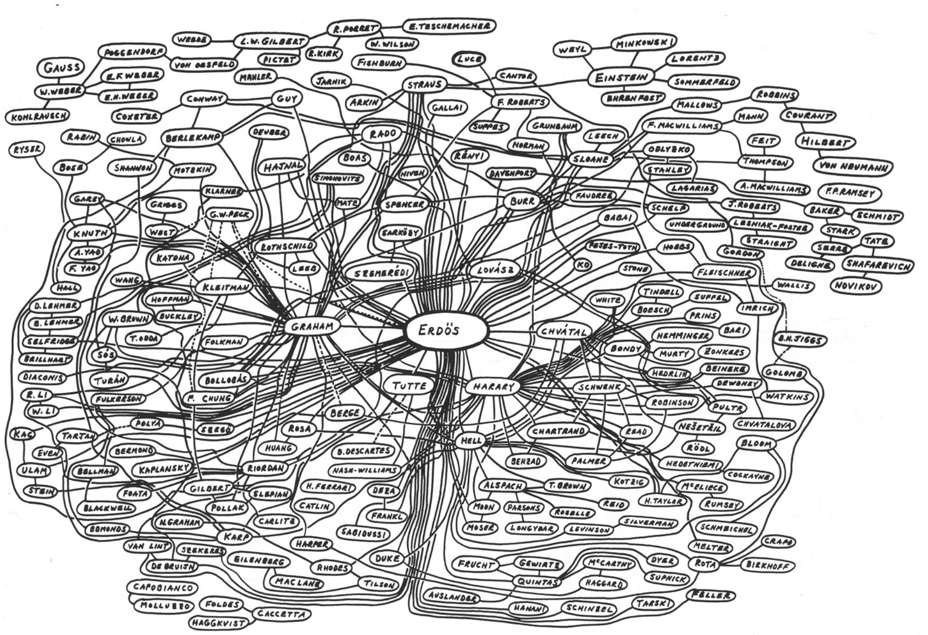

Figure 2.12. Ron Graham's hand-drawn picture of a part of the mathematics collaboration graph, centered on Paul Erdös [188]. (Image from http://www.oakland.edu/enp/cgraph.jpg)

P1: SBT
cuus984-net CUUS984-Easley 0 521 19533 1 November 30, 2009 16:2

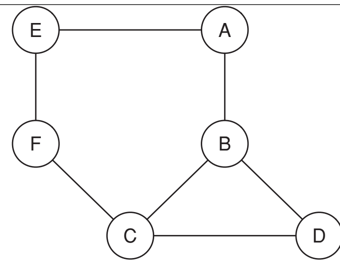

Figure 2.13. In this example, node B is pivotal for two pairs: the pair consisting of A and C, and the pair consisting of A and D. On the other hand, node D is not pivotal for any pairs.

P1: SBT
cuus984-net CUUS984-Easley 0 521 19533 1 November 30, 2009 16:2

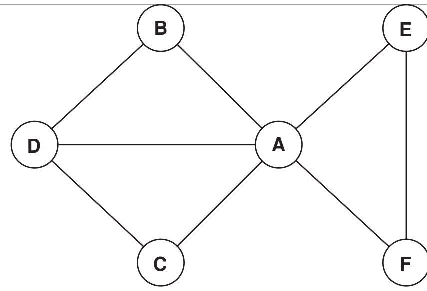

Figure 2.14. Node A is a gatekeeper. Node D is a local gatekeeper but not a gatekeeper.

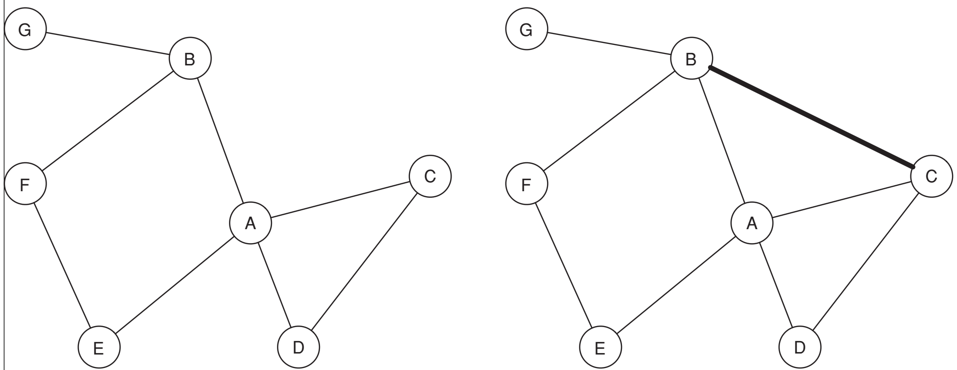

(a) (b)

Figure 3.1. The formation of the edge between *B* and *C* illustrates the effects of triadic closure, since they have a common neighbor *A*.

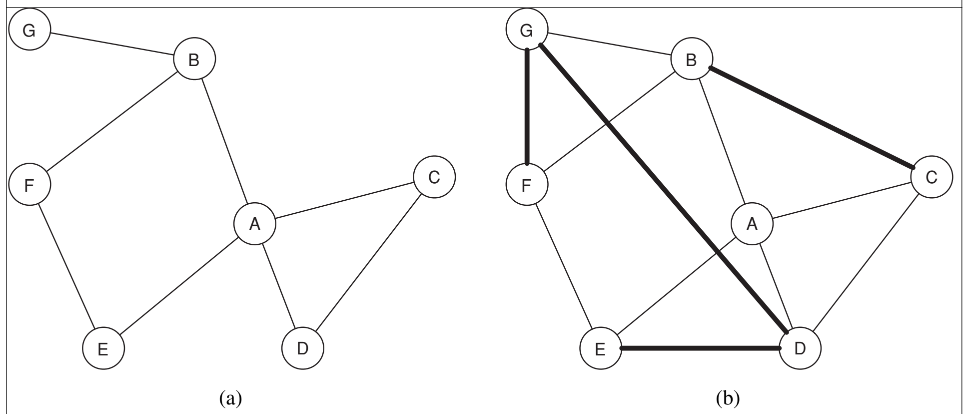

Figure 3.2. If we watch a network for a longer span of time, we can see multiple edges forming — some form through triadic closure while others (such as the *D-G* edge) form even though the two endpoints have no neighbors in common.

P1: SBT
cuus984-net CUUS984-Easley 0 521 19533 1 November 30, 2009 16:2

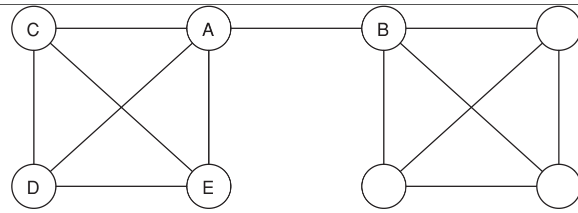

Figure 3.3. The *A*-*B* edge is a *bridge*, meaning that its removal would place *A* and *B* in distinct connected components. Bridges provide nodes with access to parts of the network that are unreachable by other means.

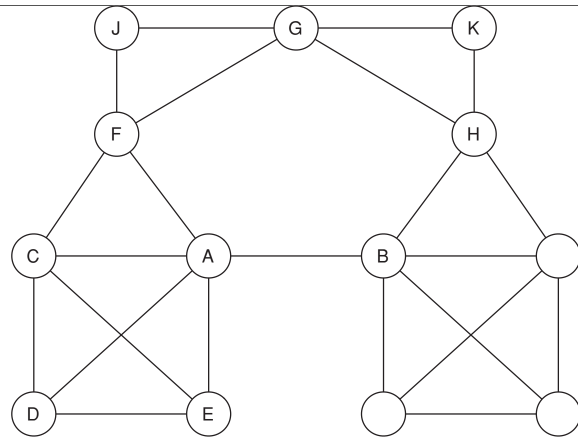

Figure 3.4. The *A-B* edge is a local bridge of span 4, since the removal of this edge would increase the distance between *A* and *B* to 4.

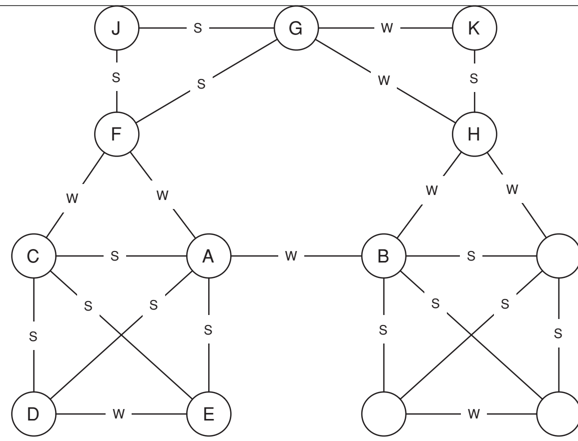

Figure 3.5. Each edge of the social network from Figure 3.4 is labeled here as either a *strong tie* (*S*) or a *weak tie* (*W*), to indicate the strength of the relationship. The labeling in the figure satisfies the Strong Triadic Closure Property at each node: if the node has strong ties to two neighbors, then these neighbors must have at least a weak tie between them.

P1: SBT
cuus984-net CUUS984-Easley 0 521 19533 1 November 30, 2009 16:2

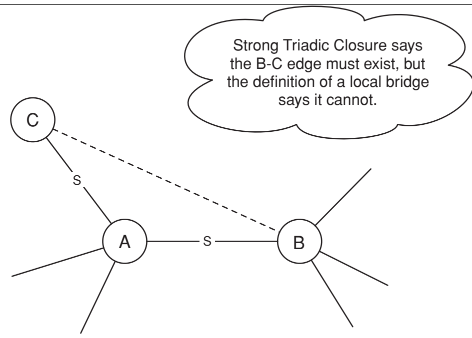

Figure 3.6. If a node satifies Strong Triadic Closure and is involved in at least two strong ties, then any local bridge it is involved in must be a weak tie. The figure illustrates the reason why: if the A-B edge is a strong tie, then there must also be an edge between B and C, meaning that the A-B edge cannot be a local bridge.

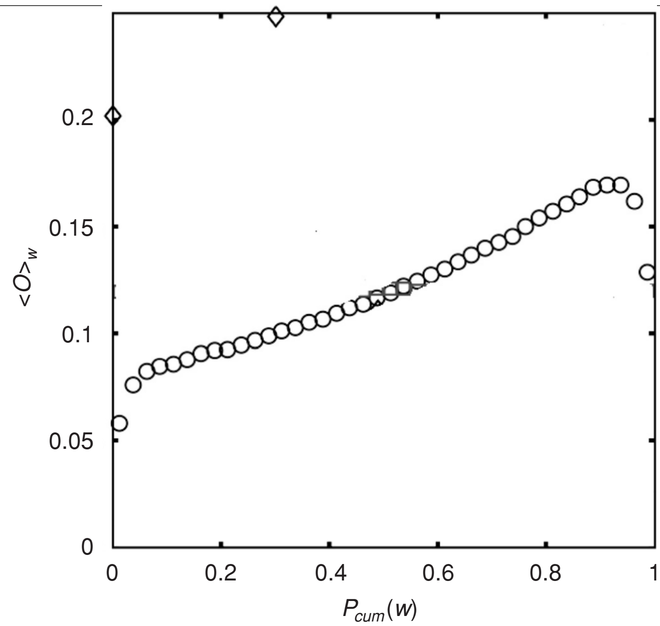

Figure 3.7. A plot of the neighborhood overlap of edges as a function of their percentile in the sorted order of all edges by tie strength. The fact that overlap increases with increasing tie strength is consistent with the theoretical predictions from Section 3.2. (Image from [328].)

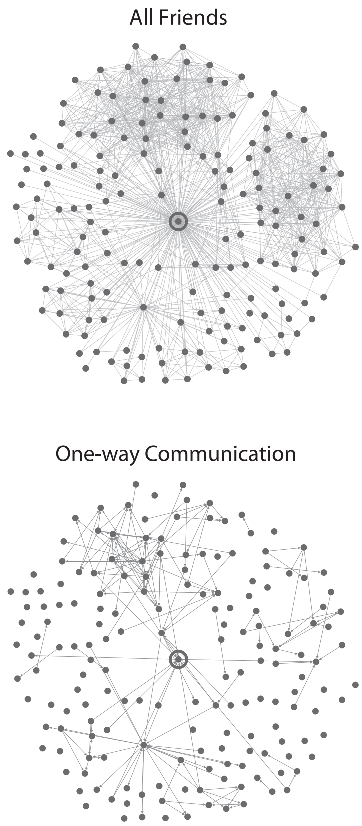

Figure 3.8. Four different views of a Facebook user's network neighborhood, showing the structure of links coresponding respectively to all declared friendships, maintained relationships, one-way communication, and reciprocal (i.e. mutual) communication. (Image from [281].)

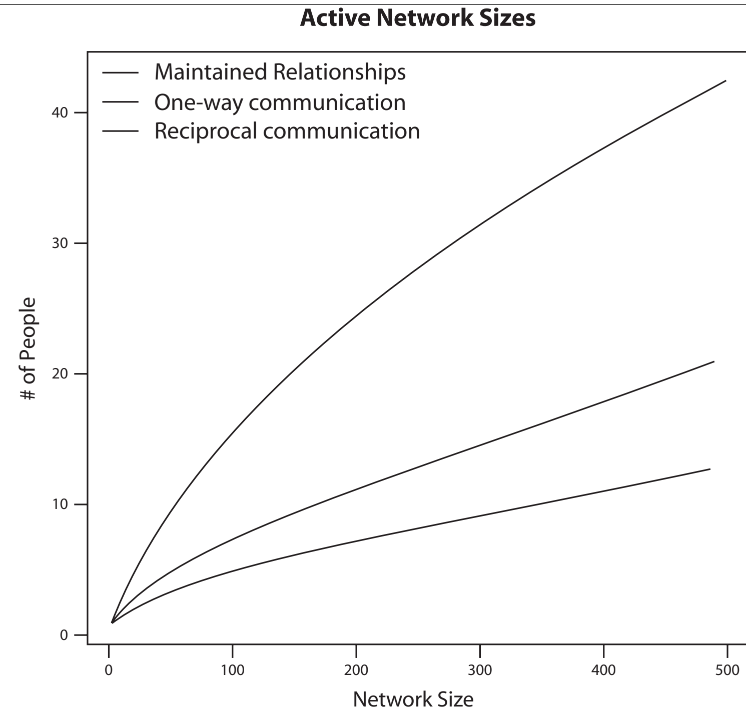

Figure 3.9. The number of links corresponding to maintained relationships, one-way communication, and reciprocal communication as a function of the total neighborhood size for users on Facebook. (Image from [281].)

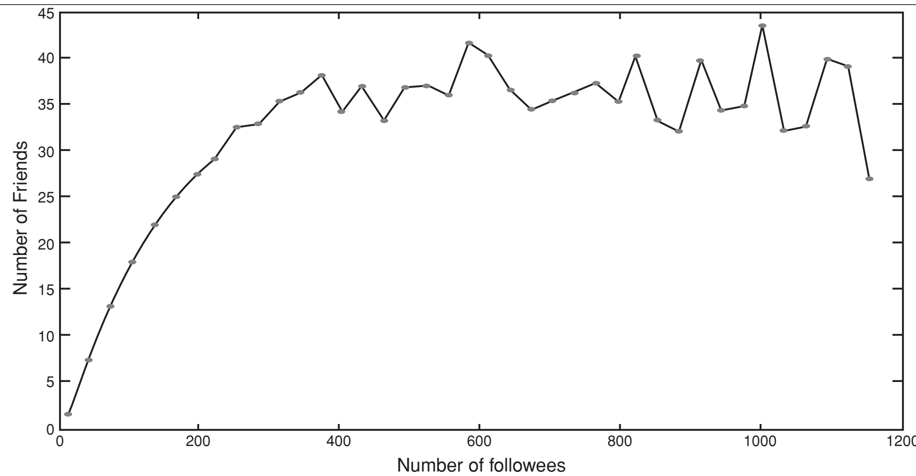

Figure 3.10. The total number of a user's strong ties (defined by multiple directed messages) as a function of the number of followees he or she has on Twitter. (Image from [218].)

P1: SBT
cuus984-net CUUS984-Easley 0 521 19533 1 November 30, 2009 16:2

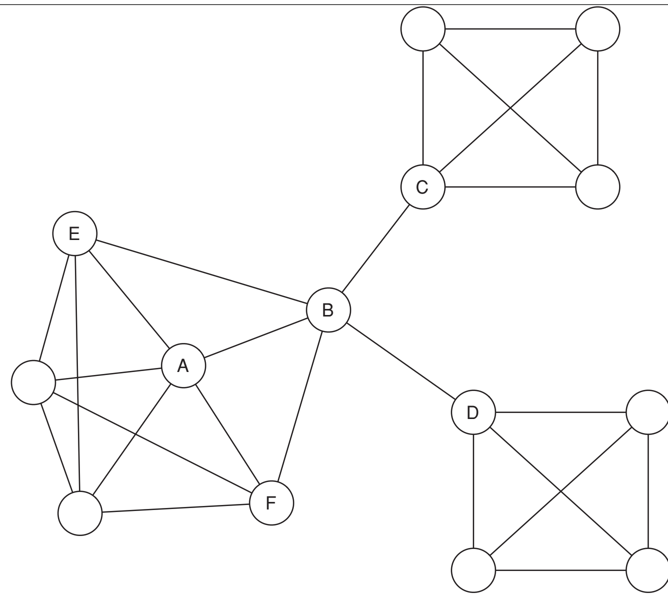

Figure 3.11. The contrast between densely-knit groups and boundary-spanning links is reflected in the different positions of nodes A and B in the underlying social network.

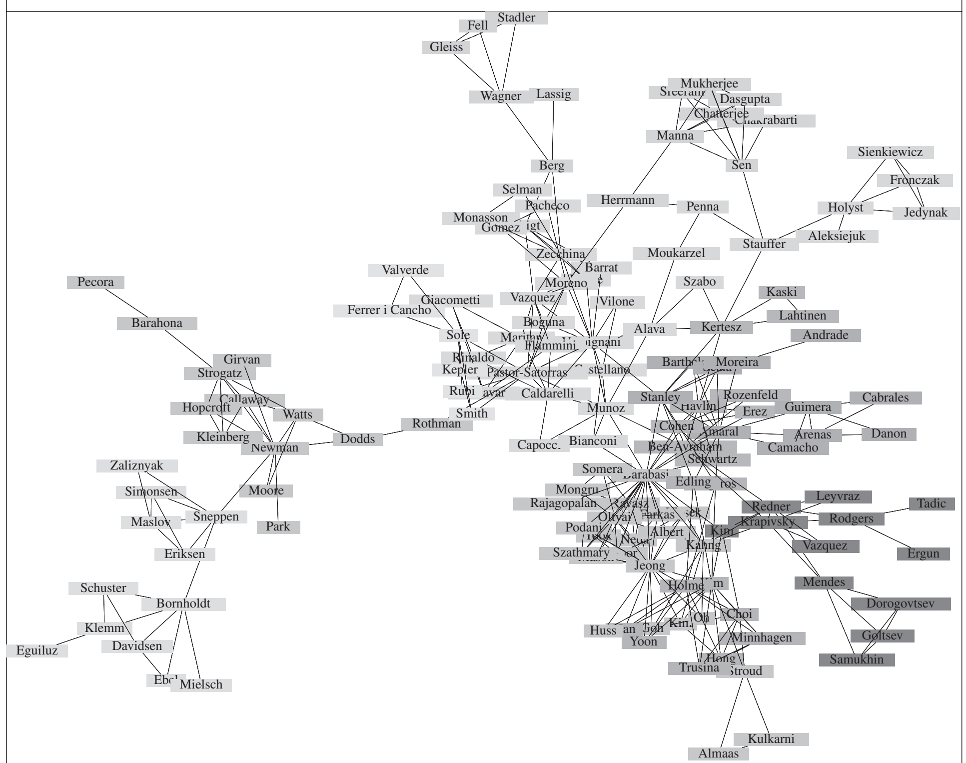

Figure 3.12. A co-authorship network of physicists and applied mathematicians working on networks [316]. Within this professional community, more tightly-knit subgroups are evident from the network structure.

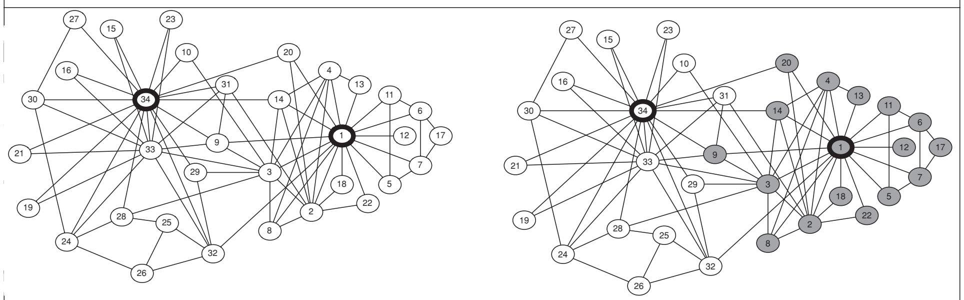

(a) (b)

Figure 3.13. A karate club studied by Wayne Zachary [409] — a dispute during the course of the study caused it to split into two clubs. Could the boundaries of the two clubs be predicted from the network structure?

P1: SBT
cuus984-net CUUS984-Easley 0 521 19533 1 November 30, 2009 16:2

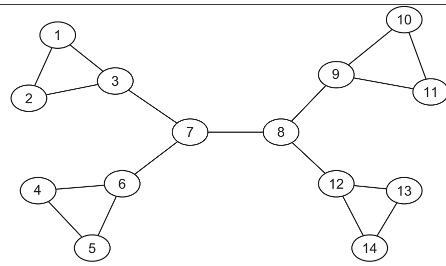

(a)

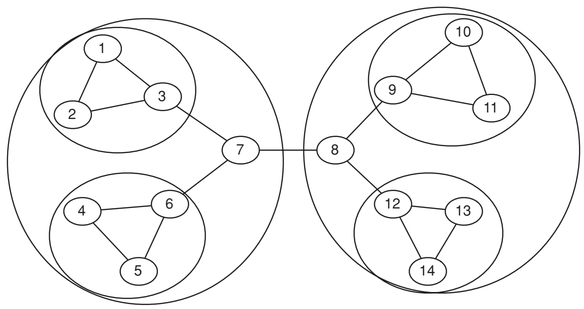

(b)

Figure 3.14. In many networks, there are tightly-knit regions that are intuitively apparent, and they can even display a *nested* structure, with smaller regions nesting inside larger ones.

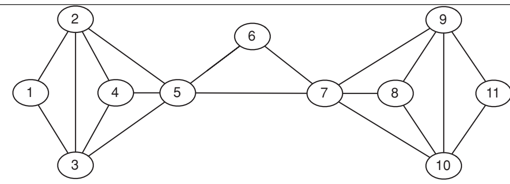

Figure 3.15. A network can display tightly-knit regions even when there are no bridges or local bridges along which to separate it.

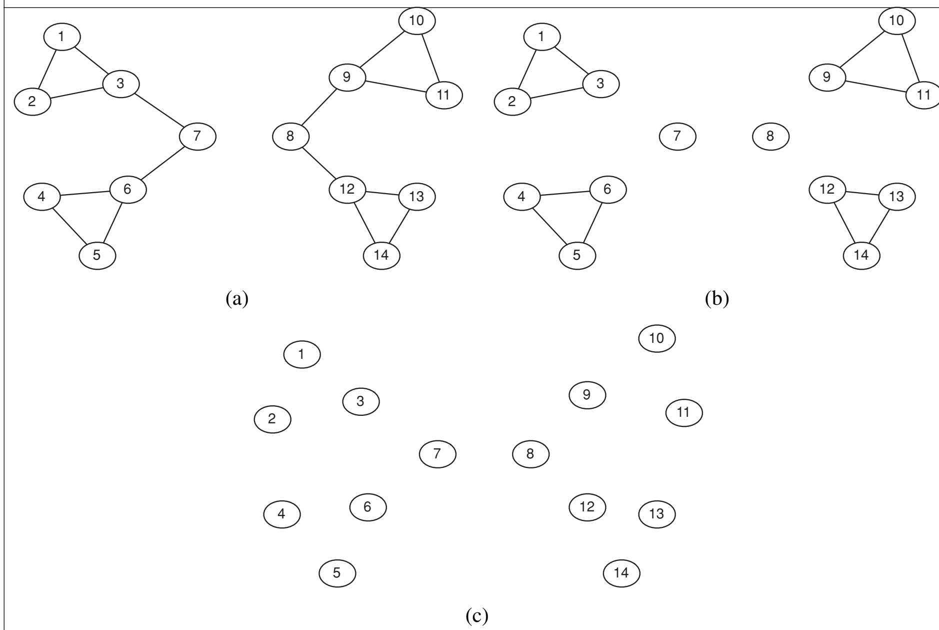

Figure 3.16. The steps of the Girvan-Newman method on the network from Figure 3.14(a).

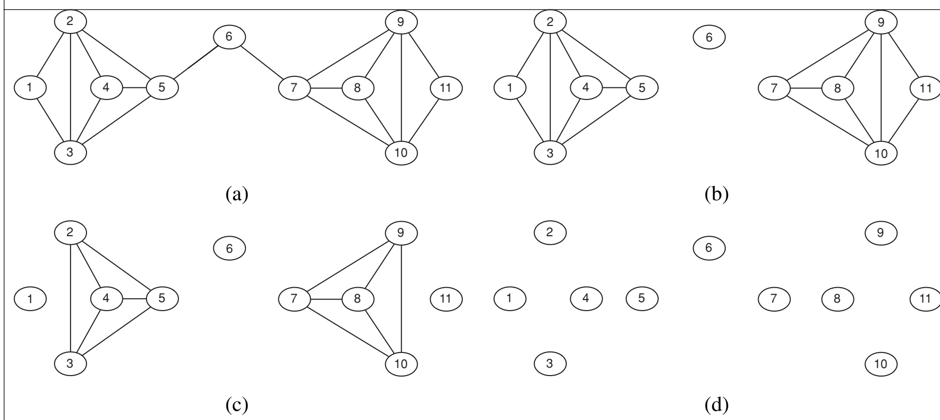

Figure 3.17. The steps of the Girvan-Newman method on the network from Figure 3.15.

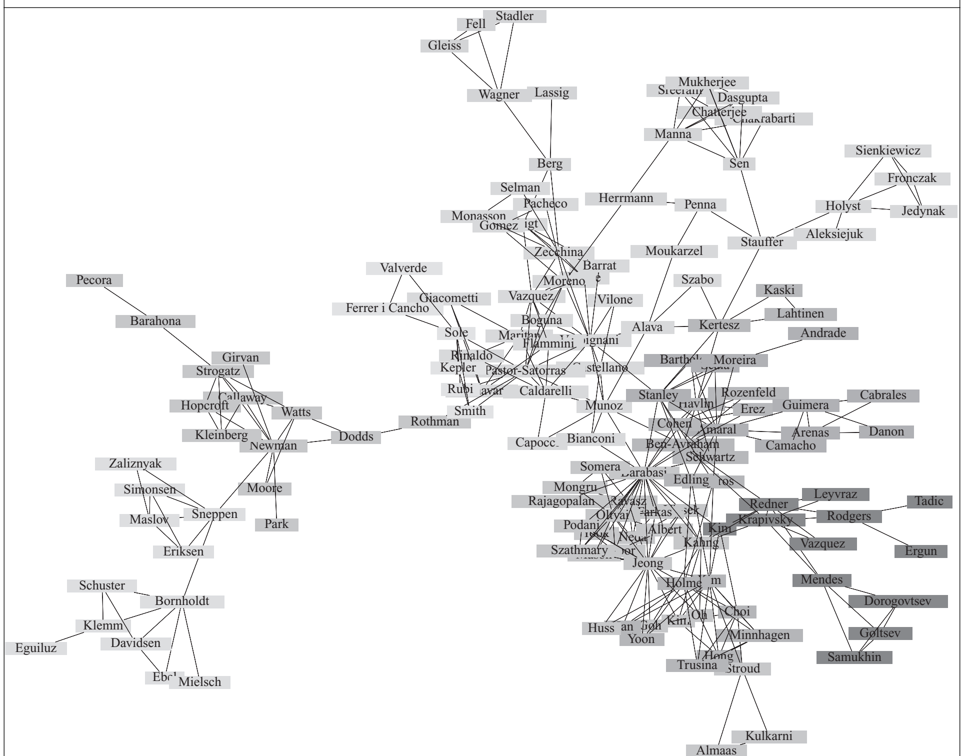

Figure 3.18. The tightly-knit regions identified by the Girvan-Newman method in the co-authorship network from Figure 3.12.

P1: SBT
cuus984-net CUUS984-Easley 0 521 19533 1 November 30, 2009 16:2

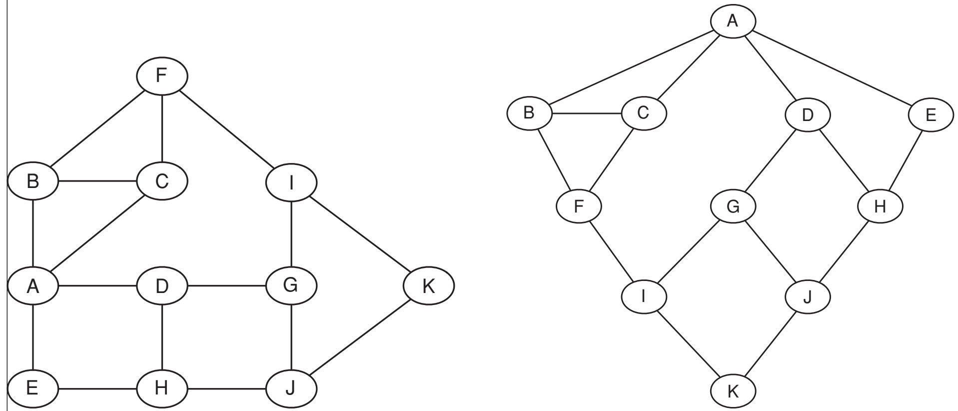

(a) (b)

Figure 3.19. The first step in the efficient method for computing betweenness values is to perform a breadth-first search of the network. Here the results of breadth-first from node *A* are shown; over the course of the method, breadth-first search is performed from each node in turn.

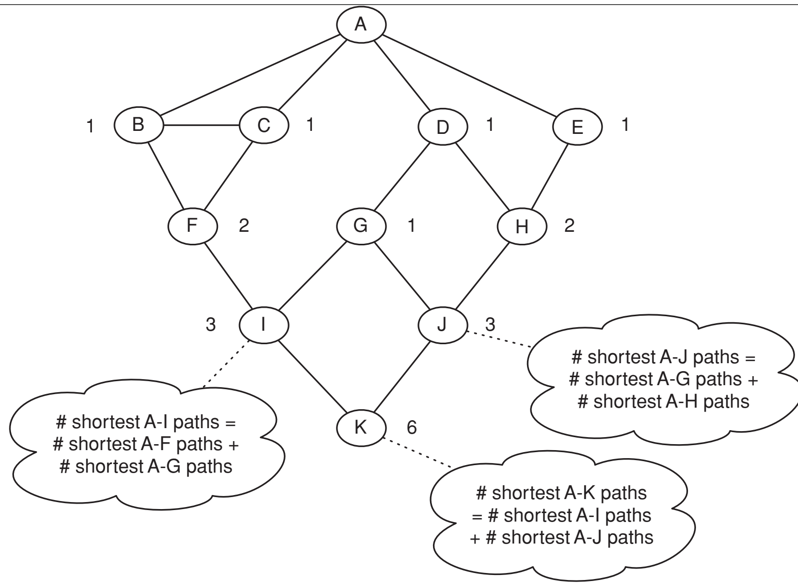

Figure 3.20. The second step in computing betweenness values is to count the number of shortest paths from a starting node *A* to all other nodes in the network. This can be done by adding up counts of shortest paths, moving downward through the breadth-first search structure.

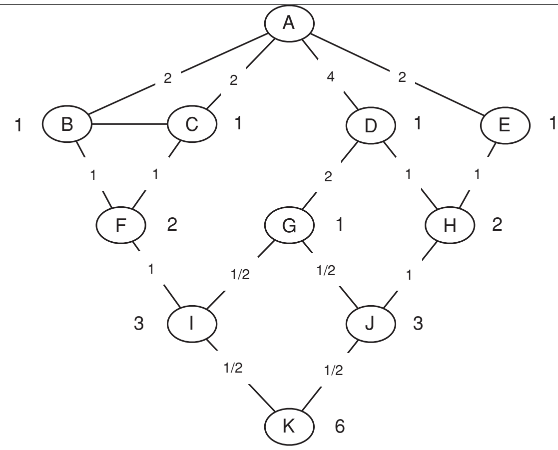

Figure 3.21. The final step in computing betweenness values is to determine the flow values from a starting node A to all other nodes in the network. This is done by working up from the lowest layers of the breadth-first search, dividing up the flow above a node in proportion to the number of shortest paths coming into it on each edge.

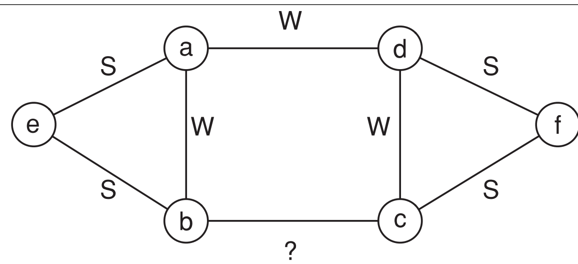

Figure 3.22.

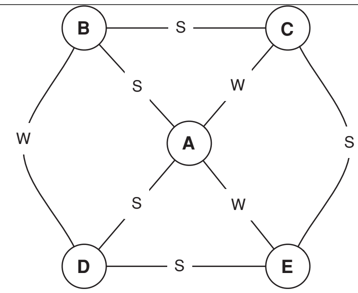

Figure 3.23. .

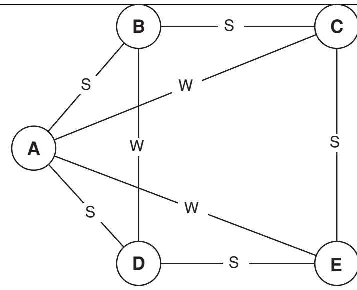

Figure 3.24. A graph with a strong/weak labeling.

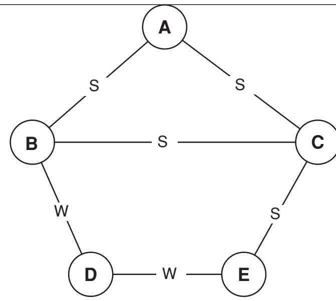

Figure 3.25.

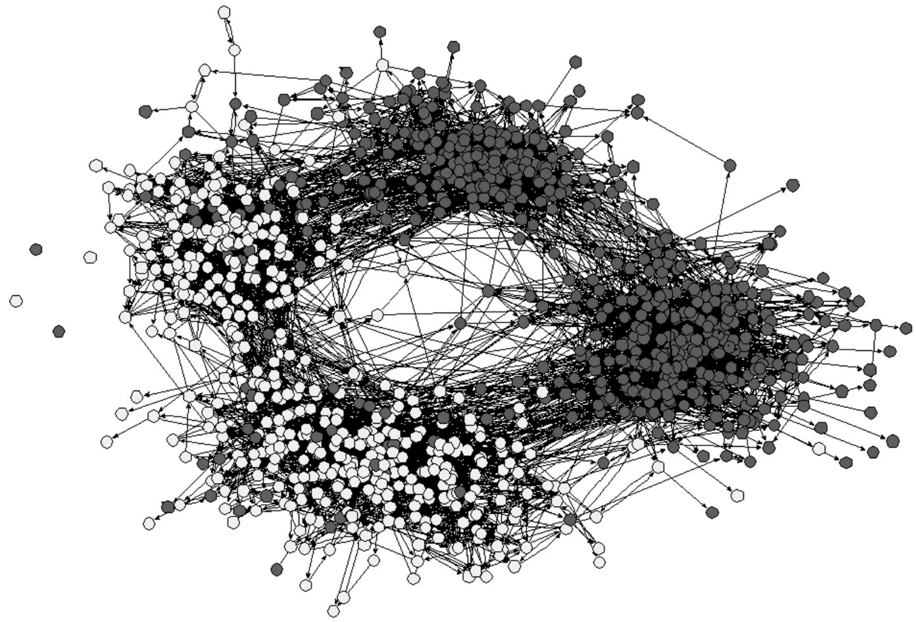

Figure 4.1. Homophily can produce a division of a social network into densely-connected, homogeneous parts that are weakly connected to each other. In this social network from a town's middle school and high school, two such divisions in the network are apparent: one based on race (with students of different races drawn as differently colored circles), and the other based on friendships in the middle and high schools respectively [299].

P1: SBT
cuus984-net CUUS984-Easley 0 521 19533 1 November 30, 2009 16:2

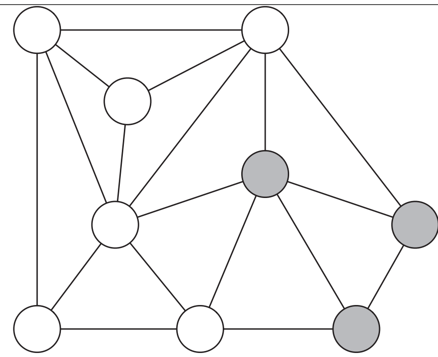

Figure 4.2. Using a numerical measure, one can determine whether small networks such as this one (with nodes divided into two types) exhibit homophily.

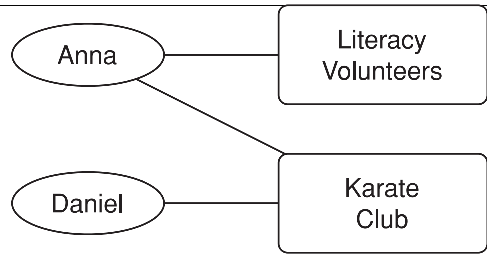

Figure 4.3. An affiliation network is a bipartite graph that shows which individuals are affiliated with which groups or activities. Here, Anna participates in both of the social foci on the right, while Daniel participates in only one.

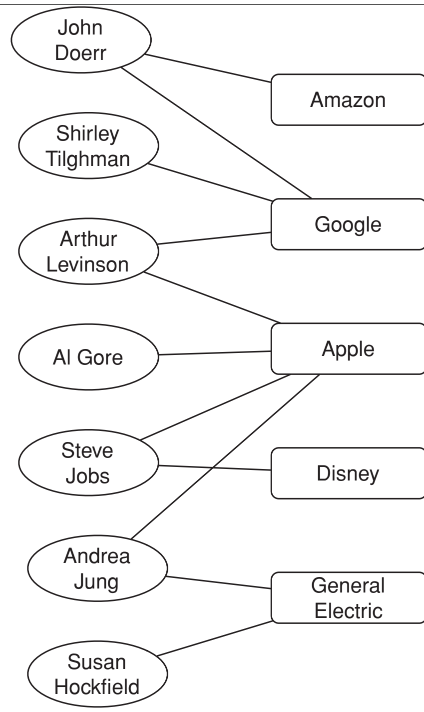

Figure 4.4. One type of affiliation network that has been widely studied is the memberships of people on corporate boards of directors [296]. A very small portion of this network (as of 2009) is shown here. The structural pattern of memberships can reveal subtleties in the interactions among both the board members and the companies.

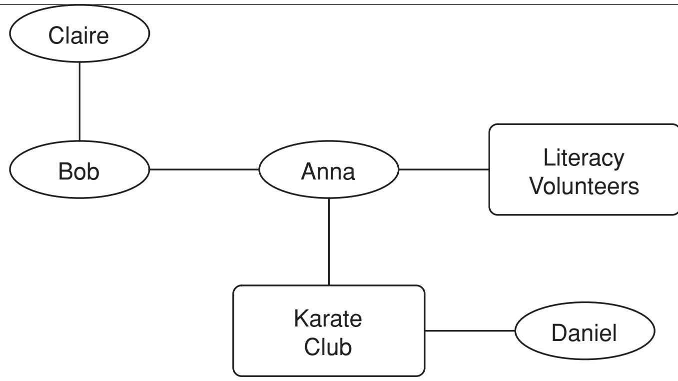

Figure 4.5. A social-affiliation network shows both the friendships between people and their affiliation with different social foci.

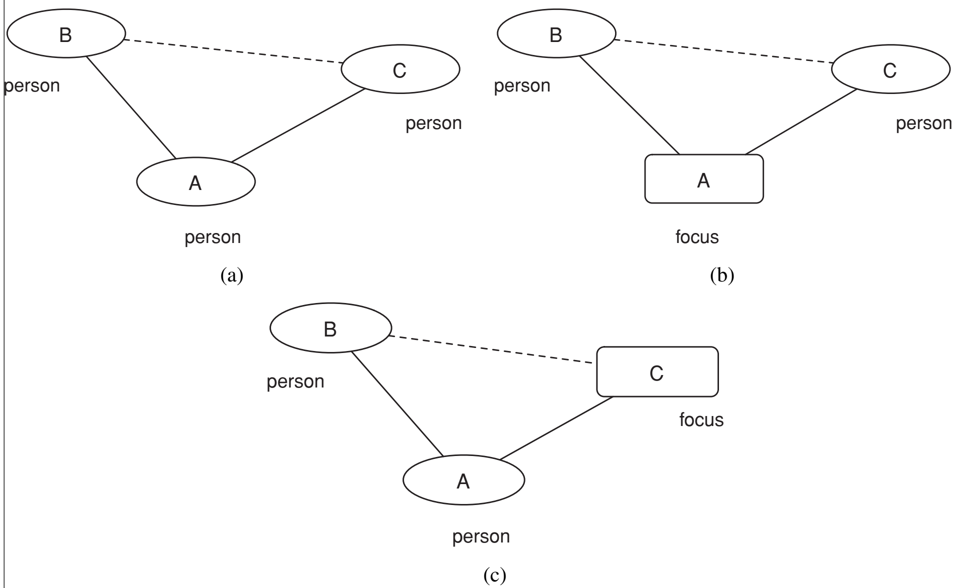

Figure 4.6. Each of triadic closure, focal closure, and membership influence corresponds to the closing of a triangle in a social-affiliation network.

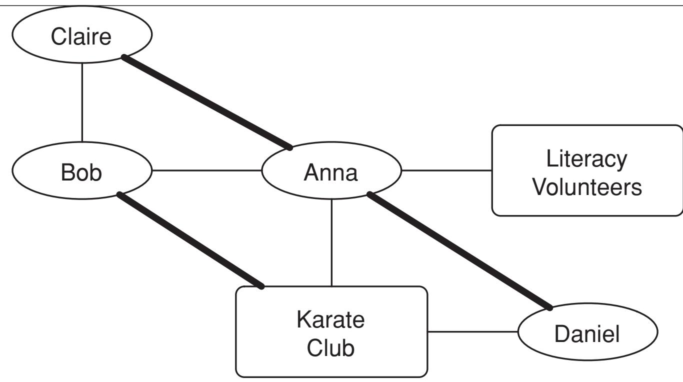

Figure 4.7. In a social-affiliation network containing both people and foci, edges can form under the effect of several different kinds of closure processes: two people with a friend in common, two people with a focus in common, or a person joining a focus that a friend is already involved in.

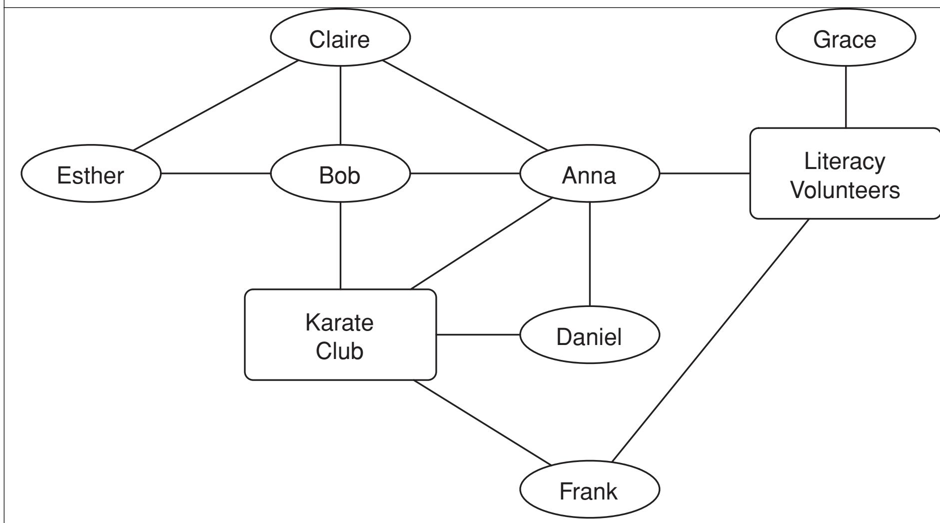

Figure 4.8. A larger network that contains the example from Figure 4.7. Pairs of people can have more than friend (or more than one focus) in common; how does this increase the likelihood that an edge will form between them?

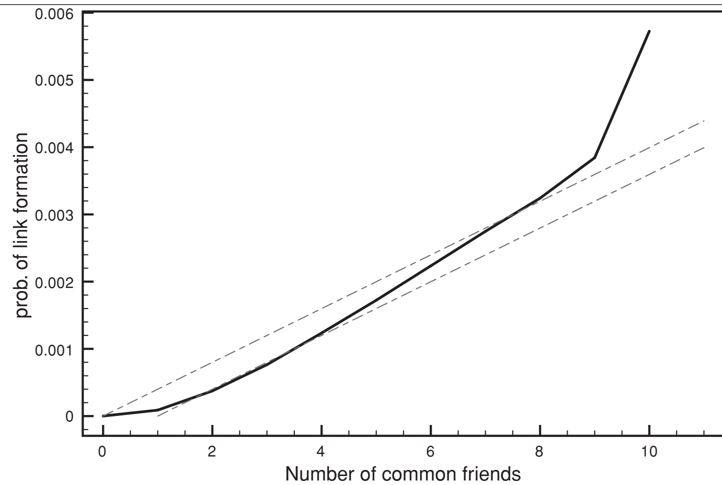

Figure 4.9. Quantifying the effects of triadic closure in an e-mail dataset [255]. The curve determined from the data is shown in the solid black line; the dotted curves show a comparison to probabilities computed according to two simple baseline models in which common friends provide independent probabilities of link formation.

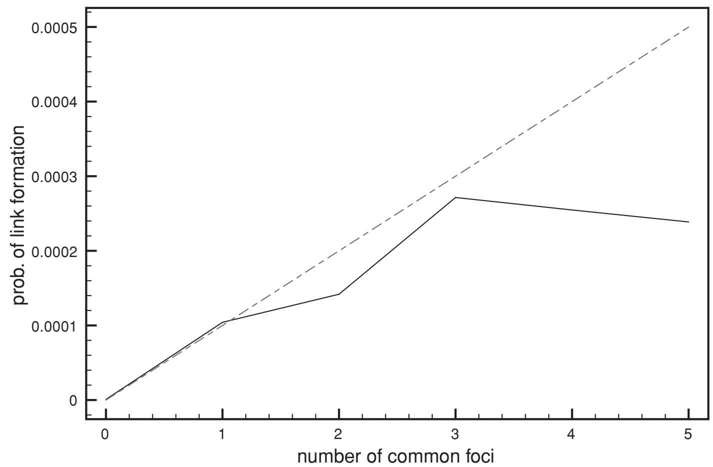

Figure 4.10. Quantifying the effects of focal closure in an e-mail dataset [255]. Again, the curve determined from the data is shown in the solid black line, while the dotted curve provides a comparison to a simple baseline.

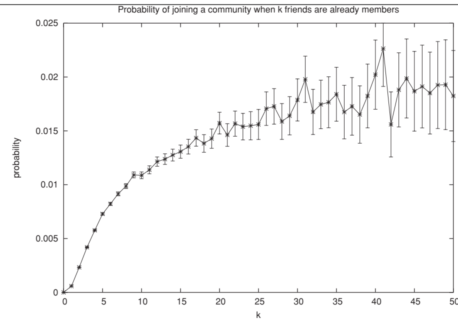

(a)

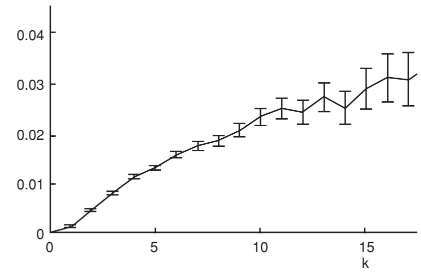

(b)

Figure 4.11. Quantifying the effects of membership closure in two large on-line datasets [32, 121].

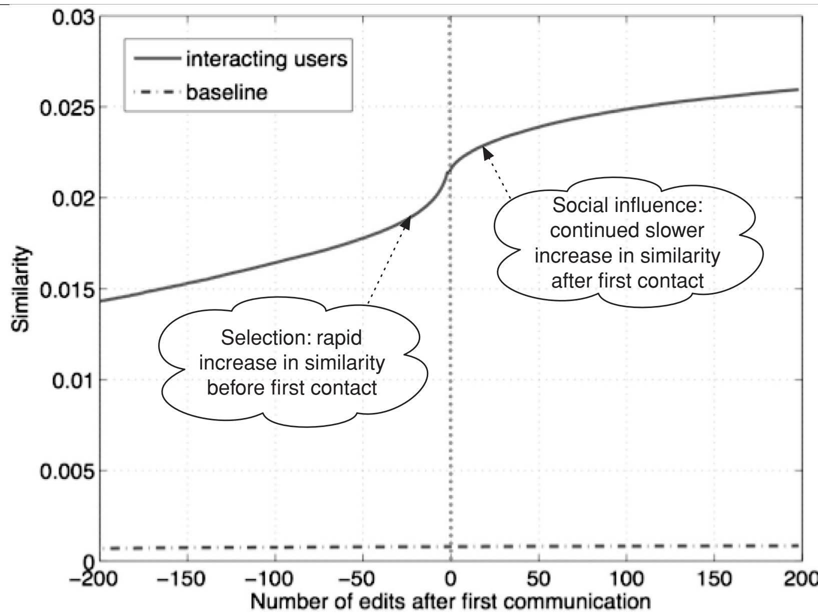

Figure 4.12. The average similarity of two editors on Wikipedia, relative to the time (0) at which they first communicated [121]. Time, on the x-axis, is measured in discrete units, where each unit corresponds to a single Wikipedia action taken by either of the two editors. The curve increases both before and after the first contact at time 0, indicating that both selection and social influence play a role; the increase in similarity is steepest just before time 0.

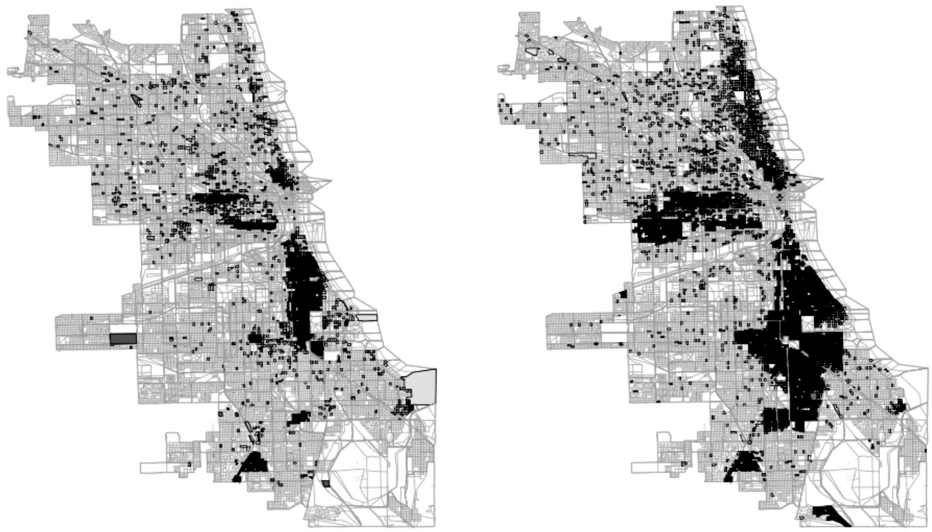

(a) *Chicago, 1940* (b) *Chicago, 1960*

Figure 4.13. The tendency of people to live in racially homogeneous neighborhoods produces spatial patterns of segregation that are apparent both in everyday life and when superimposed on a map — as here, in these maps of Chicago from 1940 and 1960 [297]. In blocks colored yellow and orange the percentage of African-Americans is below 25, while in blocks colored brown and black the percentage is above 75.

P1: SBT
cuus984-net CUUS984-Easley 0 521 19533 1 November 30, 2009 16:2

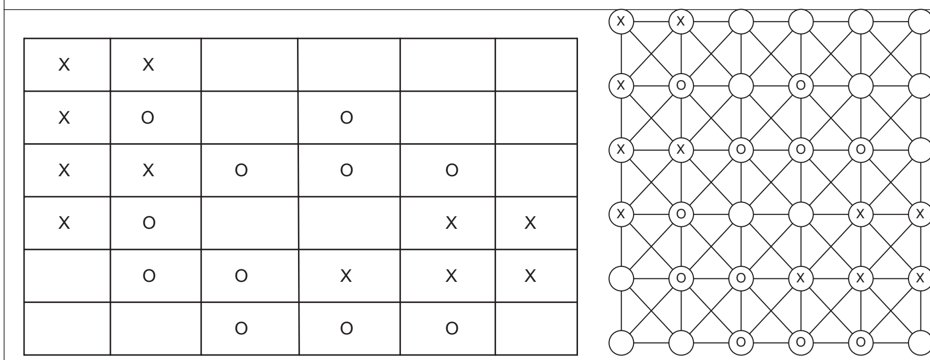

(a) (b)

Figure 4.14. In Schelling's segregation model, agents of two different types (`X` and `O`) occupy cells on a grid. The neighbor relationships among the cells can be represented very simply as a graph. Agents care about whether they have at least some neighbors of the same type.

X1*	X2*				
X3	O1*		O2		
X4	X5	O3	O4	O5*	
X6*	O6			X7	X8
	O7	O8	X9*	X10	X11
		O9	O10	O11*	

(a)

X3	X6	O1	O2		
X4	X5	O3	O4		
	O6	X2	X1	X7	X8
O11	O7	O8	X9	X10	X11
	O5	O9	O10*		

(b)

Figure 4.15. After arranging agents in cells of the grid, we first determine which agents are *unsatisfied*, with fewer than t other agents of the same type as neighbors. In one round, each of these agents moves to a cell where they will be satified; this may cause other agents to become unsatisfied, in which case a new round of movement begins.

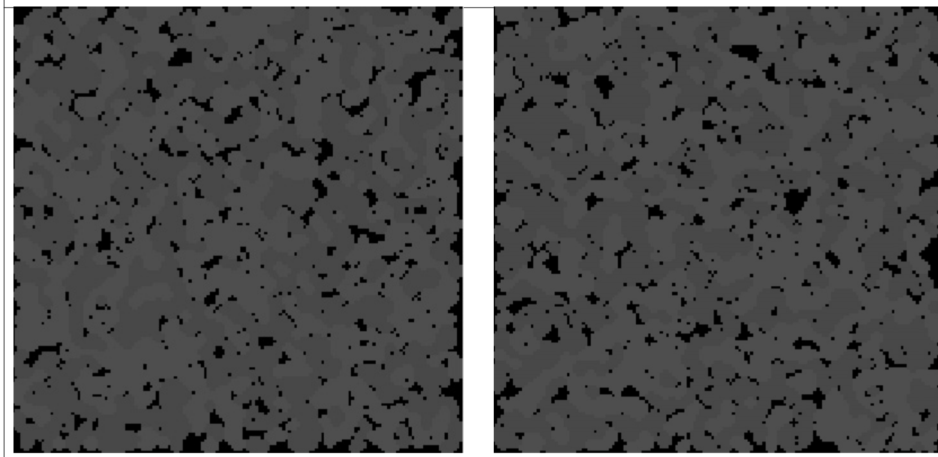

(a) (b)

Figure 4.16. Two runs of a simulation of the Schelling model with a threshold t of 3, on a 150-by-150 grid with 10,000 agents of each type.

X	X	O	O	X	X
X	X	O	O	X	X
O	O	X	X	O	O
O	O	X	X	O	O
X	X	O	O	X	X
X	X	O	O	X	X

Figure 4.17. With a threshold of 3, it is possible to arrange agents in an integrated pattern: all agents are satisfied, and everyone who is not on the boundary on the grid has an equal number of neighbors of each type.

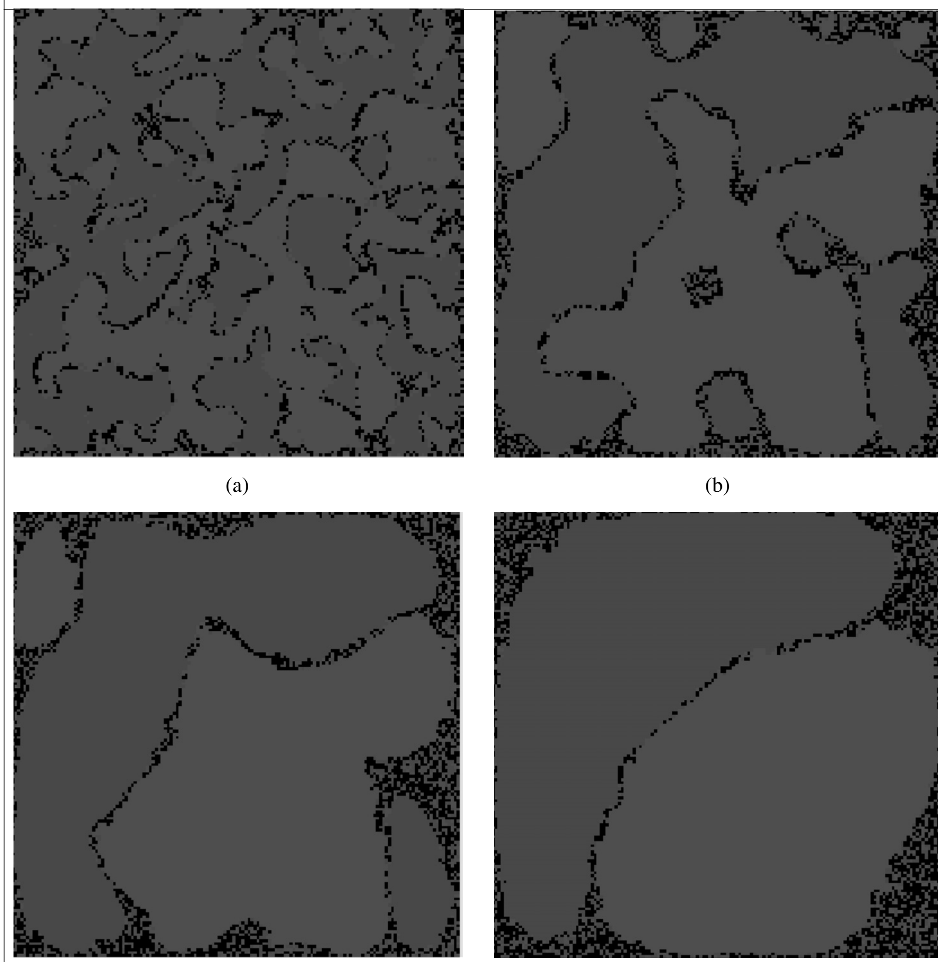

(a) (b) (c) (d)

Figure 4.18. Four intermediate points in a simulation of the Schelling model with a threshold t of 4, on a 150-by-150 grid with 10,000 agents of each type. As the rounds of movement progress, large homogeneous regions on the grid grow at the expense of smaller, narrower regions.

P1: SBT
cuus984-net CUUS984-Easley 0 521 19533 1 November 30, 2009 16:2

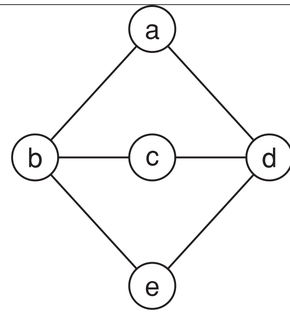

Figure 4.19. A social network where triadic closure may occur.

P1: SBT
cuus984-net CUUS984-Easley 0 521 19533 1 November 30, 2009 16:2

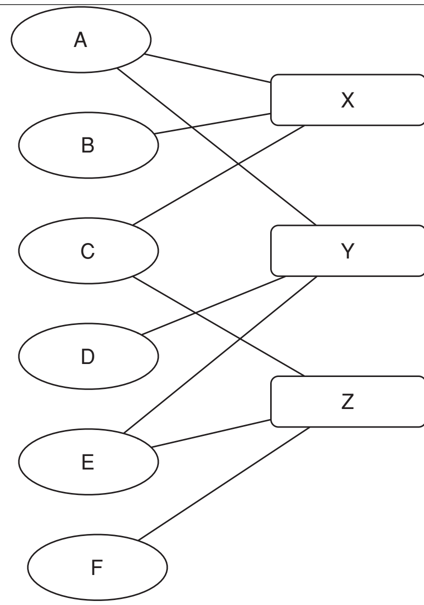

Figure 4.20. An affiliation network on six people labeled A–F, and three foci labeled X, Y, and Z.

P1: SBT
cuus984-net CUUS984-Easley 0 521 19533 1 November 30, 2009 16:2

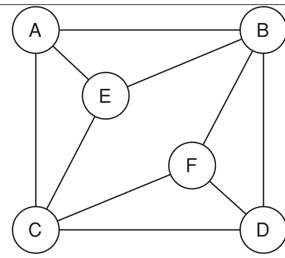

Figure 4.21. A graph on people arising from an (unobserved) affiliation network.

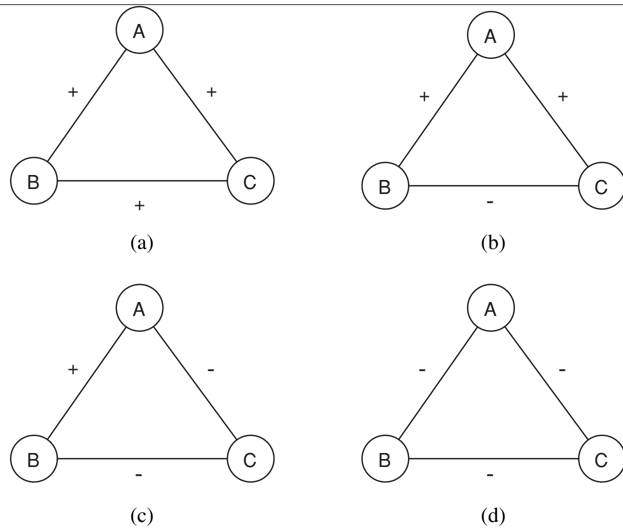

Figure 5.1. Structural balance: Each labeled triangle must have 1 or 3 positive edges.

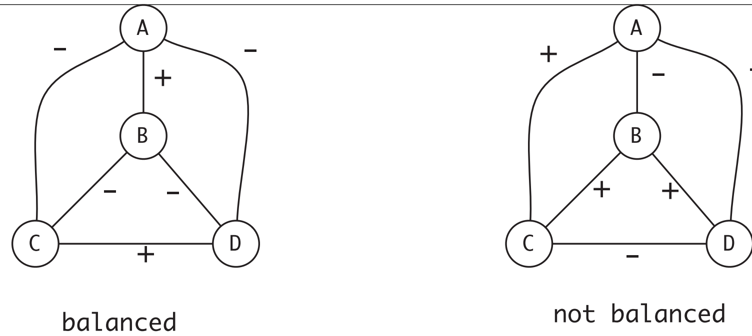

Figure 5.2. The labeled four-node complete graph on the left is balanced; the one on the right is not.

P1: SBT
cuus984-net CUUS984-Easley 0 521 19533 1 November 30, 2009 16:2

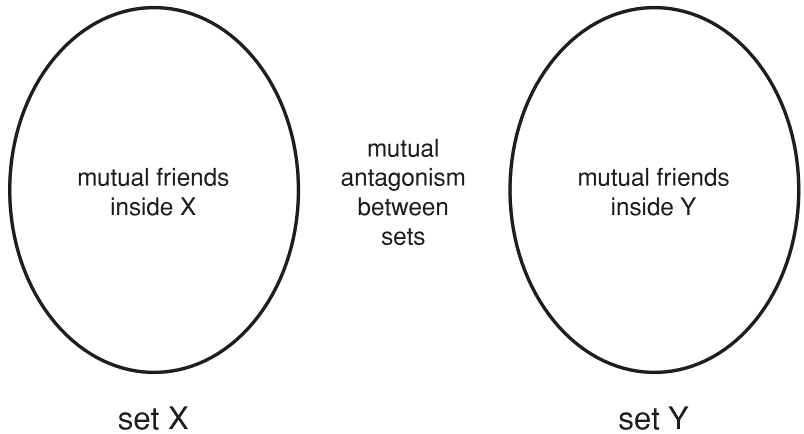

Figure 5.3. If a complete graph can be divided into two sets of mutual friends, with complete mutual antagonism between the two sets, then it is balanced. Furthermore, this is the only way for a complete graph to be balanced.

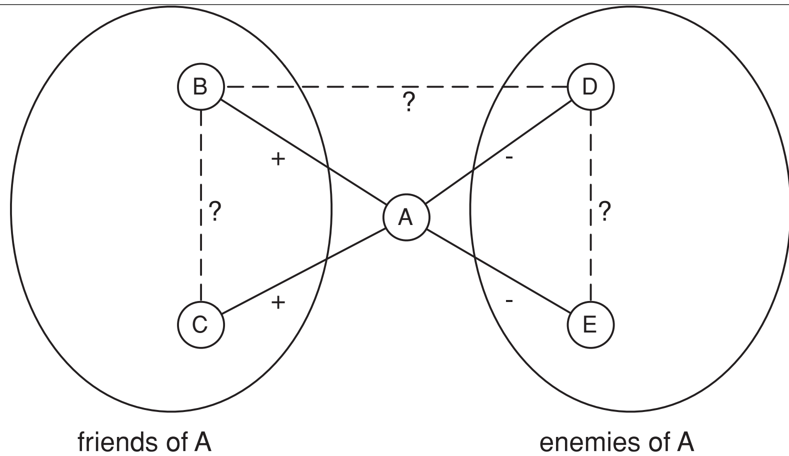

Figure 5.4. A schematic illustration of our analysis of balanced networks. (There may be other nodes not illustrated here.)

P1: SBT
cuus984-net CUUS984-Easley 0 521 19533 1 November 30, 2009 16:2

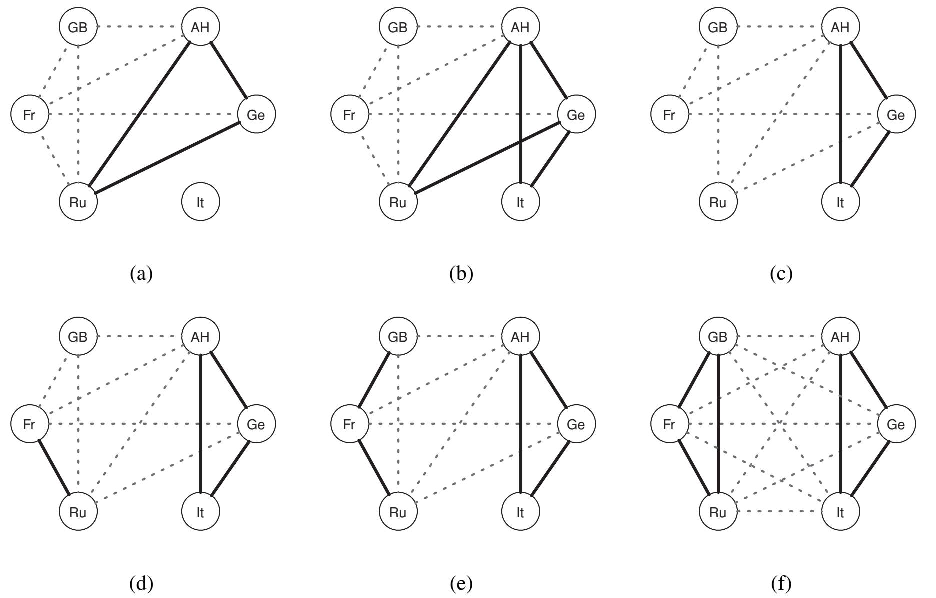

Figure 5.5. The evolution of alliances in Europe, 1872-1907 (the nations GB, Fr, Ru, It, Ge, and AH are Great Britain, France, Russia, Italy, Germany, and Austria-Hungary respectively). Solid dark edges indicate friendship while dotted red edges indicate enmity. Note how the network slides into a balanced labeling — and into World War I. This figure and example are from Antal, Krapivsky, and Redner [21].

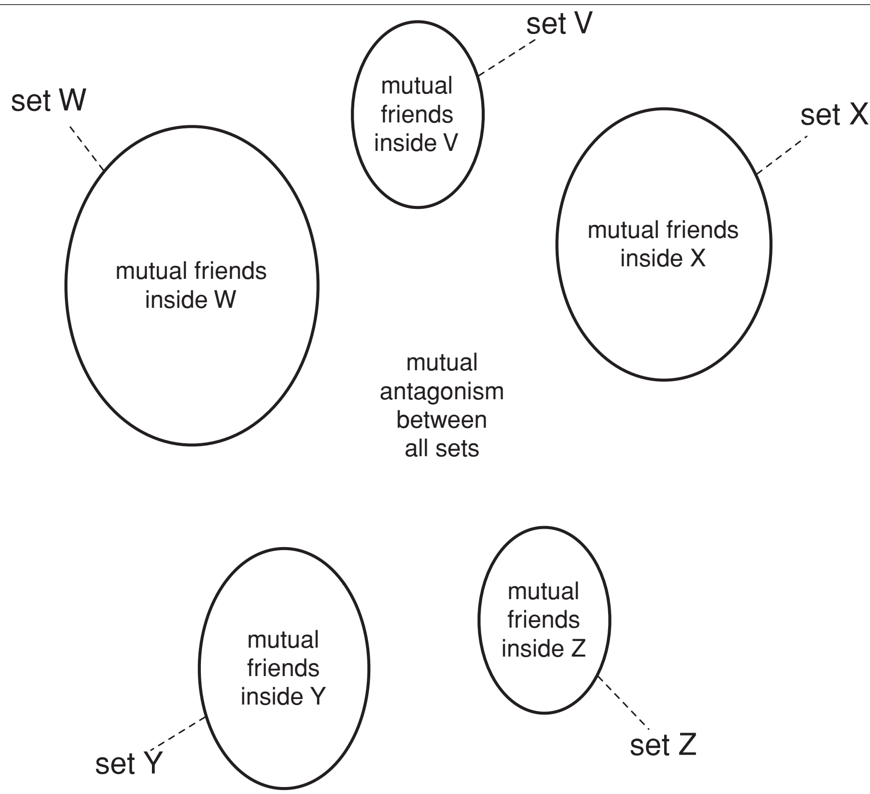

Figure 5.6. A complete graph is weakly balanced precisely when it can be divided into multiple sets of mutual friends, with complete mutual antagonism between each pair of sets.

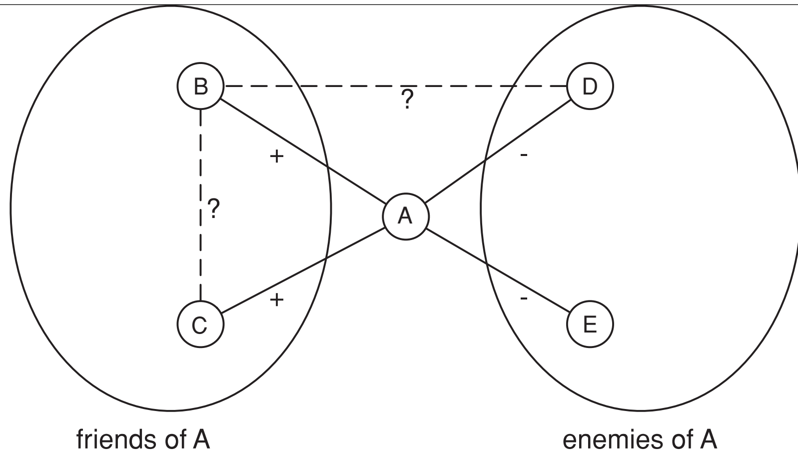

Figure 5.7. A schematic illustration of our analysis of weakly balanced networks. (There may be other nodes not illustrated here.)

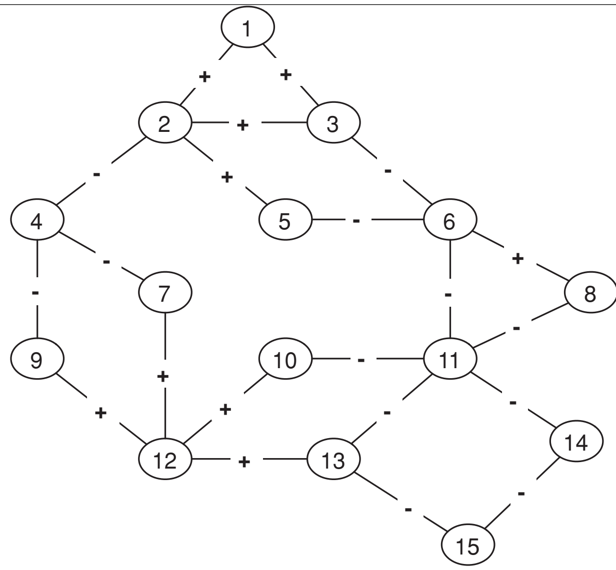

Figure 5.8. In graphs that are not complete, we can still define notions of structural balance when the edges that are present have positive or negative signs indicating friend or enemy relations.

P1: SBT
cuus984-net CUUS984-Easley 0 521 19533 1 November 30, 2009 16:2

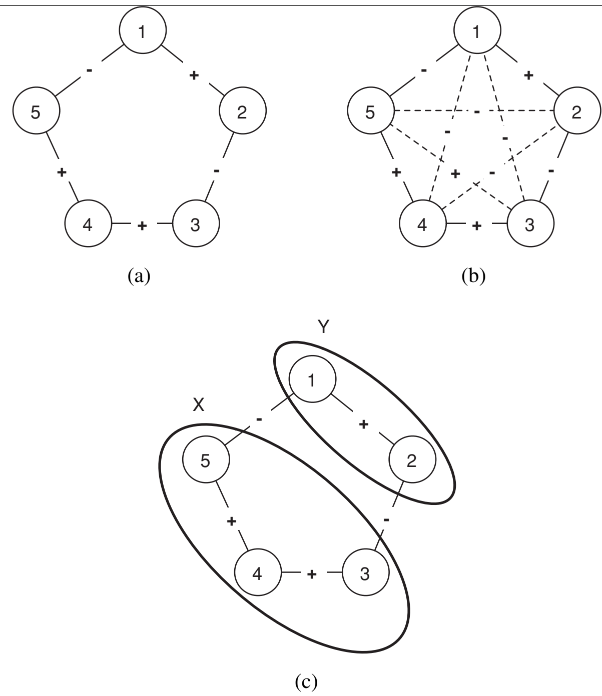

Figure 5.9. There are two equivalent ways to define structural balance for general (non-complete) graphs. One definition asks whether it is possible to fill in the remaining edges so as to produce a signed complete graph that is balanced. The other definition asks whether it is possible to divide the nodes into two sets X and Y so that all edges inside X and inside Y are positive, and all edges between X and Y are negative.

P1: SBT
cuus984-net CUUS984-Easley 0 521 19533 1 November 30, 2009 16:2

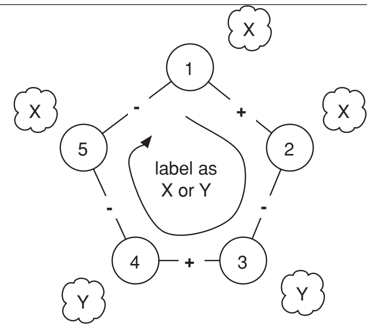

Figure 5.10. If a signed graph contains a cycle with an odd number of edges, then it is not balanced. Indeed, if we pick of one of the nodes and try to place it in X, then following the set of friend/enemy relations around the cycle will produce a conflict by the time we get to the starting node.

P1: SBT
cuus984-net CUUS984-Easley 0 521 19533 1 November 30, 2009 16:2

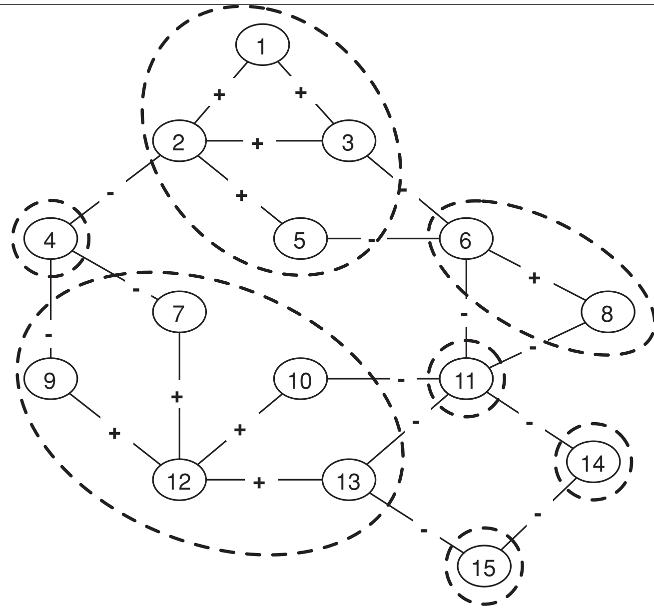

Figure 5.11. To determine if a signed graph is balanced, the first step is to consider only the positive edges, find the connected components using just these edges, and declare each of these components to be a *supernode*. In any balanced division of the graph into X and Y, all nodes in the same supernode will have to go into the same set.

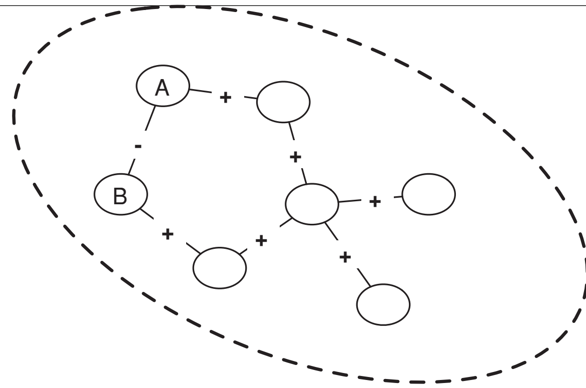

Figure 5.12. Suppse a negative edge connects two nodes A and B that belong to the same supernode. Since there is also a path consisting entirely of positive edges that connects A and B through the inside of the supernode, putting this negative edge together with the all-positive path produces a cycle with an odd number of negative edges.

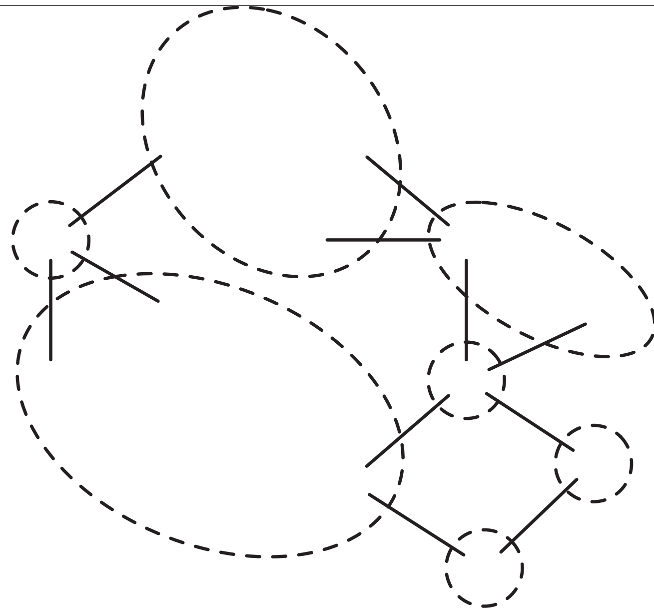

Figure 5.13. The second step in determining whether a signed graph is balanced is to look for a labeling of the supernodes so that adjacent supernodes (which necessarily contain mutual enemies) get opposite labels. For this purpose, we can ignore the original nodes of the graph and consider a *reduced graph* whose nodes are the supernodes of the original graph.

P1: SBT
cuus984-net CUUS984-Easley 0 521 19533 1 November 30, 2009 16:2

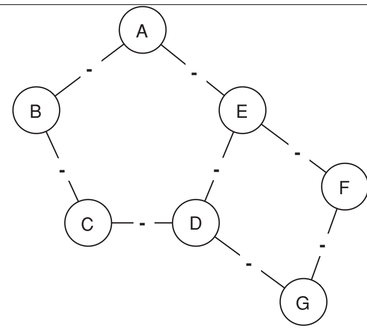

Figure 5.14. A more standard drawing of the reduced graph from the previous figure. A negative cycle is visually apparent in this drawing.

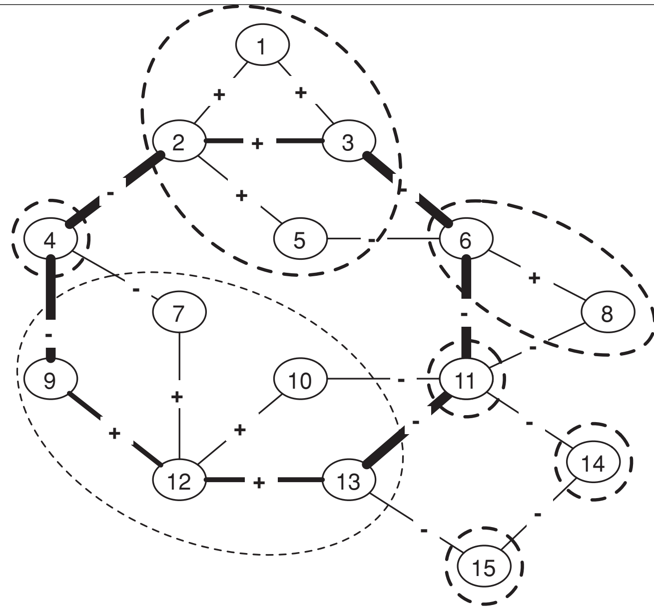

Figure 5.15. Having found a negative cycle through the supernodes, we can then turn this into a cycle in the original graph by filling in paths of positive edges through the inside of the supernodes. The resulting cycle has an odd number of negative edges.

P1: SBT
cuus984-net CUUS984-Easley 0 521 19533 1 November 30, 2009 16:2

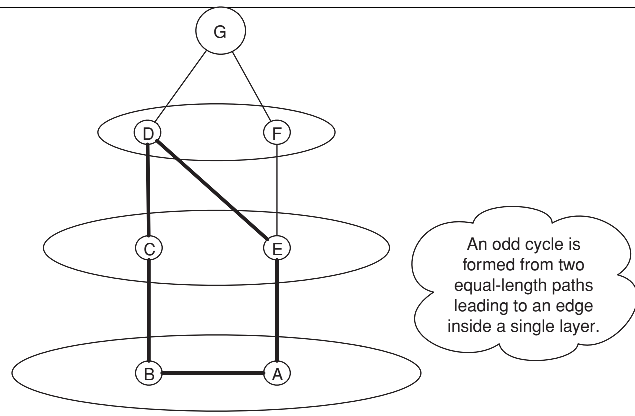

Figure 5.16. When we perform a breadth-first search of the reduced graph, there is either an edge connecting two nodes in the same layer or there isn't. If there isn't, then we can produce the desired division into X and Y by putting alternate layers in different sets. If there is such an edge (such as the edge joining A and B in the figure), then we can take two paths of the same length leading to the two ends of the edge, which together with the edge itself forms an odd cycle.

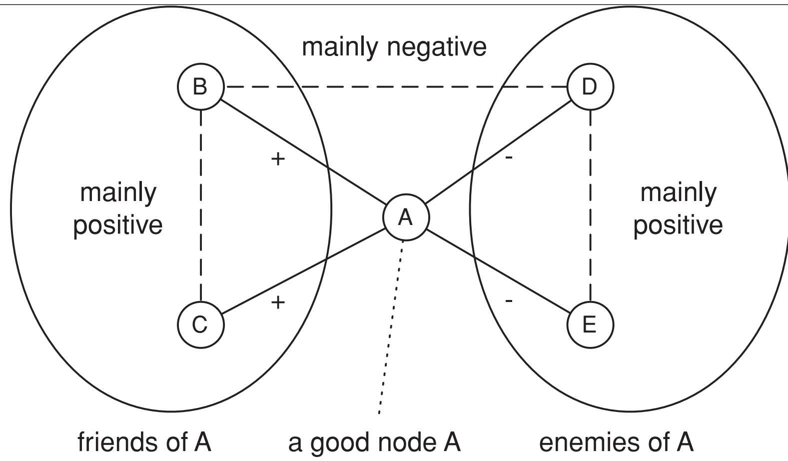

Figure 5.17. The characterization of approximately balanced complete graphs follows from an analysis similar to the proof of the original Cartwright-Harary Theorem. However, we have to be more careful in dividing the graph by first finding a "good" node that isn't involved in too many unbalanced triangles.

P1: SBT
cuus984-net CUUS984-Easley 0 521 19533 1 November 30, 2009 16:2

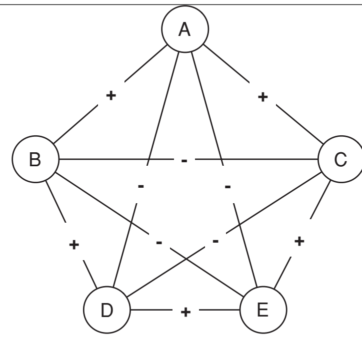

Figure 5.18. A network with five positive edges and five negative edges.

P1: SBT
cuus984-net CUUS984-Easley 0 521 19533 1 November 30, 2009 16:2

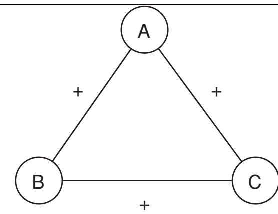

Figure 5.19. A 3-node social network in which all pairs of nodes know each other, and all pairs of nodes are friendly toward each other.

P1: SBT
cuus984-net CUUS984-Easley 0 521 19533 1 November 30, 2009 16:2

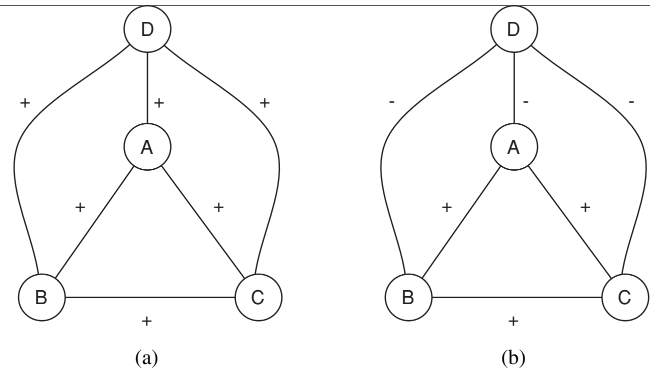

Figure 5.20. There are two distinct ways in which node *D* can join the social network from Figure 5.19 without becoming involved in any unbalanced triangles.

P1: SBT
cuus984-net CUUS984-Easley 0 521 19533 1 November 30, 2009 16:2

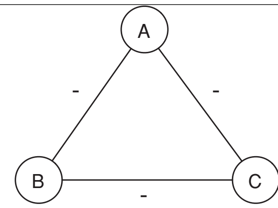

Figure 5.21. All three nodes are mutual enemies.

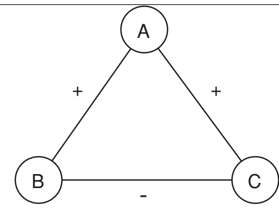

Figure 5.22. Node *A* is friends with nodes *B* and *C*, who are enemies with each other.

P1: SBT
cuus984-net CUUS984-Easley 0 521 19533 1 November 30, 2009 16:2

		Your Partner	
		Presentation	*Exam*
You	*Presentation*	90, 90	86, 92
	Exam	92, 86	88, 88

Figure 6.1. Exam or Presentation?

P1: SBT
cuus984-net CUUS984-Easley 0 521 19533 1 November 30, 2009 16:2

		Suspect 2	
		NC	C
Suspect 1	NC	$-1, -1$	$-10, 0$
	C	$0, -10$	$-4, -4$

Figure 6.2. Prisoner's Dilemma

P1: SBT
cuus984-net CUUS984-Easley 0 521 19533 1 November 30, 2009 16:2

		Athlete 2	
		Don't Use Drugs	*Use Drugs*
Athlete 1	*Don't Use Drugs*	3, 3	1, 4
	Use Drugs	4, 1	2, 2

Figure 6.3. Performance-Enhancing Drugs

		Your Partner: *Presentation*	Your Partner: *Exam*
You	*Presentation*	98, 98	94, 96
	Exam	96, 94	92, 92

Figure 6.4. Exam-or-Presentation Game with an easier exam.

		Firm 2	
		Low-Priced	*Upscale*
Firm 1	*Low-Priced*	.48, .12	.60, .40
	Upscale	.40, .60	.32, .08

Figure 6.5. Marketing Strategy

		Firm 2: A	Firm 2: B	Firm 2: C
Firm 1	A	4, 4	0, 2	0, 2
	B	0, 0	1, 1	0, 2
	C	0, 0	0, 2	1, 1

Figure 6.6. Three-Client Game

P1: SBT
cuus984-net CUUS984-Easley 0 521 19533 1 November 30, 2009 16:2

		Your Partner	
		PowerPoint	*Keynote*
You	*PowerPoint*	1, 1	0, 0
	Keynote	0, 0	1, 1

Figure 6.7. Coordination Game

		Your Partner	
		PowerPoint	*Keynote*
You	*PowerPoint*	1, 1	0, 0
	Keynote	0, 0	2, 2

Figure 6.8. Unbalanced Coordination Game

		Your Partner	
		PowerPoint	*Keynote*
You	*PowerPoint*	1, 2	0, 0
	Keynote	0, 0	2, 1

Figure 6.9. Battle of the Sexes

P1: SBT
cuus984-net CUUS984-Easley 0 521 19533 1 November 30, 2009 16:2

		Hunter 2	
		Hunt Stag	*Hunt Hare*
Hunter 1	*Hunt Stag*	4, 4	0, 3
	Hunt Hare	3, 0	3, 3

Figure 6.10. Stag Hunt

		Your Partner: *Presentation*	Your Partner: *Exam*
You	*Presentation*	90, 90	82, 88
	Exam	88, 82	88, 88

Figure 6.11. Exam-or-Presentation Game (Stag Hunt version)

		Animal 2	
		D	H
Animal 1	D	3, 3	1, 5
	H	5, 1	0, 0

Figure 6.12. Hawk-Dove Game

		Your Partner	
		Presentation	*Exam*
You	*Presentation*	90, 90	86, 92
	Exam	92, 86	76, 76

Figure 6.13. Exam or Presentation? (Hawk-Dove version)

		Player 2: H	Player 2: T
Player 1	H	$-1, +1$	$+1, -1$
	T	$+1, -1$	$-1, +1$

Figure 6.14. Matching Pennies

P1: SBT
cuus984-net CUUS984-Easley 0 521 19533 1 November 30, 2009 16:2

		Defense	
		Defend Pass	*Defend Run*
Offense	*Pass*	0, 0	10, −10
	Run	5, −5	0, 0

Figure 6.15. Run-Pass Game

		Goalie	
		L	R
Kicker	L	$0.58, -0.58$	$0.95, -0.95$
	R	$0.93, -0.93$	$0.70, -0.70$

Figure 6.16. The Penalty-Kick Games (from empirical data [331]).

		Your Partner *PowerPoint*	Your Partner *Keynote*
You	*PowerPoint*	1, 1	0, 0
You	*Keynote*	0, 0	2, 2

Figure 6.17. Unbalanced Coordination Game

P1: SBT
cuus984-net CUUS984-Easley 0 521 19533 1 November 30, 2009 16:2

		Your Partner: *Presentation*	Your Partner: *Exam*
You	*Presentation*	90, 90	86, 92
	Exam	92, 86	88, 88

Figure 6.18. Exam or Presentation?

P1: SBT
cuus984-net CUUS984-Easley 0 521 19533 1 November 30, 2009 16:2

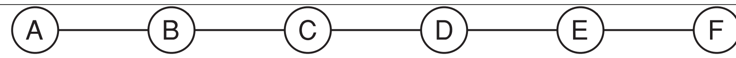

Figure 6.19. In the Facility Location Game, each player has strictly dominated strategies but no dominant strategy.

		Firm 2 B	Firm 2 D	Firm 2 F
Firm 1	A	1, 5	2, 4	3, 3
Firm 1	C	4, 2	3, 3	4, 2
Firm 1	E	3, 3	2, 4	5, 1

Figure 6.20. Facility Location Game

P1: SBT
cuus984-net CUUS984-Easley 0 521 19533 1 November 30, 2009 16:2

		Firm 2	
		B	D
Firm 1	C	4, 2	3, 3
	E	3, 3	2, 4

Figure 6.21. Smaller Facility Location Game

		Firm 2
		D
Firm 1	C	3, 3

Figure 6.22. Even smaller Facility Location Game

P1: SBT
cuus984-net CUUS984-Easley 0 521 19533 1 November 30, 2009 16:2

		Hunter 2	
		Hunt Stag	*Hunt Hare*
Hunter 1	*Hunt Stag*	3, 3	0, 3
	Hunt Hare	3, 0	3, 3

Figure 6.23. Stag Hunt: A version with a weakly dominated strategy

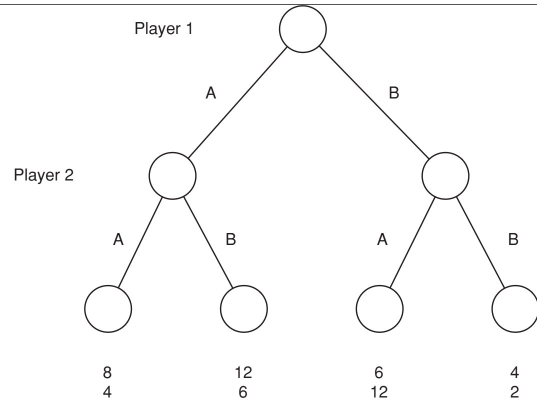

Figure 6.24. A simple game in extensive form.

P1: SBT
cuus984-net CUUS984-Easley 0 521 19533 1 November 30, 2009 16:2

		Firm 2			
		AA, AB	AA, BB	BA, AB	BA, BB
Firm 1	A	8, 4	8, 4	12, 6	12, 6
	B	6, 12	4, 2	6, 12	4, 2

Figure 6.25. Conversion to normal form.

P1: SBT
cuus984-net CUUS984-Easley 0 521 19533 1 November 30, 2009 16:2

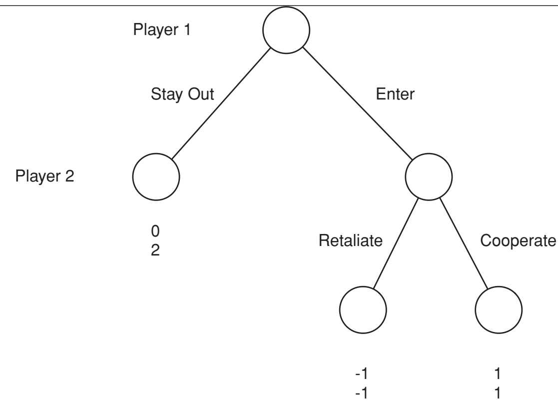

Figure 6.26. Extensive-form representation of the Market Entry Game.

P1: SBT
cuus984-net CUUS984-Easley 0 521 19533 1 November 30, 2009 16:2

		Firm 2	
		R	C
Firm 1	S	0, 2	0, 2
	E	−1, −1	1, 1

Figure 6.27. Normal Form of the Market Entry Game

Player B

		L	M	R
Player A	t	0, 3	6, 2	1, 1
	m	2, 3	0, 1	7, 0
	b	5, 3	4, 2	3, 1

Figure 6.28. Payoff Matrix

		Player B	
		L	*R*
Player A	*U*	1, 2	3, 2
	D	2, 4	0, 2

UnFig01-page211.

		Player B		
		L	*M*	*R*
	U	1, 1	2, 3	1, 6
Player A	*M*	3, 4	5, 5	2, 2
	D	1, 10	4, 7	0, 4

UnFig02-page211.

		Player B	
		L	*R*
Player A	*U*	2, 15	4, 20
	D	6, 6	10, 8

UnFig03-page212.

		Player B	
		L	R
Player A	U	3, 5	4, 3
	D	2, 1	1, 6

UnFig04-page212.

P1: SBT
cuus984-net CUUS984-Easley 0 521 19533 1 November 30, 2009 16:2

		Player B	
		L	*R*
Player A	*U*	1, 1	4, 2
	D	3, 3	2, 2

UnFig05-page212.

P1: SBT
cuus984-net CUUS984-Easley 0 521 19533 1 November 30, 2009 16:2

		Player B	
		L	R
Player A	U	1, 1	3, 2
	D	0, 3	4, 4

UnFig06-page213.

		Player B	
		L	*R*
Player A	*U*	5, 6	0, 10
	D	4, 4	2, 2

UnFig07-page213.

P1: SBT
cuus984-net CUUS984-Easley 0 521 19533 1 November 30, 2009 16:2

		Player B	
		L	*R*
Player A	*U*	1, 1	0, 0
	D	0, 0	4, 4

UnFig08-page213.

P1: SBT
cuus984-net CUUS984-Easley 0 521 19533 1 November 30, 2009 16:2

		Player B	
		L	*R*
Player A	*U*	8, 4	5, 5
	D	3, 3	4, 8

UnFig09-page214.

		Player B	
		L	R
Player A	U	$0, 0$	$-1, 1$
	D	$-1, 1$	$2, -2$

UnFig10-page214.

		Player B	
		L	*R*
Player A	*U*	3, 3	1, 2
	D	2, 1	3, 0

UnFig11-page214.

		Player B		
		L	*M*	*R*
Player A	*U*	2, 4	2, 1	3, 2
	D	1, 2	3, 3	2, 4

UnFig12-page215.

		Player B	
		L	R
Player A	U	2, 4	3, 2
	D	1, 2	2, 4

UnFig13-page215.

P1: SBT
cuus984-net CUUS984-Easley 0 521 19533 1 November 30, 2009 16:2

		Player B	
		L	R
Player A	U	1, 1	1, 1
	D	0, 0	2, 1

UnFig14-page216.

P1: SBT
cuus984-net CUUS984-Easley 0 521 19533 1 November 30, 2009 16:2

		Player B	
		L	*R*
Player A	*U*	4, 4, 4	0, 0, 1
	D	0, 2, 1	2, 1, 0

UnFig15-page217.

P1: SBT
cuus984-net CUUS984-Easley 0 521 19533 1 November 30, 2009 16:2

		Player B	
		L	*R*
Player A	*U*	2, 0, 0	1, 1, 1
	D	1, 1, 1	2, 2, 2

UnFig16-page217.

P1: SBT
cuus984-net CUUS984-Easley 0 521 19533 1 November 30, 2009 16:2

		Beetle 2	
		Small	*Large*
Beetle 1	*Small*	5, 5	1, 8
	Large	8, 1	3, 3

Figure 7.1. The Body-Size Game

		Virus 2	
		Φ6	ΦH2
Virus 1	Φ6	1.00, 1.00	0.65, 1.99
	ΦH2	1.99, 0.65	0.83, 0.83

Figure 7.2. The Virus Game

P1: SBT
cuus984-net CUUS984-Easley 0 521 19533 1 November 30, 2009 16:2

		Organism 2	
		S	T
Organism 1	S	a, a	b, c
	T	c, b	d, d

Figure 7.3. General Symmetric Game

		Hunter 2	
		Hunt Stag	*Hunt Hare*
Hunter 1	*Hunt Stag*	4, 4	0, 3
	Hunt Hare	3, 0	3, 3

Figure 7.4. Stag Hunt

		Hunter 2	
		Hunt Stag	*Hunt Hare*
Hunter 1	*Hunt Stag*	4, 4	0, 4
	Hunt Hare	4, 0	3, 3

Figure 7.5. Stag Hunt: A version with added benefit from hunting hare alone

P1: SBT
cuus984-net CUUS984-Easley 0 521 19533 1 November 30, 2009 16:2

		Animal 2	
		D	H
Animal 1	D	3, 3	1, 5
	H	5, 1	0, 0

Figure 7.6. Hawk-Dove Game

P1: SBT
cuus984-net CUUS984-Easley 0 521 19533 1 November 30, 2009 16:2

		Virus 2	
		Φ6	ΦH2
Virus 1	Φ6	1.00, 1.00	0.65, 1.99
	ΦH2	1.99, 0.65	0.50, 0.50

Figure 7.7. The Virus Game: Hypothetical payoffs with stronger fitness penalties to ΦH2.

P1: SBT
cuus984-net CUUS984-Easley 0 521 19533 1 November 30, 2009 16:2

		Player B x	Player B y
Player A	x	2, 2	0, 0
Player A	y	0, 0	1, 1

UnFig01-page235.

		Player B	
		x	y
Player A	x	4, 4	3, 5
	y	5, 3	5, 5

UnFig02-page236.

		Player B	
		X	Y
Player A	X	a, a	b, c
	Y	c, b	d, d

UnFig03-page236.

		Player B	
		X	Y
Player A	X	1, 1	2, x
	Y	x, 2	3, 3

UnFig04-page236.

		Player B	
		X	Y
Player A	X	a, a	b, c
	Y	c, b	d, d

UnFig05-page237.

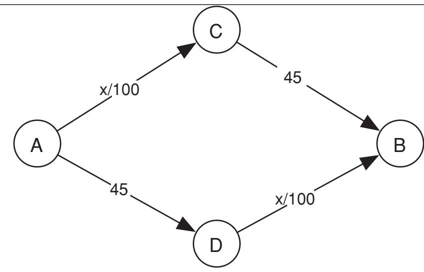

Figure 8.1. A highway network, with each edge labeled by its travel time (in minutes) when there are x cars using it. When 4000 cars need to get from A to B, they divide evenly over the two routes at equilibrium, and the travel time is 65 minutes.

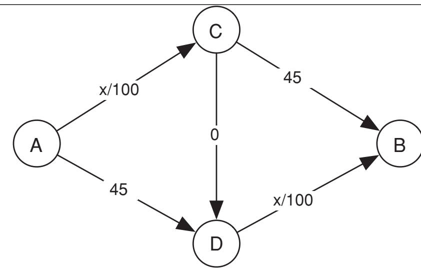

Figure 8.2. The highway network from the previous figure, after a very fast edge has been added from *C* to *D*. Although the highway system has been "upgraded," the travel time at equilibrium is now 80 minutes, since all cars use the route through *C* and *D*.

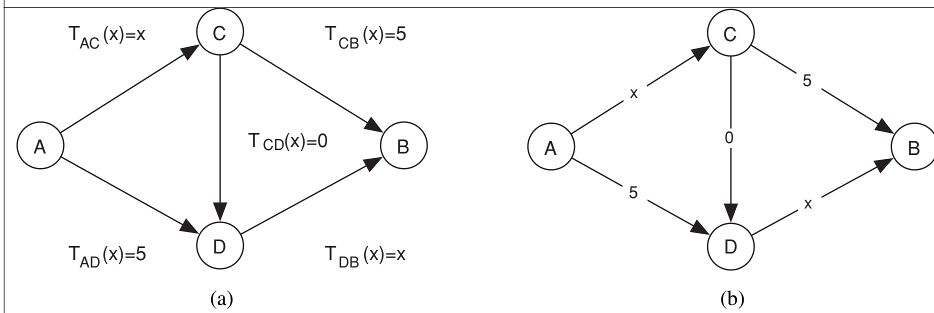

Figure 8.3. A network annotated with the travel-time function on each edge.

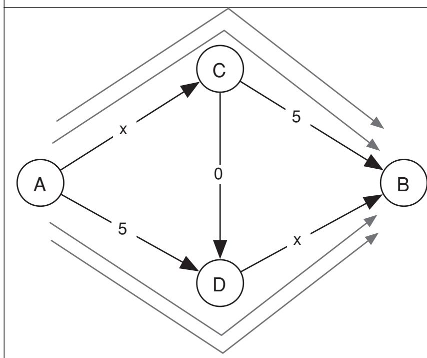

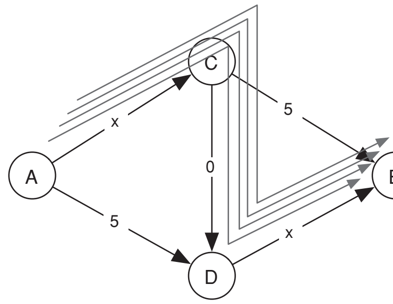

Figure 8.4. A version of Braess's Paradox: In the socially optimal traffic pattern (on the left), the social cost is 28, while in the unique Nash equilibrium (on the right), the social cost is 32.

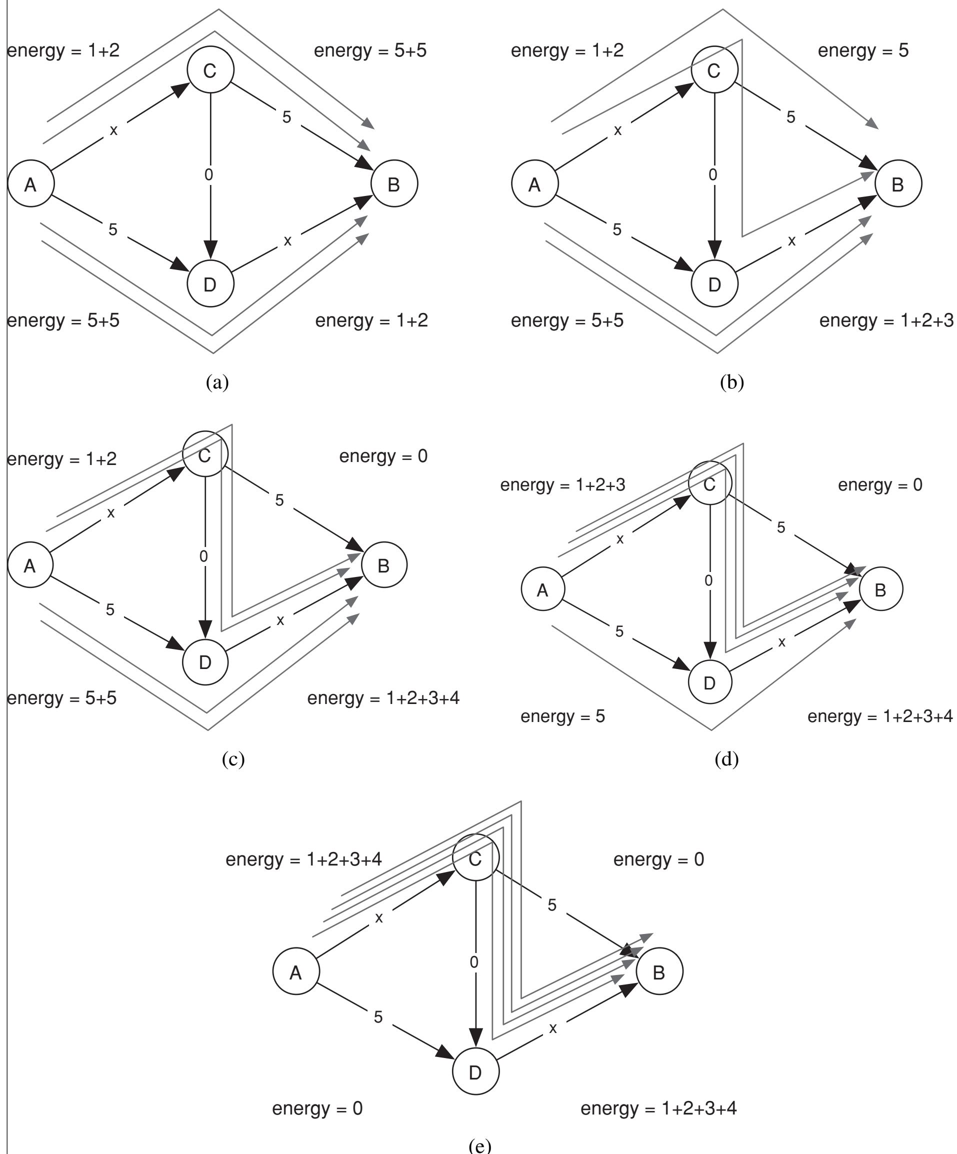

Figure 8.5. We can track the progress of best-response dynamics in the traffic game by watching how the potential energy changes.

P1: SBT
cuus984-net CUUS984-Easley 0 521 19533 1 November 30, 2009 16:2

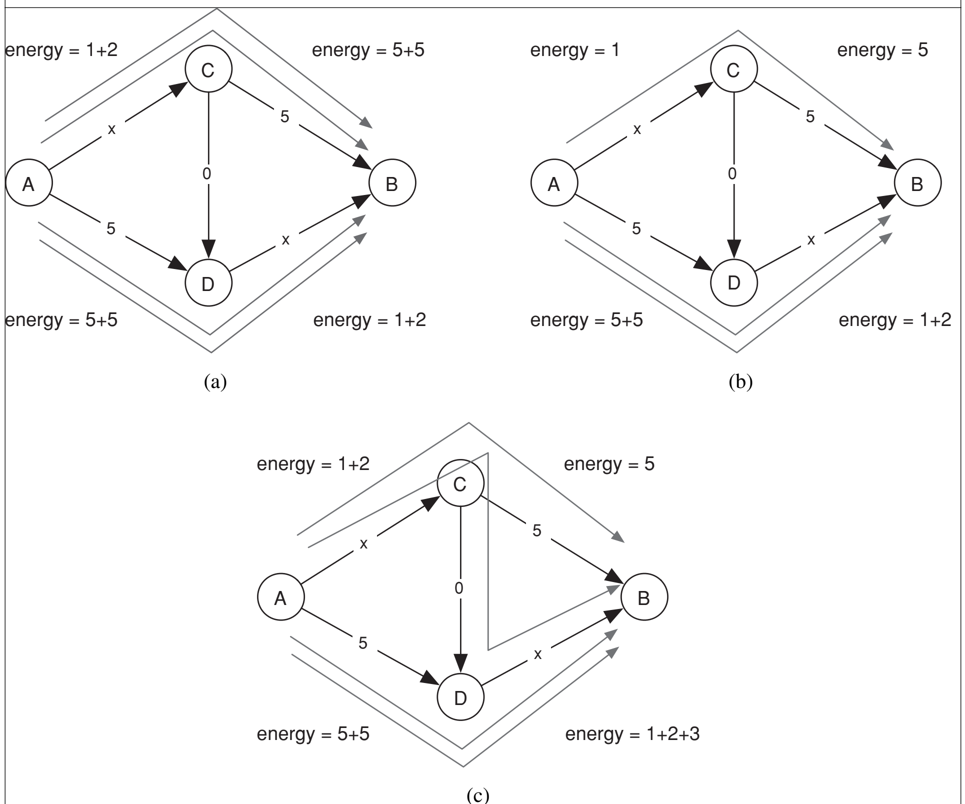

Figure 8.6. When a driver abandons one path in favor of another, the change in potential energy is exactly the improvement in the driver's travel time.

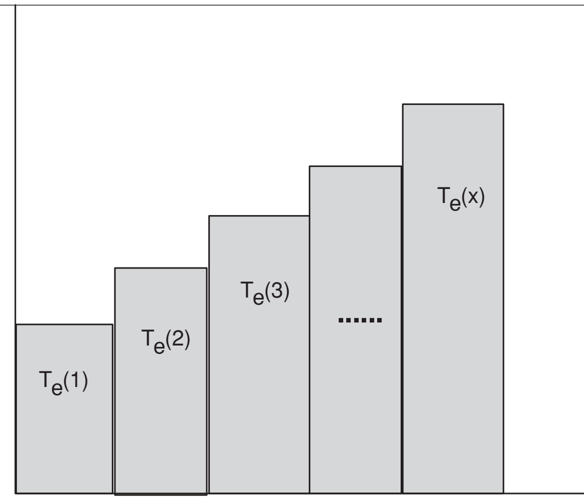

Figure 8.7. The potential energy is the area under the shaded rectangles; it is always at least half the total travel time, which is the area inside the enclosing rectangle.

P1: SBT
cuus984-net CUUS984-Easley 0 521 19533 1 November 30, 2009 16:2

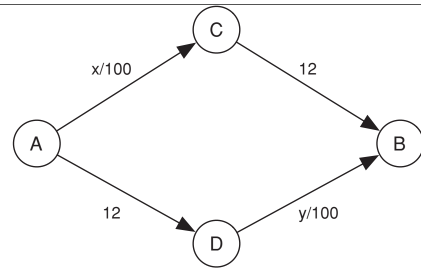

Figure 8.8. Traffic Network.

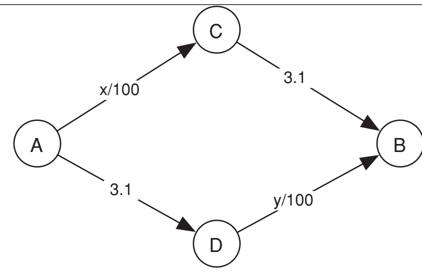

Figure 8.9. Traffic Network

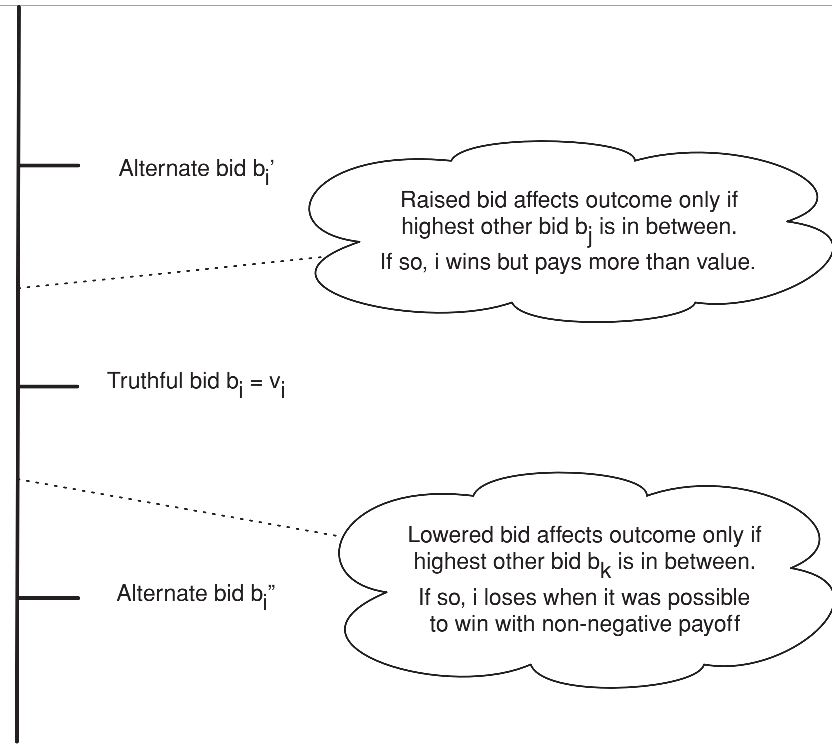

Figure 9.1. If bidder *i* deviates from a truthful bid in a second-price auction, the payoff is only affected if the change in bid changes the win/loss outcome.

P1: SBT
cuus984-net CUUS984-Easley 0 521 19533 1 November 30, 2009 16:2

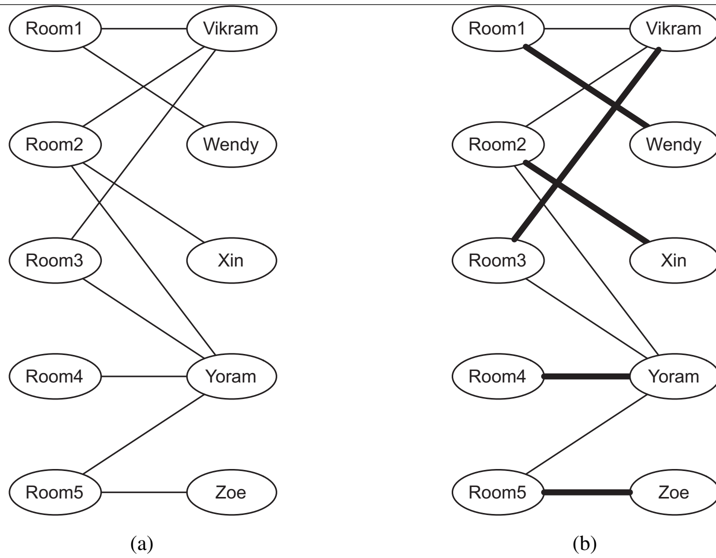

Figure 10.1. (a) An example of a bipartite graph. (b) A perfect matching in this graph, indicated via the dark edges.

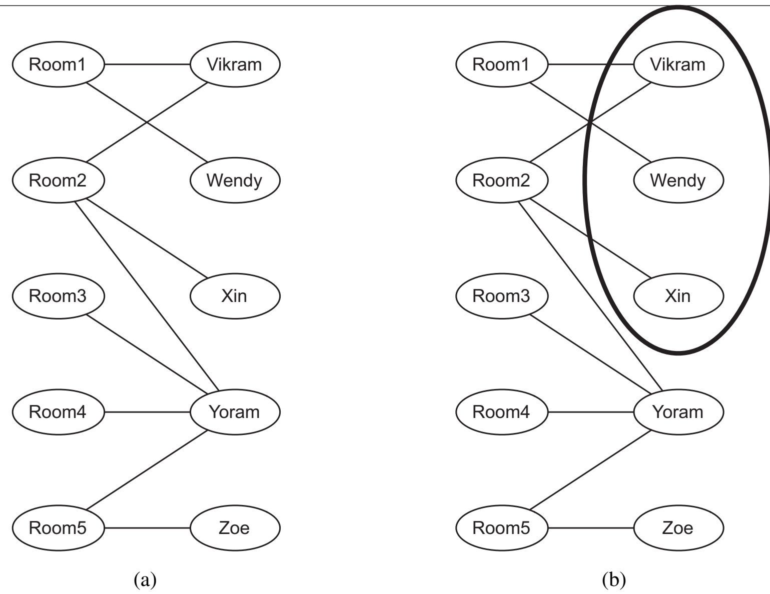

Figure 10.2. (a) A bipartite graph with no perfect matching. (b) A constricted set demonstrating there is no perfect matching.

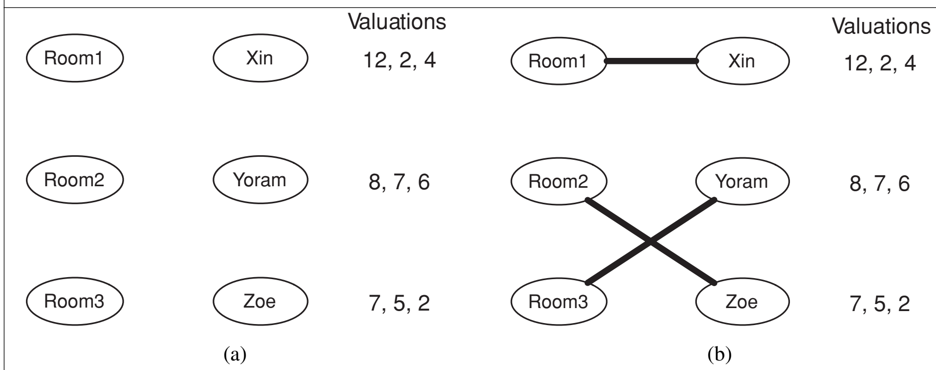

Figure 10.3. (a) A set of valuations. Each person's valuations for the objects appears as a list next to them. (b) An optimal assignment with respect to these valuations.

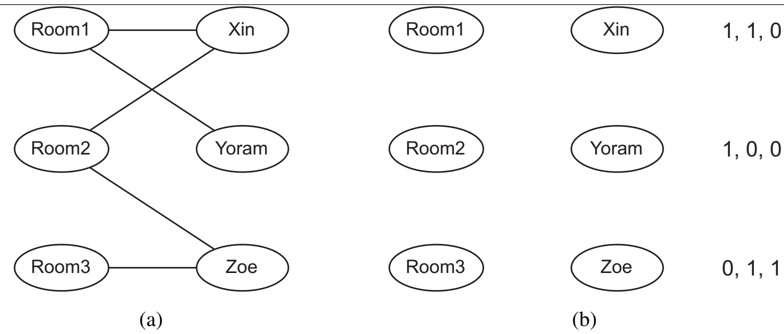

Figure 10.4. (a) A bipartite graph in which we want to search for a perfect matching. (b) A corresponding set of valuations for the same nodes so that finding the optimal assignment lets us determine whether there is a perfect matching in the original graph.

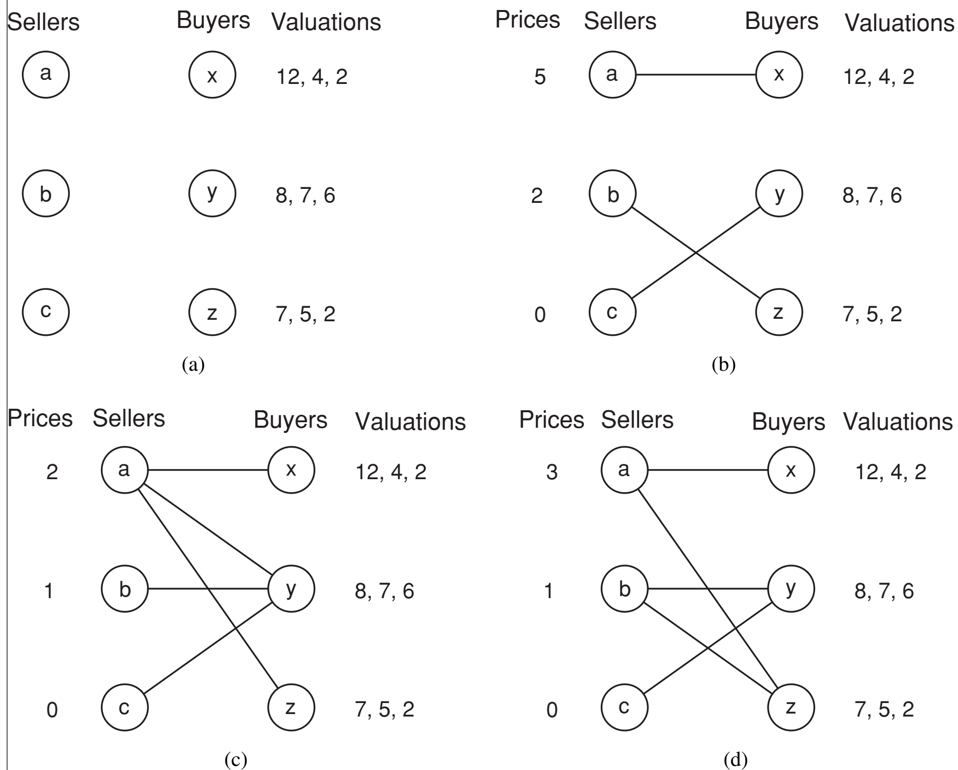

Figure 10.5. (a) Three sellers (a, b, and c) and three buyers (x, y, and z). For each buyer node, the valuations for the houses of the respective sellers appear in a list next to the node. (b) Each buyer creates a link to her preferred seller. The resulting set of edges is the preferred-seller graph for this set of prices. (c) The preferred-seller graph for prices 2, 1, 0. (d) The preferred-seller graph for prices 3, 1, 0.

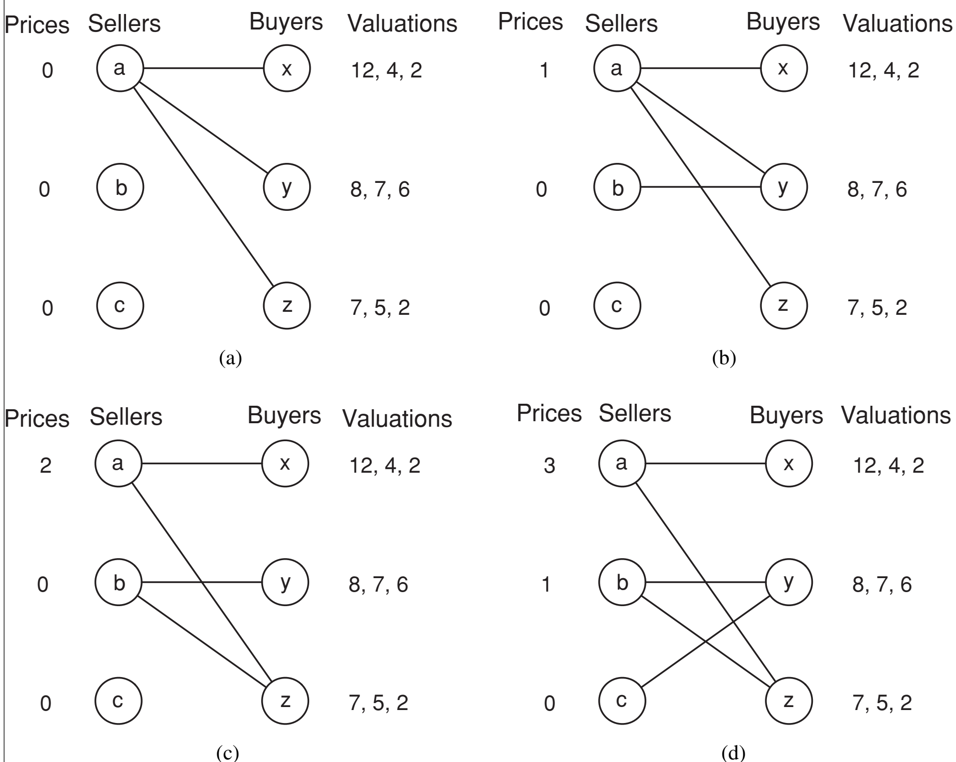

Figure 10.6. The auction procedure applied to the example from Figure 10.5. Each separate picture shows steps (i) and (ii) of successive rounds, in which the preferred-seller graph for that round is constructed.

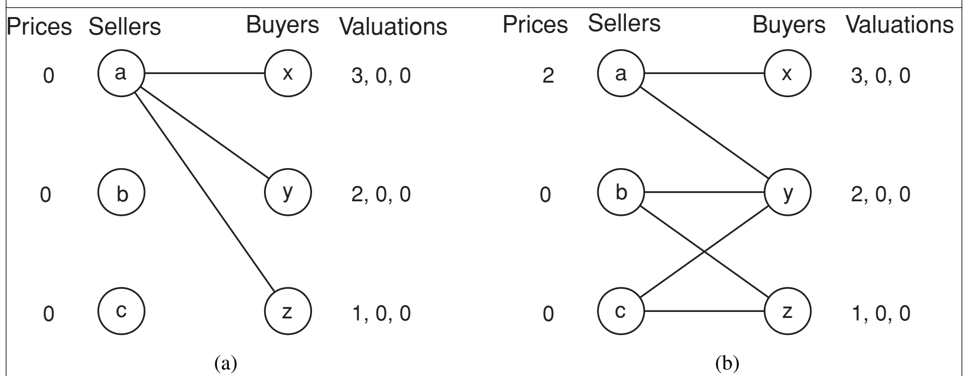

Figure 10.7. A single-item auction can be represented by the bipartite graph model: the item is represented by one seller node, and then there are additional seller nodes for which all buyers have 0 valuation. (a) The start of the bipartite graph auction. (b) The end of the bipartite graph auction, when buyer x gets the item at the valuation of buyer y.

P1: SBT
cuus984-net CUUS984-Easley 0 521 19533 1 November 30, 2009 16:2

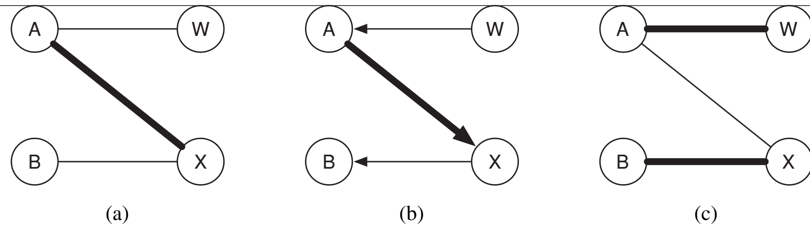

Figure 10.8. (a) A matching that does not have maximum size. (b) What a matching does not have maximum size, we can try to find an *augmenting path* that connects unmatched nodes on opposite sides while alternating between non-matching and matching edges. (c) If we then swap the edges on this path — taking out the matching edges on the path and replacing them with the non-matching edges — then we obtain a larger matching.

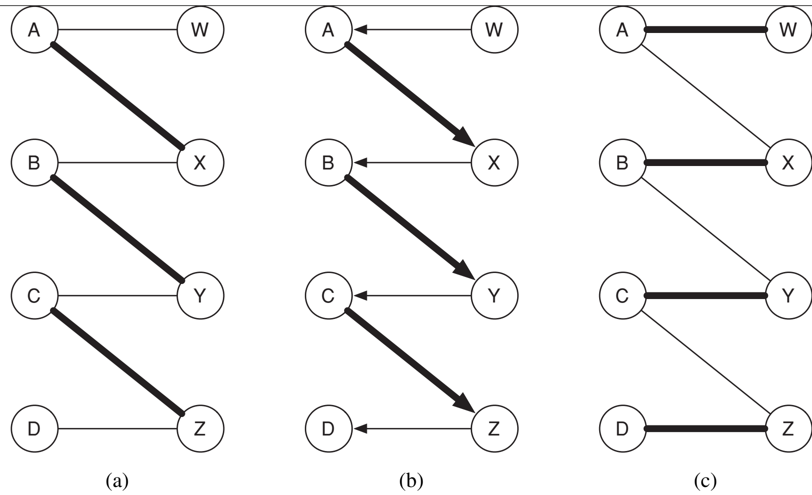

Figure 10.9. The principle used in Figure 10.8 can be applied to larger bipartite graphs as well, sometimes producing long augmenting paths.

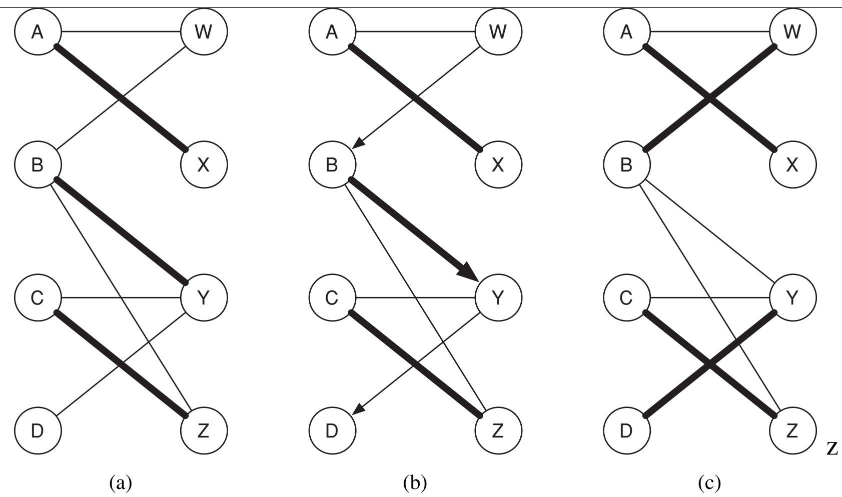

Figure 10.10. In more complex graphs, finding an augmenting path can require a more careful search, in which choices lead to "dead ends" while others connect two unmatched nodes.

P1: SBT
cuus984-net CUUS984-Easley 0 521 19533 1 November 30, 2009 16:2

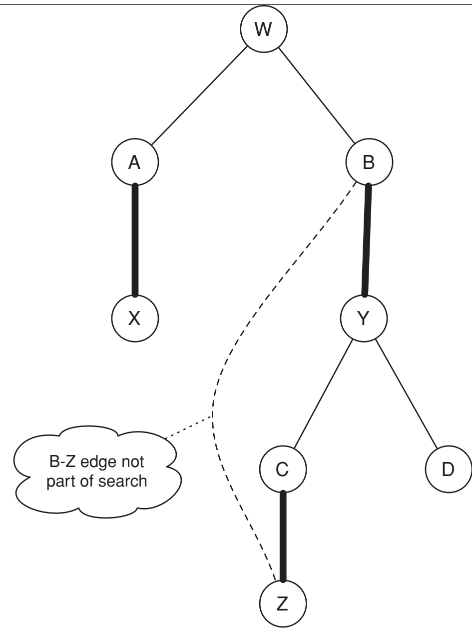

Figure 10.11. In an alternating breadth-first search, one constructs layers that alternately use non-matching and matching edges; if a unmatched node is ever reached, this results in an augmenting path.

P1: SBT
cuus984-net CUUS984-Easley 0 521 19533 1 November 30, 2009 16:2

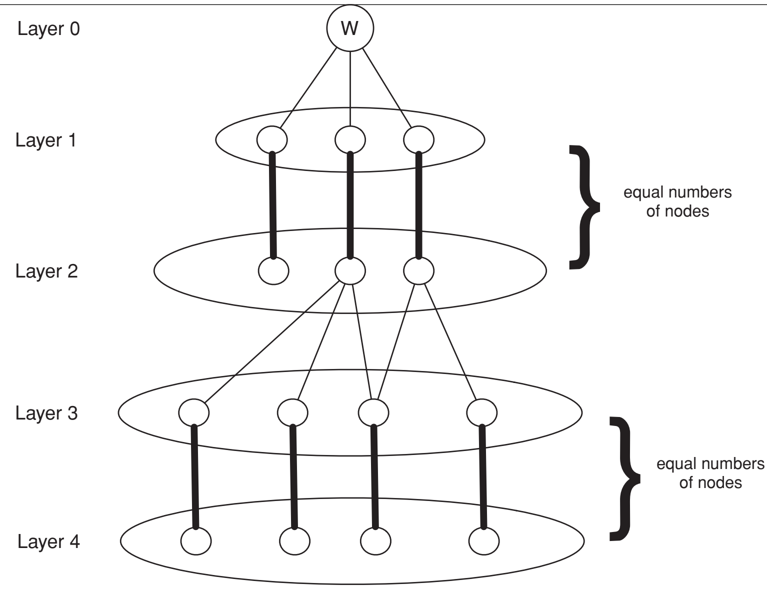

Figure 10.12. A schematic view of alternating breadth-first search, which produces pairs of layers of equal size.

P1: SBT
cuus984-net CUUS984-Easley 0 521 19533 1 November 30, 2009 16:2

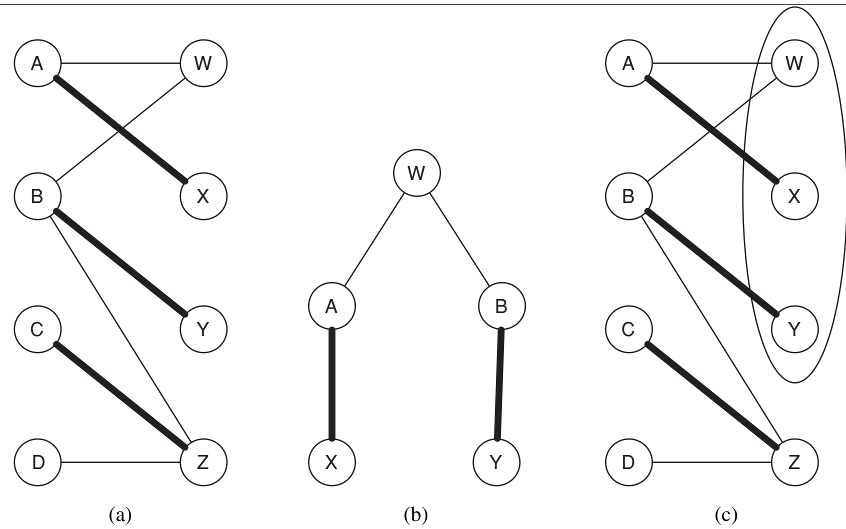

Figure 10.13. (a) A matching that has maximum size, but is not perfect. (b) For such a matching, the search for an augment path using alternating breadth-first search will fail. (c) The failure of this search exposes a constricted set: the set of nodes belonging to the even layers.

P1: SBT
cuus984-net CUUS984-Easley 0 521 19533 1 November 30, 2009 16:2

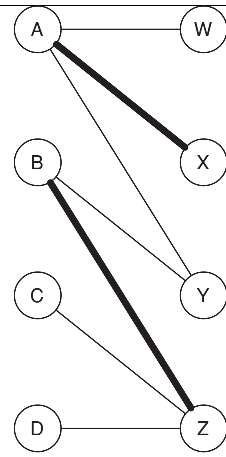

Figure 10.14. If the alternating breadth-first search fails from *any* node on the right-hand side, this is enough to expose a constricted set and hence prove there is no perfect matching. However, it is still possible that an alternating breadth-first search could still succeed from some other node. (In this case, the search from W would fail, but the search from Y would succeed.)

Figure 10.15. The map for a parking-space market. (Image from Google Maps, http://maps.google.com/)

P1: SBT
cuus984-net CUUS984-Easley 0 521 19533 1 November 30, 2009 16:2

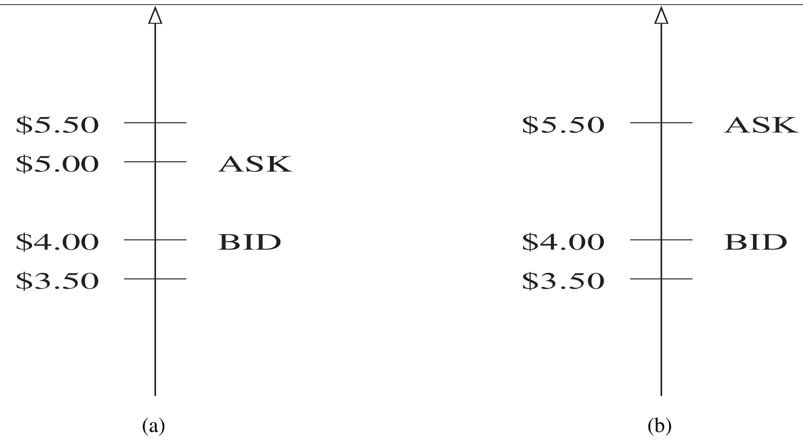

Figure 11.1. (a) A book of limit orders for a stock with a bid of $4 and an ask of $5. (b) A book of limit orders for a stock with a bid of $4 and an ask of $5.50.

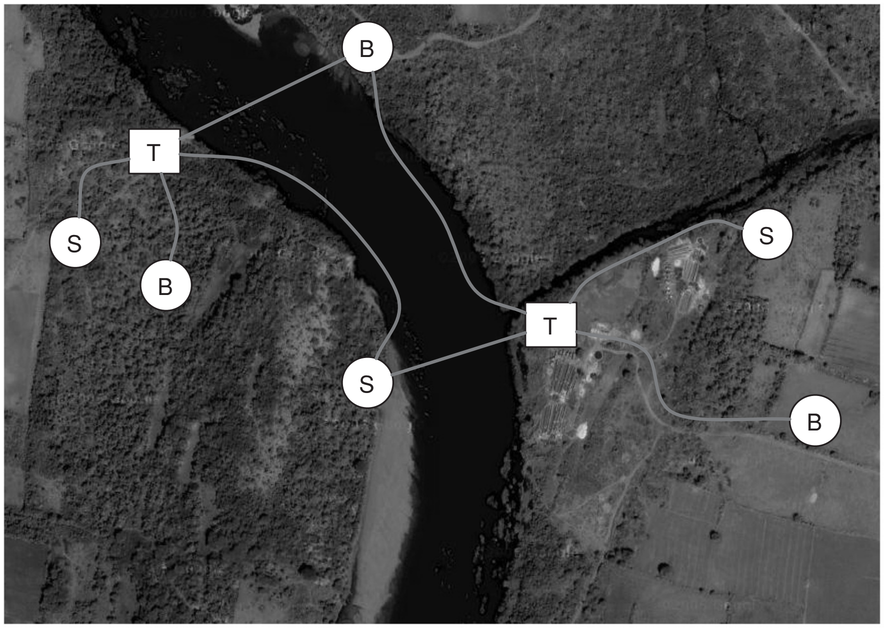

Figure 11.2. Trading networks for agricultural markets can be based on geographic constraints, giving certain buyers (nodes labeled B) and sellers (nodes labeled S) greater access to traders (nodes labeled T).

P1: SBT
cuus984-net CUUS984-Easley 0 521 19533 1 November 30, 2009 16:2

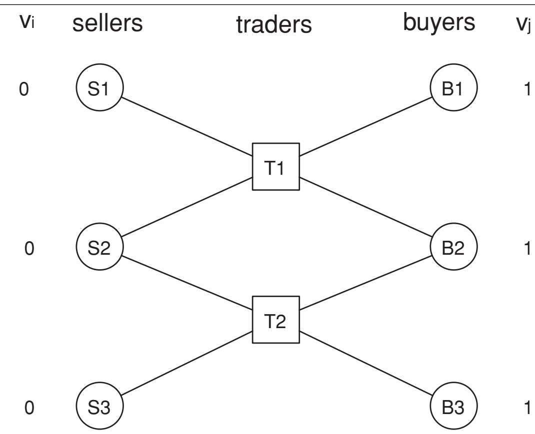

Figure 11.3. A standardized view of the trading network from Figure 11.2: Sellers are represented by circles on the left, buyers are represented by circles on the right, and traders are represented by squares in the middle. The value that each seller and buyer places on a copy of the good is written next to the respective node that represents them.

(a) (b)

Figure 11.4. (a) Each trader posts bid prices to the sellers he is connected to, and ask prices to the buyers he is connected to. (b) This in turn determines a flow of goods, as sellers and buyers each choose the offer that is most favorable to them.

P1: SBT
cuus984-net CUUS984-Easley 0 521 19533 1 November 30, 2009 16:2

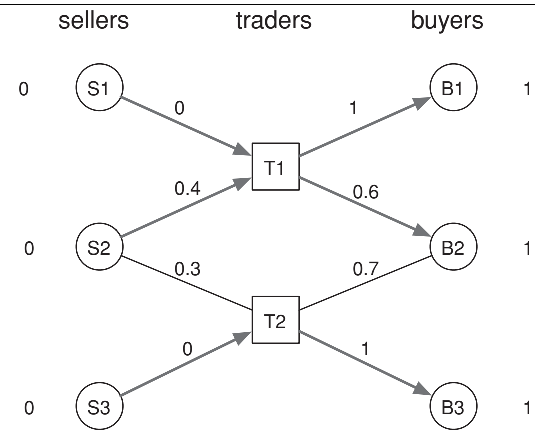

Figure 11.5. Relative to the choice of strategies in Figure 11.4(b), trader $T1$ has a way to improve his payoff by undercutting $T2$ and performing the transaction that moves $S2$'s copy of the good to $B2$.

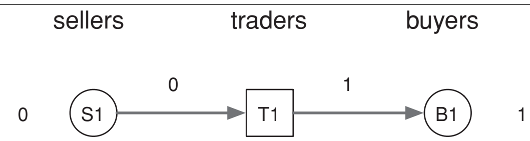

Figure 11.6. A simple example of a trading network in which the trader has a monopoly and extracts all of the surplus from trade.

P1: SBT
cuus984-net CUUS984-Easley 0 521 19533 1 November 30, 2009 16:2

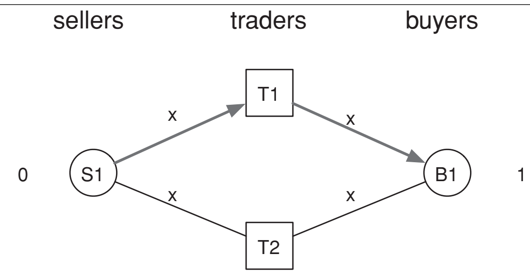

Figure 11.7. A trading network in which there is perfect competition between the two traders, T1 and T2. The equilibrium has a common bid and ask of x, where x can be any real number between 0 and 1.

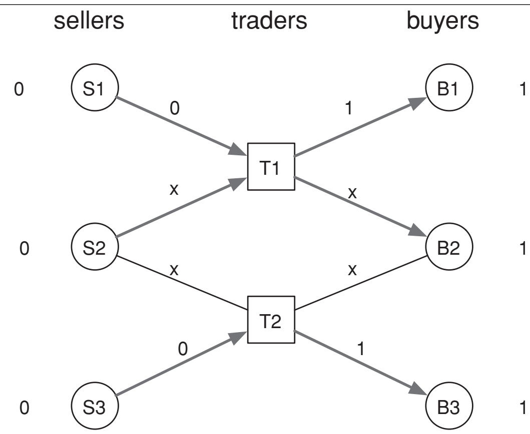

Figure 11.8. The equilibria for the trading network from Section 11.2. This network can be analyzed using the ideas from the simpler networks representing monopoly and perfect competition.

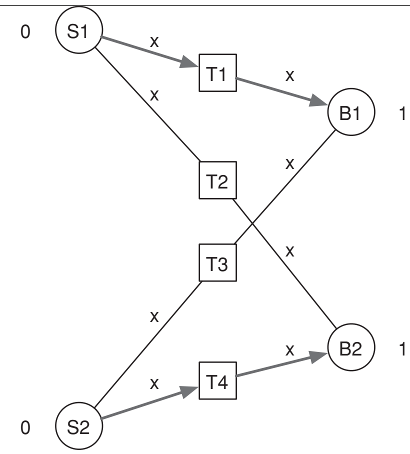

Figure 11.9. A form of *implicit perfect competition*: all bid/ask spreads will be zero in equilibrium, even though no trader directly "competes" with any other trader for the same buyer-seller pair.

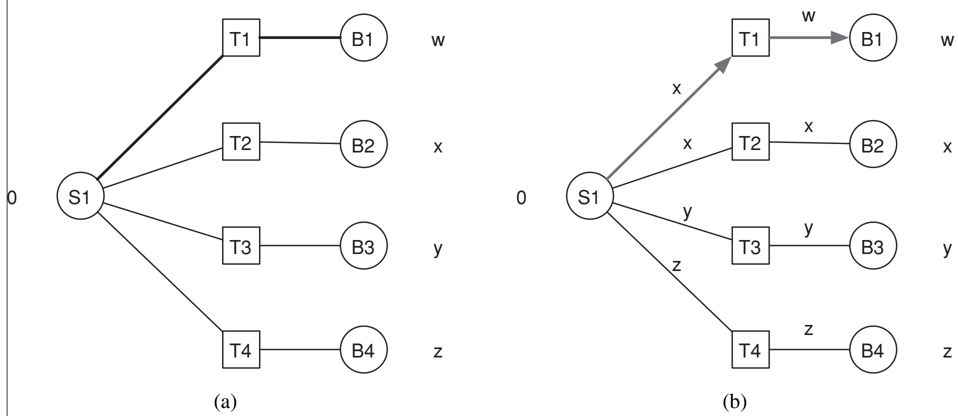

Figure 11.10. (a) A single-item auction can be represented using a trading network. (b) Equilibrium prices and flow of goods. The resulting equilibrium implements the second-price rule from Chapter 9.

P1: SBT
cuus984-net CUUS984-Easley 0 521 19533 1 November 30, 2009 16:2

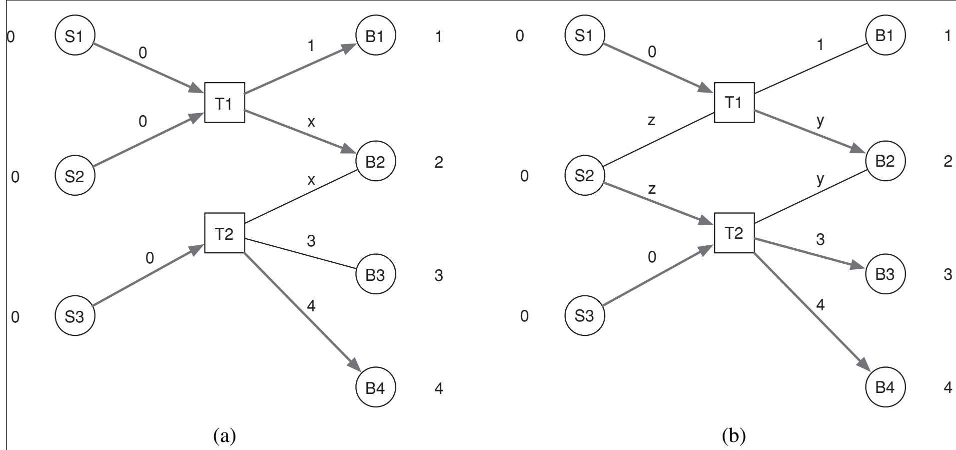

Figure 11.11. (a) Equilibrium before the new $S2$-$T2$ link is added. (b) When the $S2$-$T2$ edge is added, a number of changes take place in the equilibrium. Among these changes is the fact that buyer $B1$ no longer gets a copy of the good, and $B3$ gets one instead.

P1: SBT
cuus984-net CUUS984-Easley 0 521 19533 1 November 30, 2009 16:2

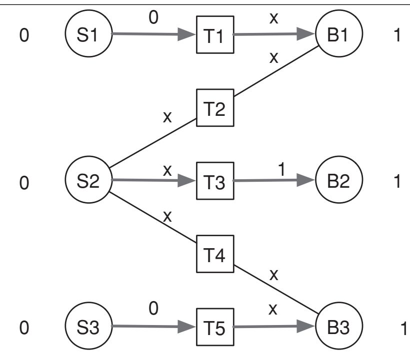

Figure 11.12. Whether a trader can make a profit may depend on the choice of equilibrium. In this trading network, when $x = 1$, traders $T1$ and $T5$ make a profit, while when $x = 0$, only trader $T3$ makes a profit.

P1: SBT
cuus984-net CUUS984-Easley 0 521 19533 1 November 30, 2009 16:2

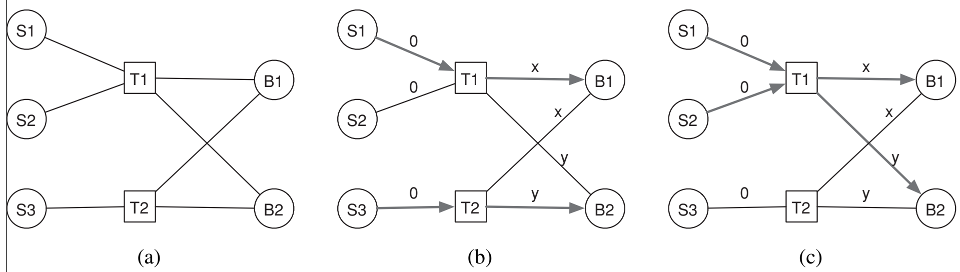

Figure 11.13. Despite a form of monopoly power in this network, neither trader can make a profit in any equilibrium.

P1: SBT
cuus984-net CUUS984-Easley 0 521 19533 1 November 30, 2009 16:2

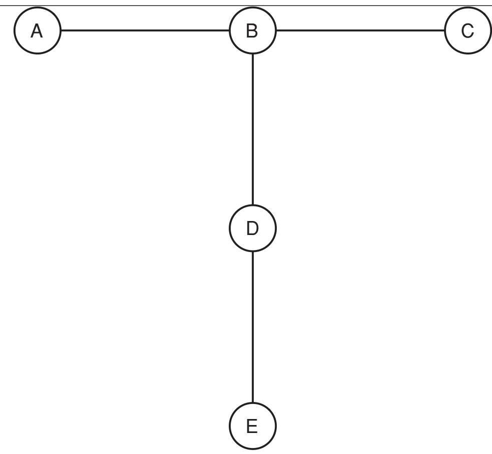

Figure 12.1. A social network on five people, with node *B* occupying an intuitively powerful position.

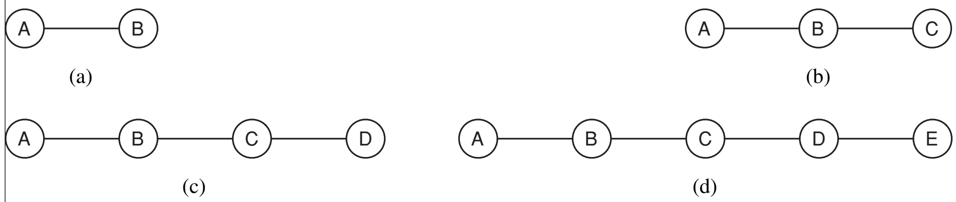

Figure 12.2. Paths of lengths 2, 3, 4, and 5 form instructive examples of different phenomena in exchange networks.

P1: SBT
cuus984-net CUUS984-Easley 0 521 19533 1 November 30, 2009 16:2

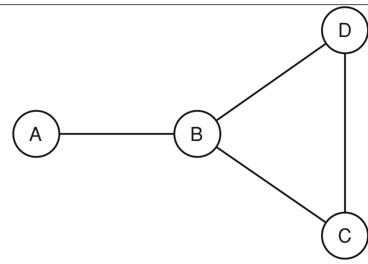

Figure 12.3. An exchange network with a weak power advantage for node B.

P1: SBT
cuus984-net CUUS984-Easley 0 521 19533 1 November 30, 2009 16:2

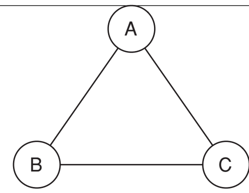

Figure 12.4. An exchange network in which negotiations never stabilize.

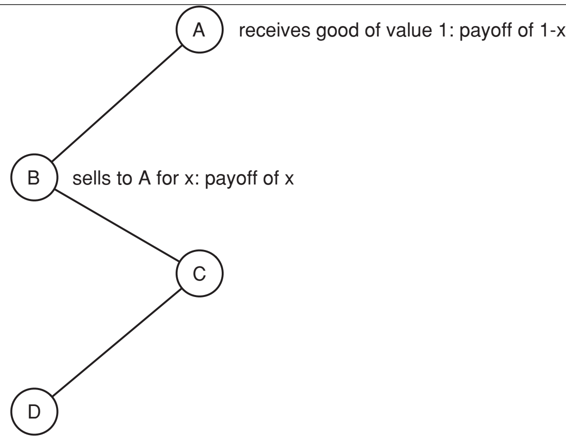

Figure 12.5. An exchange network built from the 4-node path can also be viewed as a buyer-seller network with 2 sellers and 2 buyers.

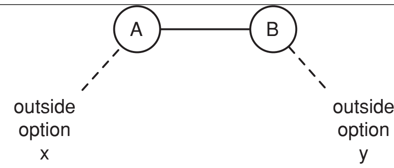

Figure 12.6. Two nodes bargaining with outside options.

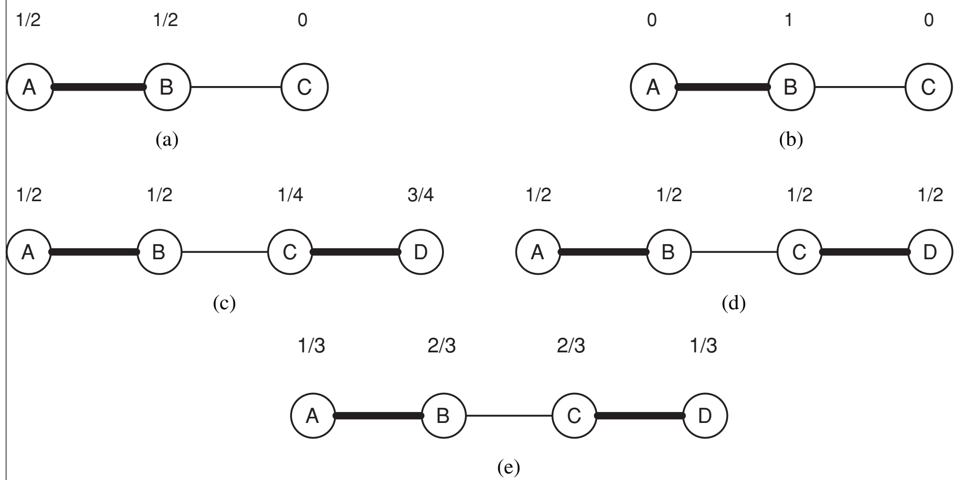

Figure 12.7. Some examples of stable and unstable outcomes of network exchange on the 3-node path and the 4-node path. The darkened edges constitute matchings showing who exchanges with whom, and the numbers above the nodes represent the values.

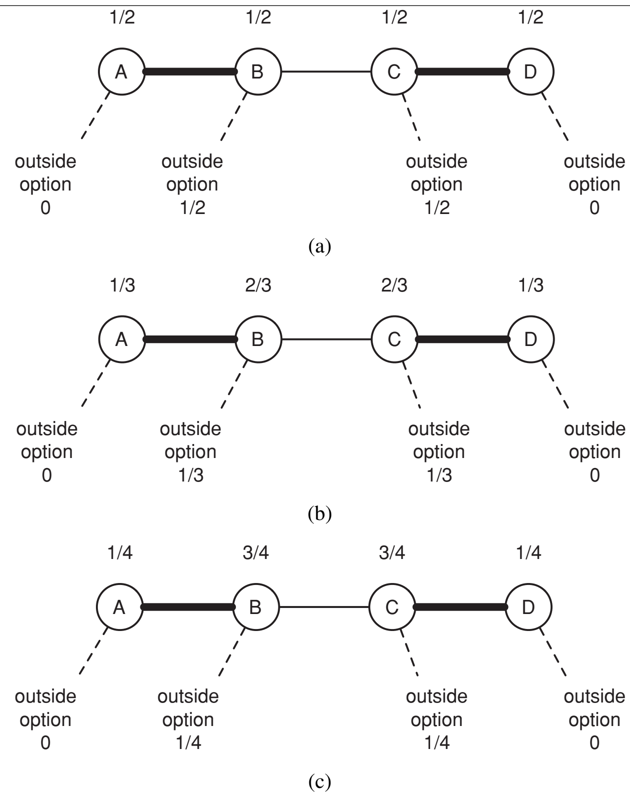

Figure 12.8. The difference between balanced and unbalanced outcomes.

P1: SBT
cuus984-net CUUS984-Easley 0 521 19533 1 November 30, 2009 16:2

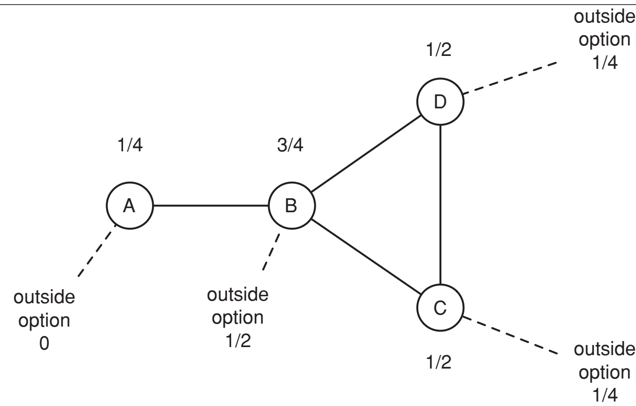

Figure 12.9. A balanced outcome on the stem graph.

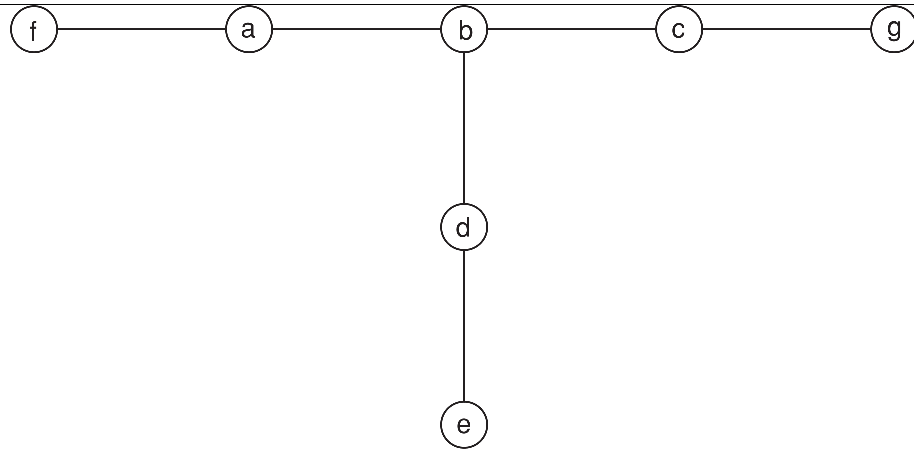

Figure 12.10. A graph used for a network exchange theory experiment.

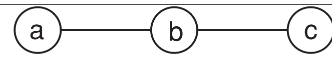

Figure 12.11.

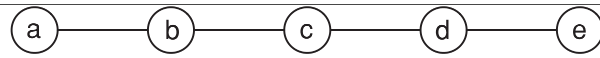

Figure 12.12. A graph used for a network exchange theory experiment.

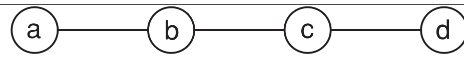

Figure 12.13.

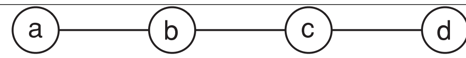

Figure 12.14. A 4-node path in a network exchange theory experiment.

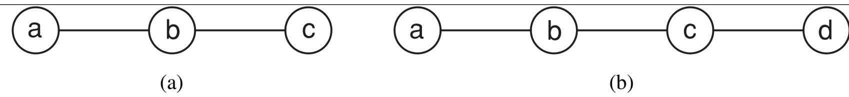

Figure 12.15. A 3-node path (right) and a 4-node path (left).

P1: SBT
cuus984-net CUUS984-Easley 0 521 19533 1 November 30, 2009 16:2

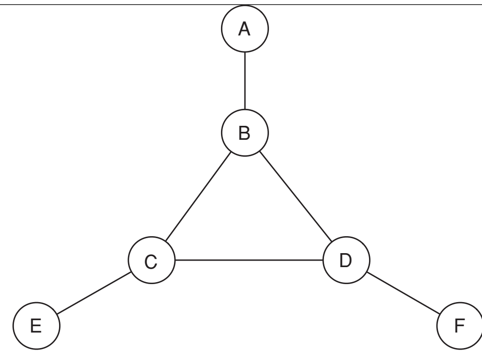

Figure 12.16. The graph for the network exchange theory experiment in part (b).

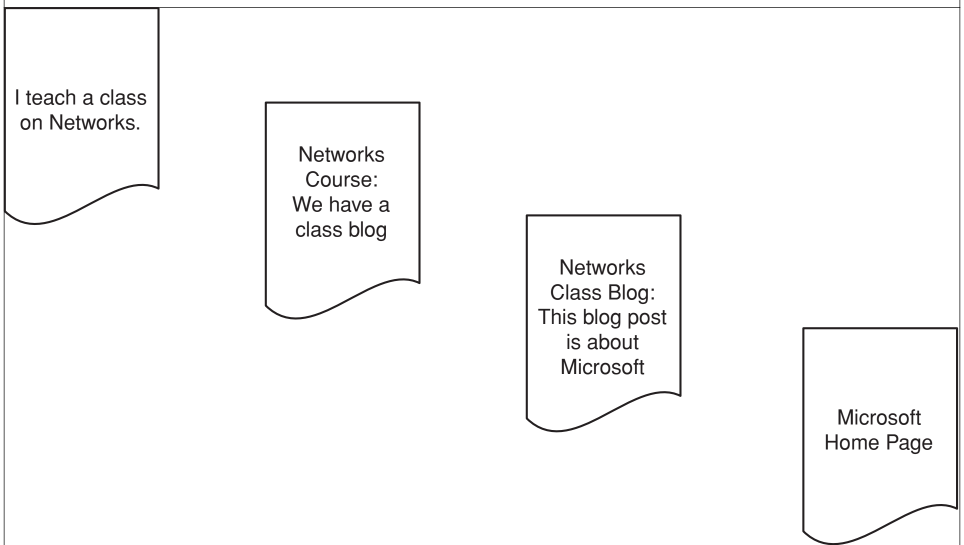

Figure 13.1. A set of four Web pages.

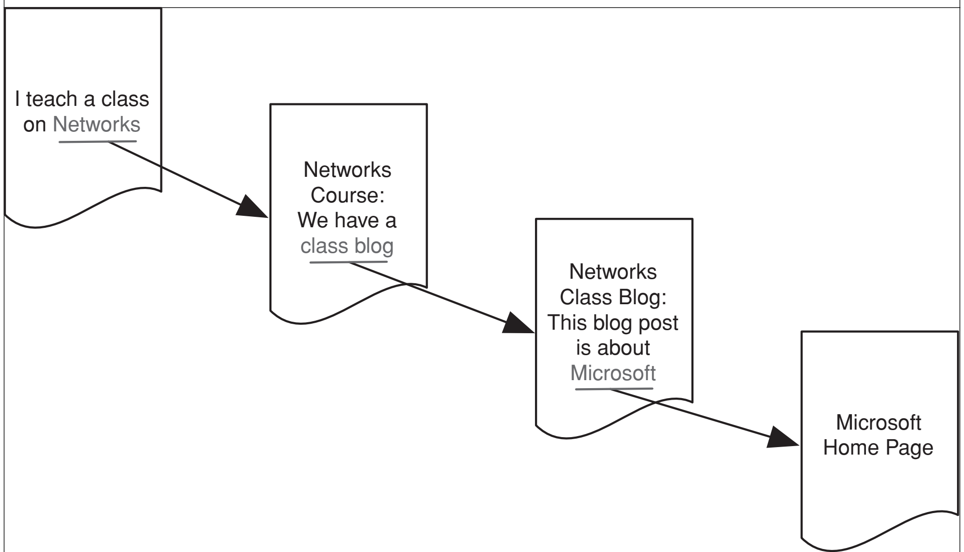

Figure 13.2. Information on the Web is organized using a network metaphor: The links among Web pages turn the Web into a directed graph.

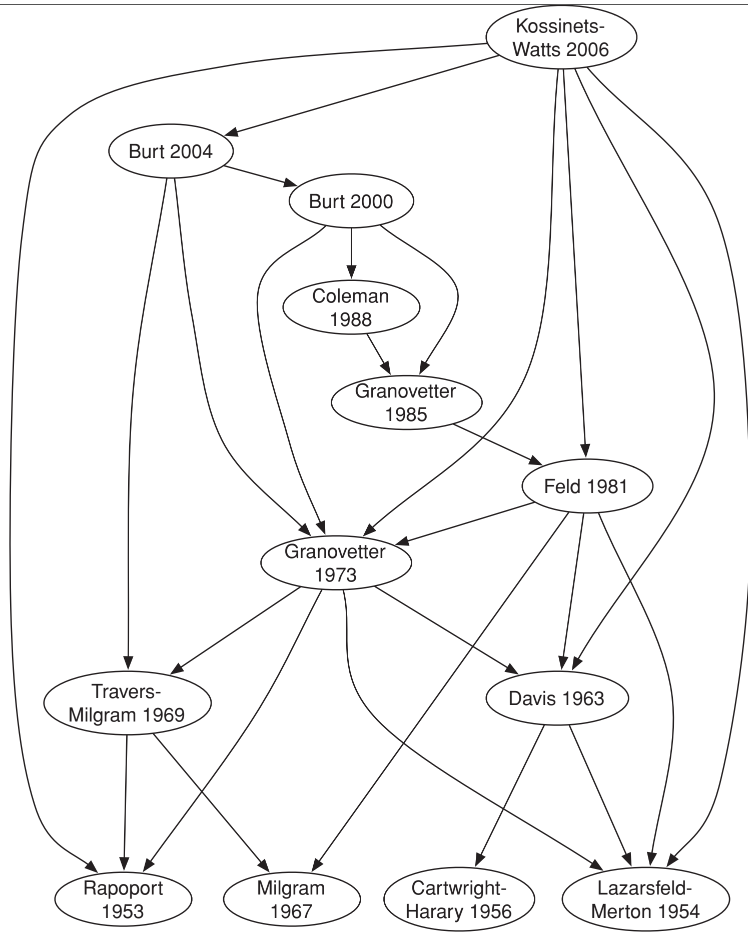

Figure 13.3. The network of citations among a set of research papers forms a directed graph that, like the Web, is a kind of information network. In contrast to the Web, however, the passage of time is much more evident in citation networks, since their links tend to point strictly backward in time.

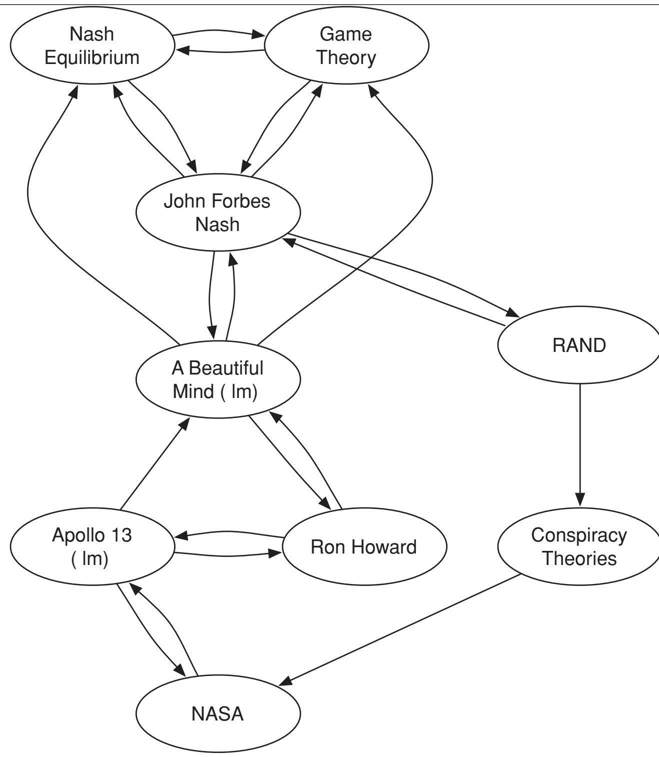

Figure 13.4. The cross-references among a set of articles in an encyclopedia forms another kind of information network that can be represented as a directed graph. The figure shows the cross-references among a set of Wikipedia articles on topic in game theory, and their connections to related topics including popular culture and government agencies.

P1: SBT
cuus984-net CUUS984-Easley 0 521 19533 1 November 30, 2009 16:2

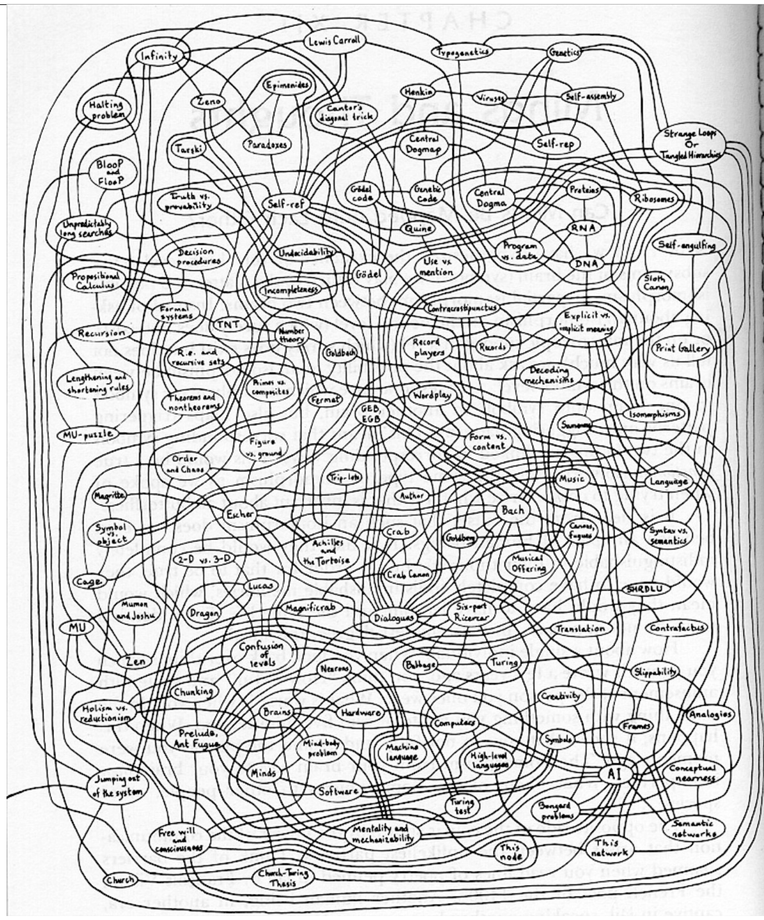

Figure 13.5. Part of Douglas Hofstadter's semantic network representing the relationships among concepts in his book *Gödel, Escher, Bach* [217]. (Image from http://caad.arch.ethz.ch/teaching/nds/ws98/script/text/img-text/hofstadter2.gif)

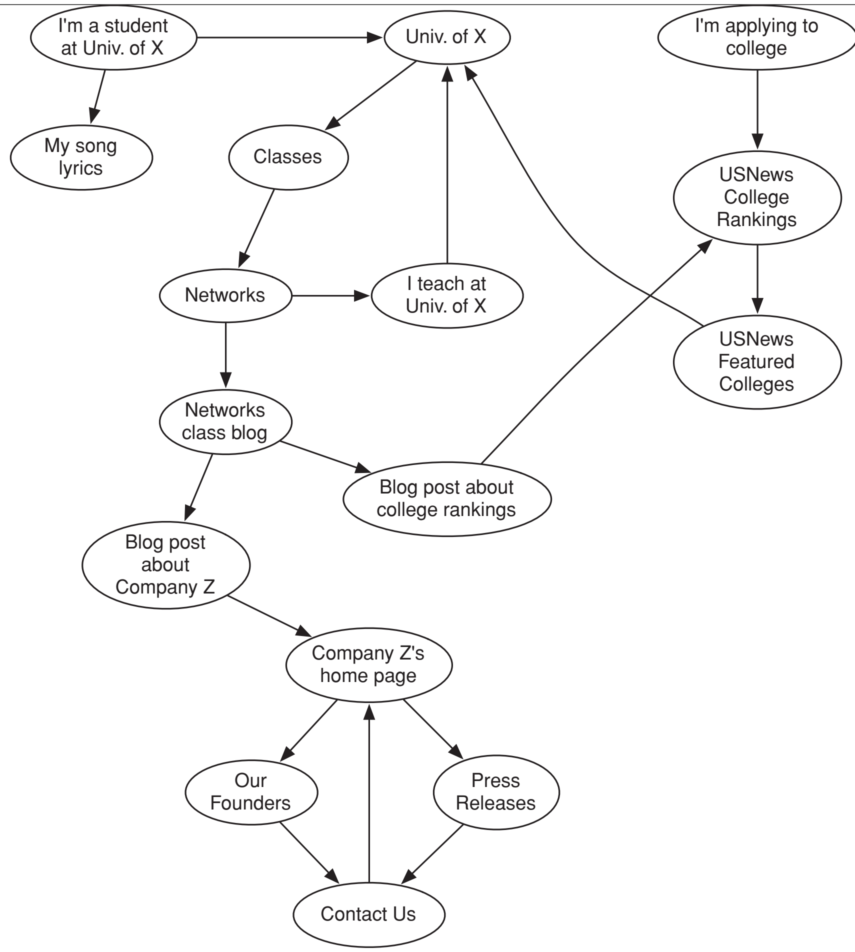

Figure 13.6. A directed graph formed by the links among a small set of Web pages.

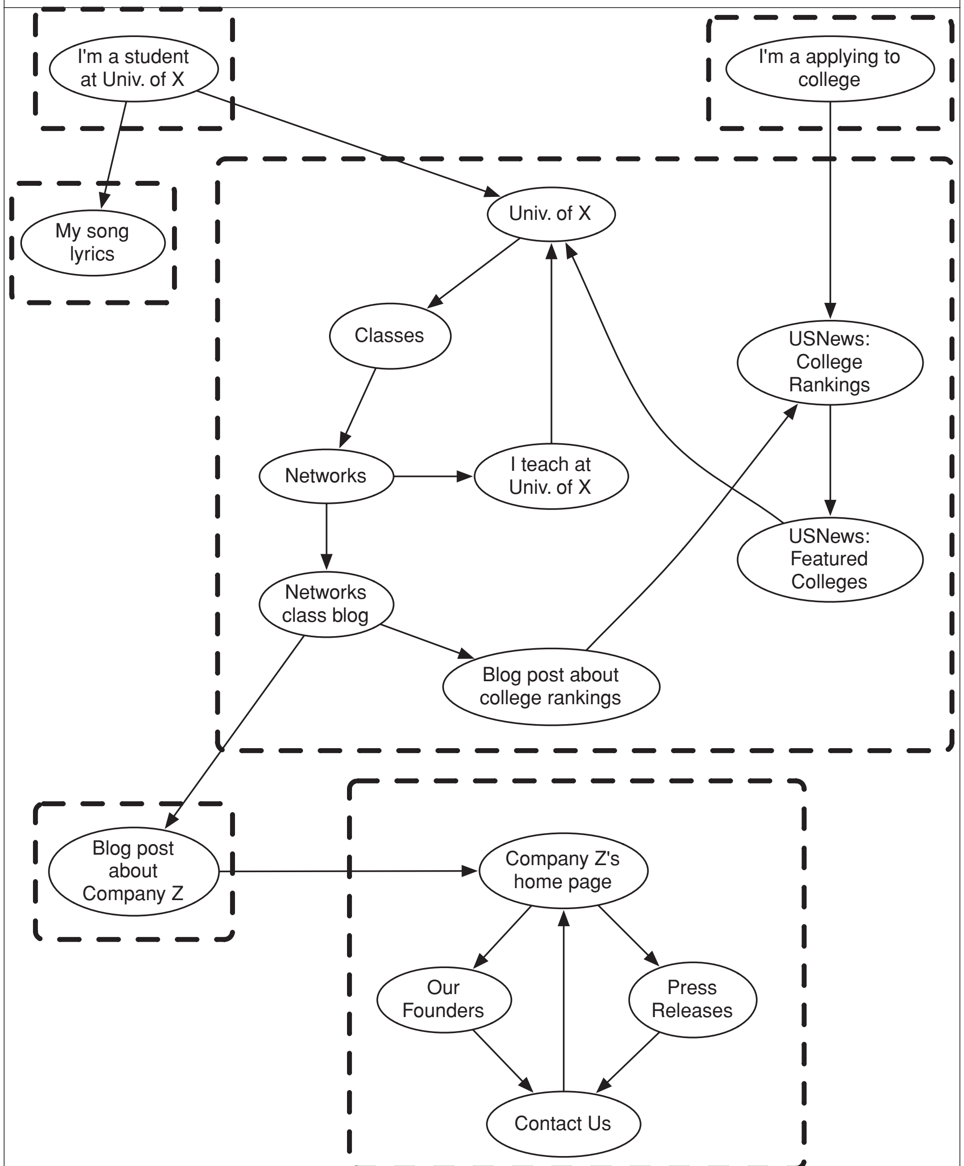

Figure 13.7. A directed graph with its strongly connected components identified.

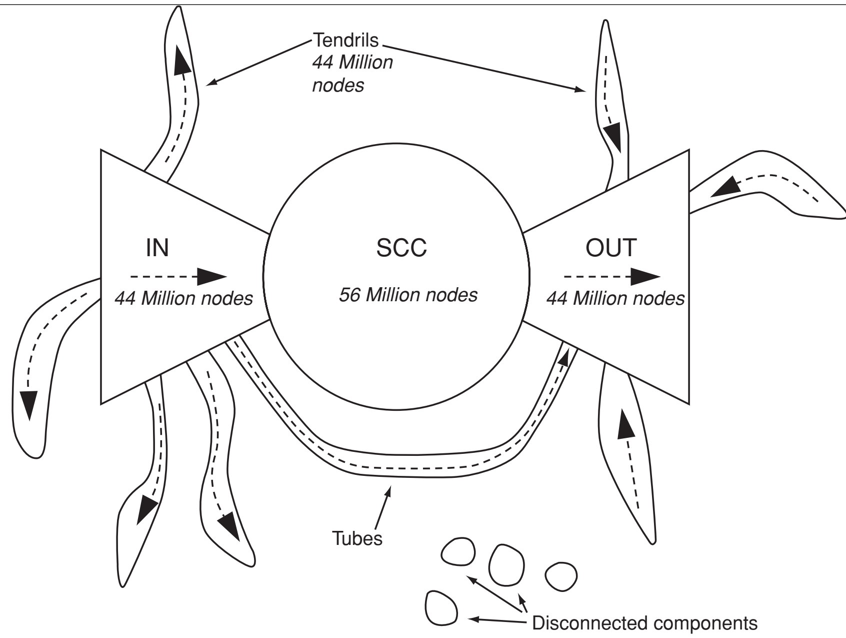

Figure 13.8. A schematic picture of the bow-structure of the Web (image from [79]).

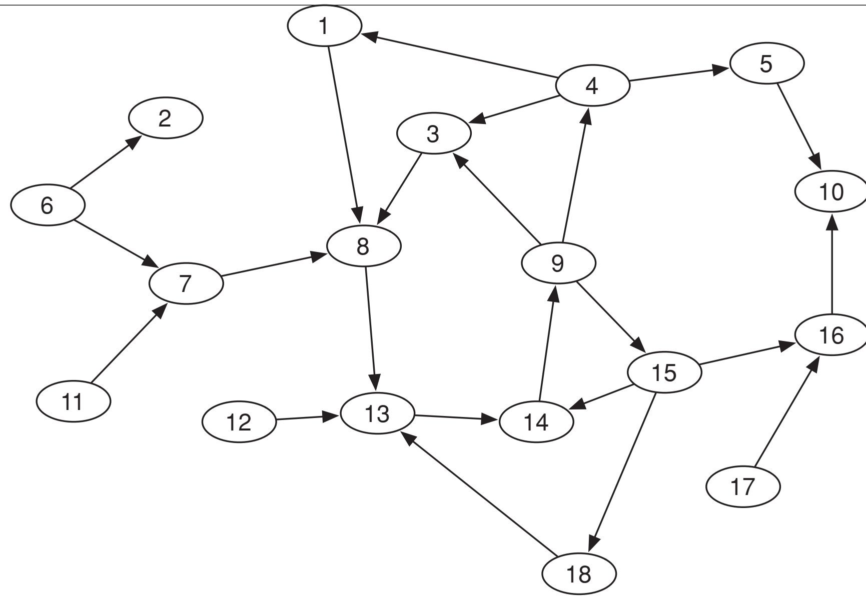

Figure 13.9. A directed graph of Web pages.

P1: SBT
cuus984-net CUUS984-Easley 0 521 19533 1 November 30, 2009 16:2

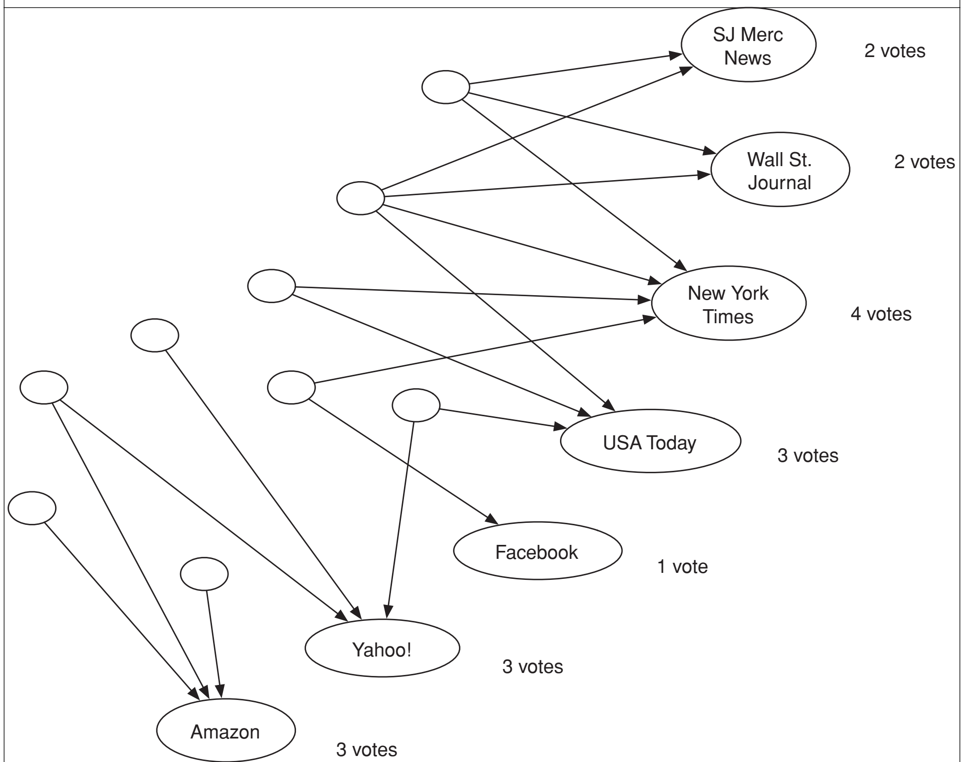

Figure 14.1. Counting in-links to pages for the query "newspapers."

P1: SBT
cuus984-net CUUS984-Easley 0 521 19533 1 November 30, 2009 16:2

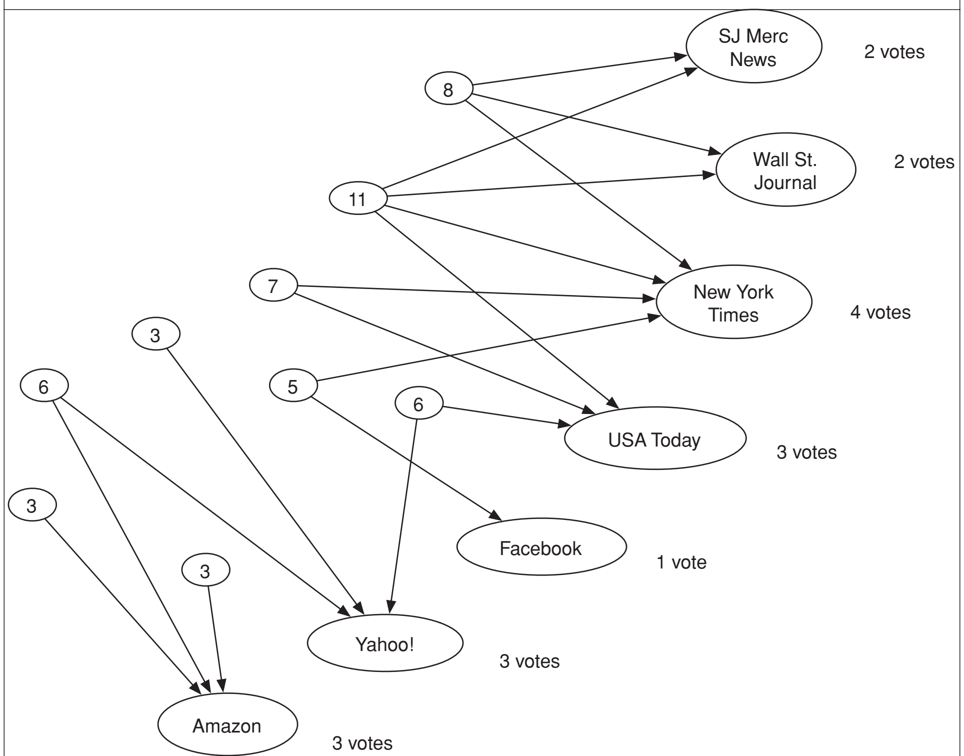

Figure 14.2. Finding good lists for the query "newspapers": each page's value as a list is written as a number inside it.

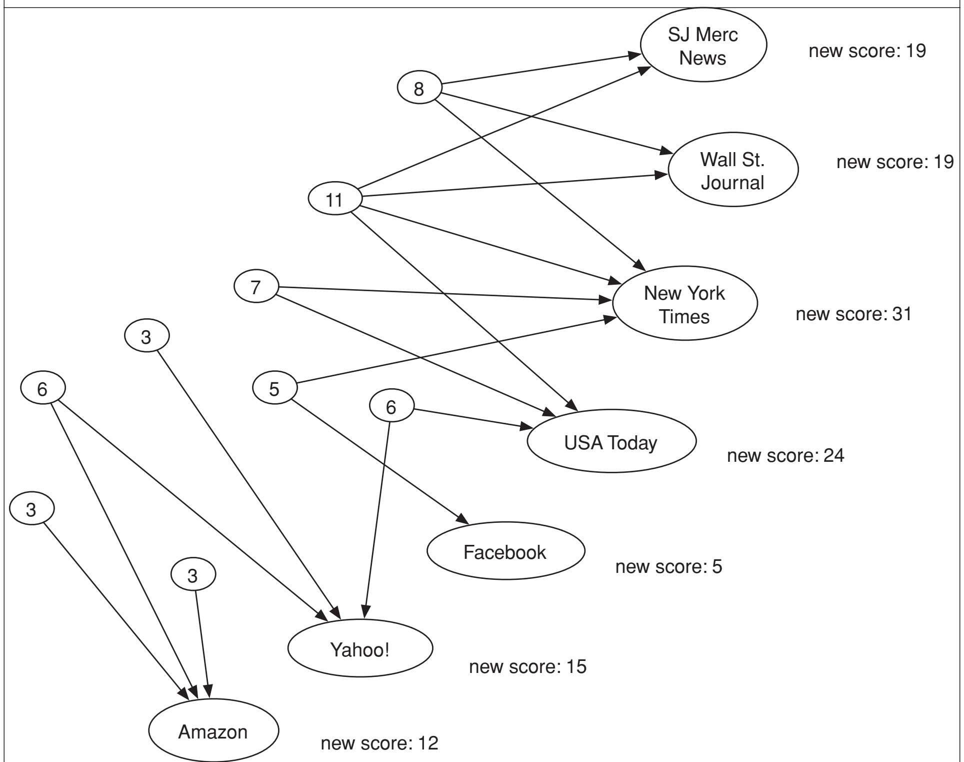

Figure 14.3. Re-weighting votes for the query "newspapers": each of the labeled page's new score is equal to the sum of the values of all lists that point to it.

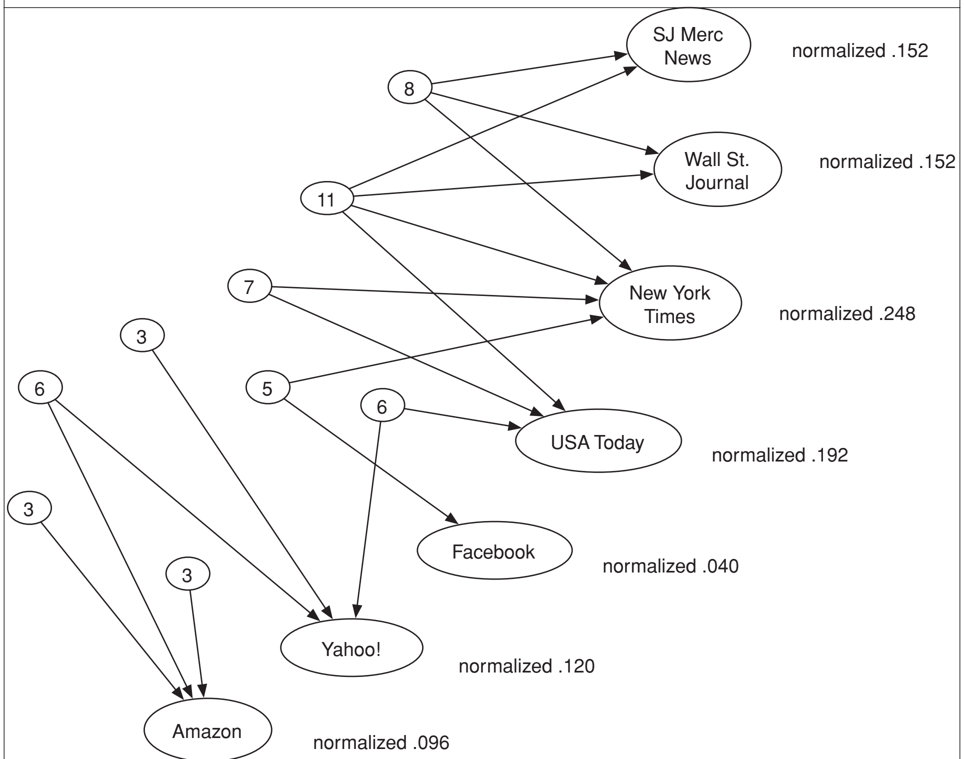

Figure 14.4. Re-weighting votes after normalizing for the query "newspapers."

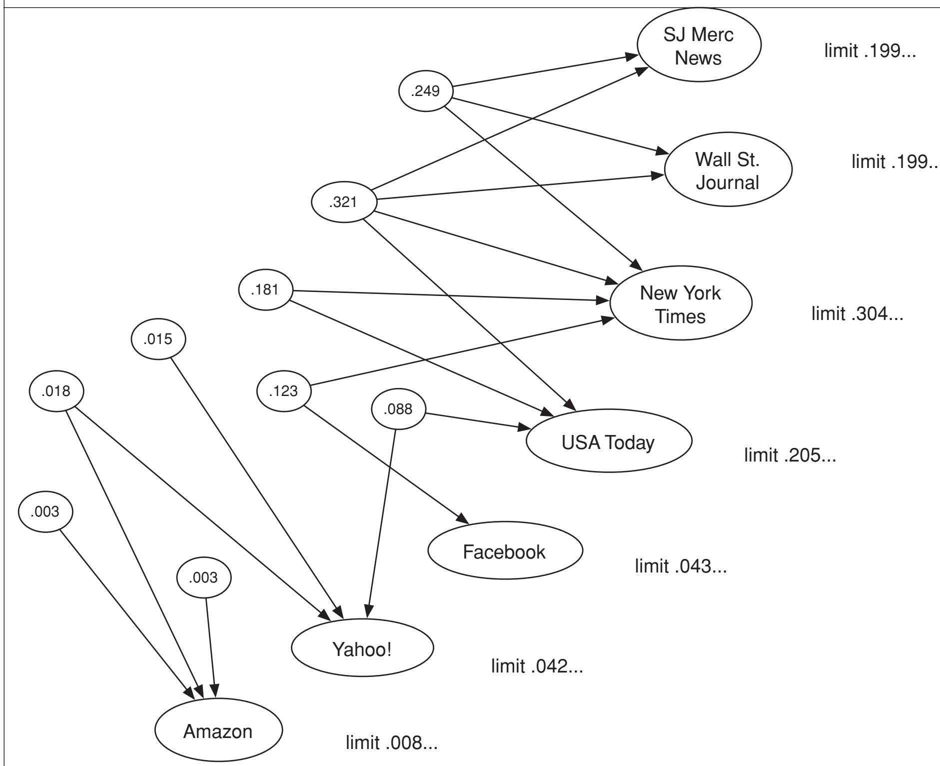

Figure 14.5. Limiting hub and authority values for the query "newspapers."

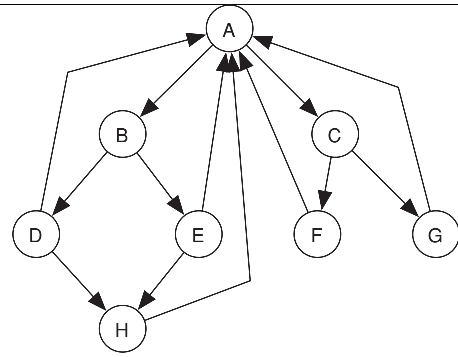

Figure 14.6. A collection of eight pages: *A* has the largest PageRank, followed by *B* and *C* (which collect endorsements from *A*).

P1: SBT
cuus984-net CUUS984-Easley 0 521 19533 1 November 30, 2009 16:2

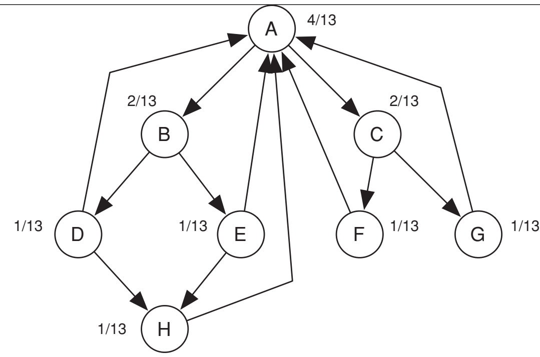

Figure 14.7. Equilibrium PageRank values for the network of eight Web pages from Figure 14.6.

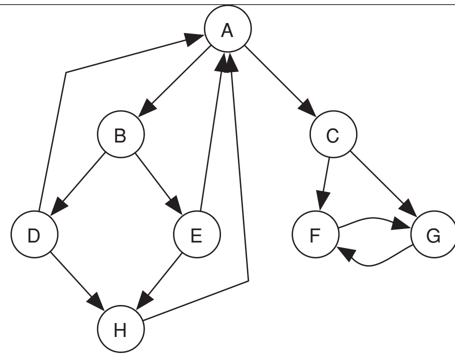

Figure 14.8. The same collection of eight pages, but F and G have changed their links to point to each other instead of to A. Without a smoothing effect, all the PageRank would go to F and G.

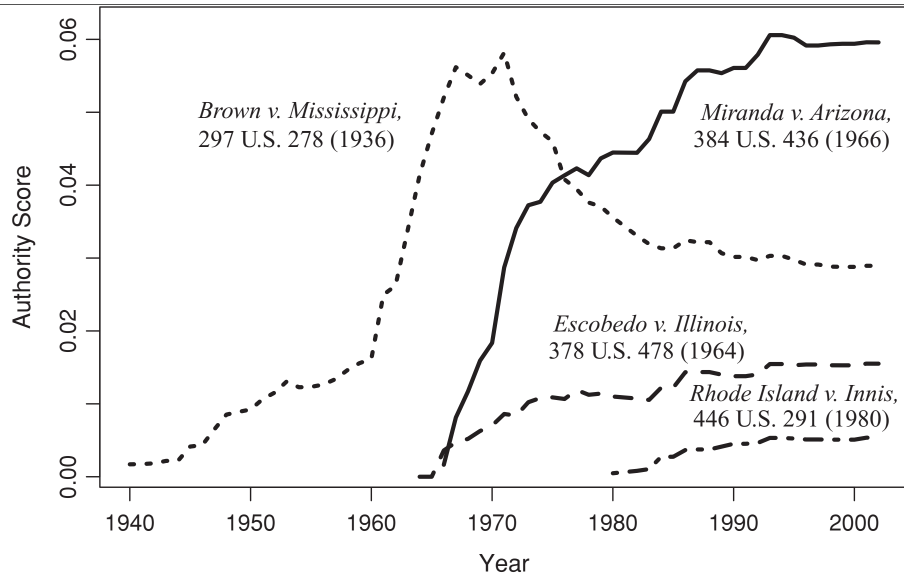

Figure 14.9. The rising and falling authority of key Fifth Amendment cases from the 20th century illustrates some of the relationships among them. (Image from [165].)

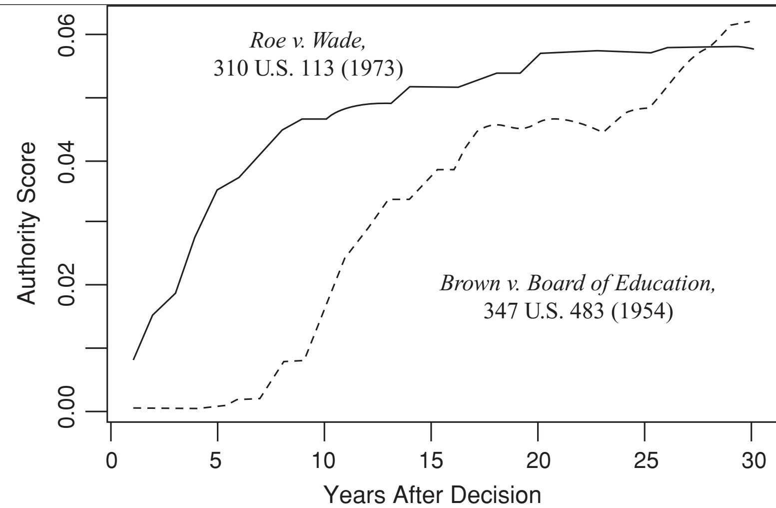

Figure 14.10. *Roe v. Wade* and *Brown v. Board of Education* acquired authority at very different speeds. (Image from [165].)

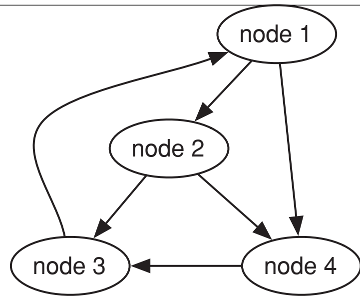

$$\begin{bmatrix} 0 & 1 & 0 & 1 \\ 0 & 0 & 1 & 1 \\ 1 & 0 & 0 & 0 \\ 0 & 0 & 1 & 0 \end{bmatrix}$$

Figure 14.11. The directed hyperlinks among Web pages can be represented using an *adjacency matrix M*: the entry M_{ij} is equal to 1 if there is a link from node i to node j, and $M_{ij} = 0$ otherwise.

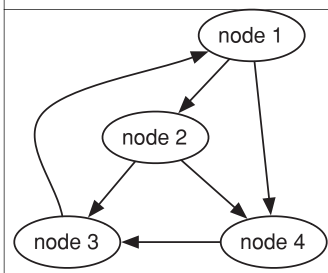

$$\begin{bmatrix} 0 & 1 & 0 & 1 \\ 0 & 0 & 1 & 1 \\ 1 & 0 & 0 & 0 \\ 0 & 0 & 1 & 0 \end{bmatrix} \begin{bmatrix} 2 \\ 6 \\ 4 \\ 3 \end{bmatrix} = \begin{bmatrix} 9 \\ 7 \\ 2 \\ 4 \end{bmatrix}$$

Figure 14.12. By representing the link structure using an adjacency matrix, the Hub and Authority Update Rules become matrix-vector multiplication.

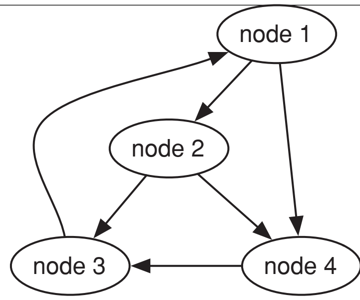

$$\begin{bmatrix} 0 & 1/2 & 0 & 1/2 \\ 0 & 0 & 1/2 & 1/2 \\ 1 & 0 & 0 & 0 \\ 0 & 0 & 1 & 0 \end{bmatrix}$$

Figure 14.13. The flow of PageRank under the Basic PageRank Update Rule can be represented using a matrix N derived from the adjacency matrix M: the entry N_{ij} specifies the portion of i's PageRank that should be passed to j in one update step.

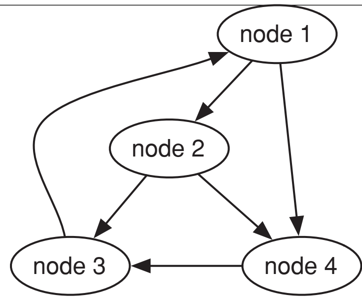

$$\begin{bmatrix} .05 & .45 & .05 & .45 \\ .05 & .05 & .45 & .45 \\ .85 & .05 & .05 & .05 \\ .05 & .05 & .85 & .05 \end{bmatrix}$$

Figure 14.14. The flow of PageRank under the Scaled PageRank Update Rule can also be represented using a matrix derived from the adjacency matrix M (shown here with scaling factor $s = 0.8$). We denote this matrix by $\tilde{N}$; the entry $\tilde{N}_{ij}$ specifies the portion of i's PageRank that should be passed to j in one update step.

P1: SBT
cuus984-net CUUS984-Easley 0 521 19533 1 November 30, 2009 16:2

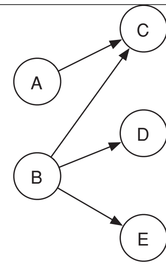

Figure 14.15.

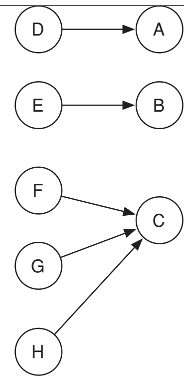

Figure 14.16. A network of Web pages.

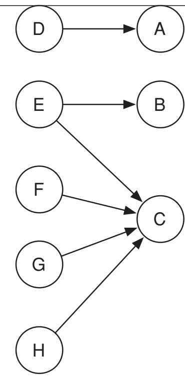

Figure 14.17. A network of Web pages.

P1: SBT
cuus984-net CUUS984-Easley 0 521 19533 1 November 30, 2009 16:2

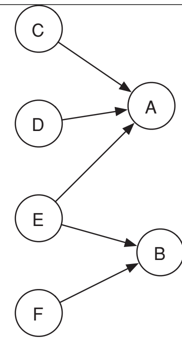

Figure 14.18.

P1: SBT
cuus984-net CUUS984-Easley 0 521 19533 1 November 30, 2009 16:2

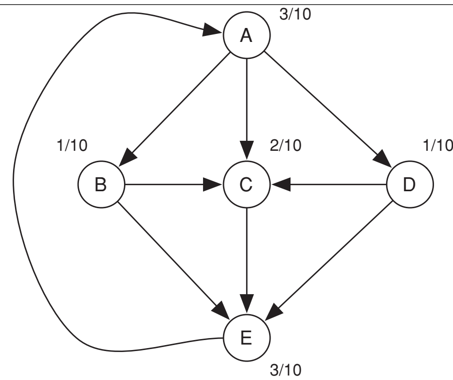

Figure 14.19. A network of Web pages.

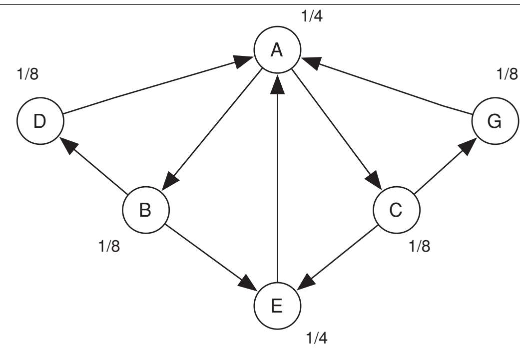

Figure 14.20. A network of Web pages.

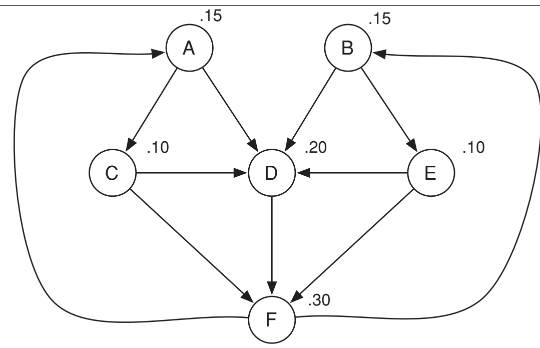

Figure 14.21. A collection of 6 Web pages, with possible PageRank values.

P1: SBT
cuus984-net CUUS984-Easley 0 521 19533 1 November 30, 2009 16:2

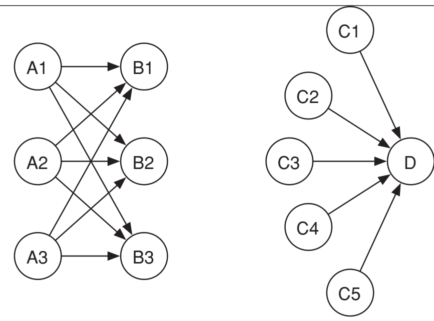

Figure 14.22.

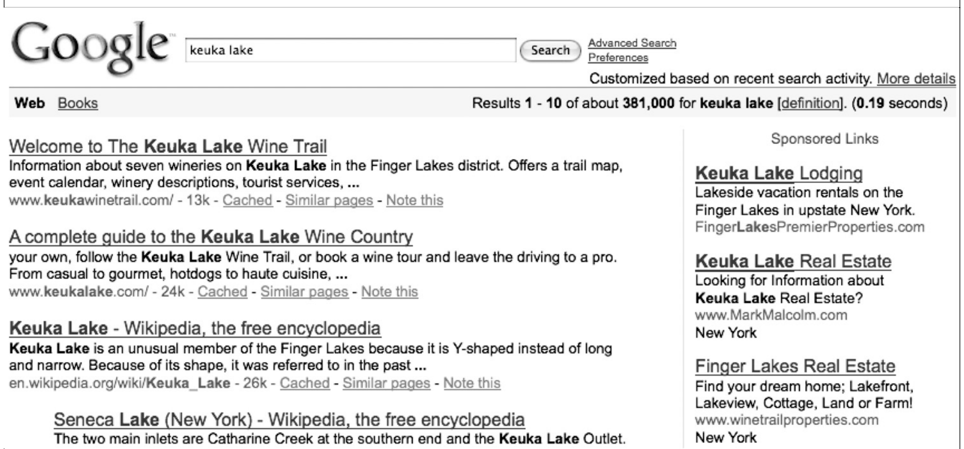

Figure 15.1. Search engines display paid advertisements (shown on the right-hand side of the page in this example) that match the query issued by a user. These appear alongside the results determined by the search engine's own ranking method (shown on the left-hand side). An auction procedure determines the selection and ordering of the ads.

P1: SBT
cuus984-net CUUS984-Easley 0 521 19533 1 November 30, 2009 16:2

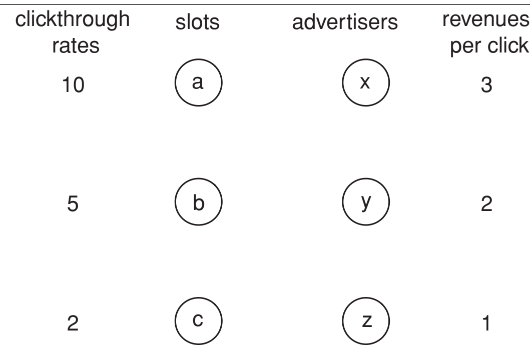

Figure 15.2. In the basic set-up of a search engine's market for advertising, there are a certain number of advertising slots to be sold to a population of potential advertisers. Each slot has a *clickthrough rate*: the number of clicks per hour it will receive, with higher slots generally getting higher clickthrough rates. Each advertisers has a *revenue per click*, the amount of money it expects to receive, on average, each time a user clicks on one of its ads and arrives at its site. We draw the advertisers in descending order of their revenue per click; for now, this is purely a pictorial convention, but in Section 15.2 we will show that the market in fact generally allocates slots to the advertisers in this order.

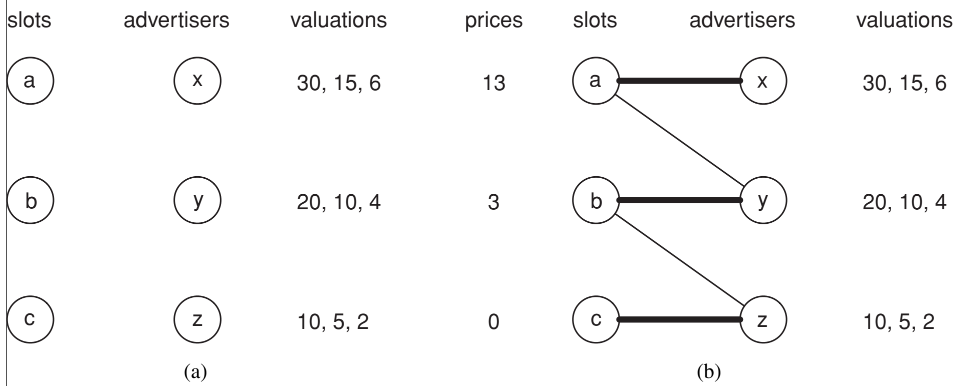

Figure 15.3. The allocation of advertising slots to advertisers can be represented as a matching market, in which the slots are the items to be sold, and the advertisers are the buyers. An advertiser's valuation for a slot is simply the product of its own revenue per click and the clickthrough rate of the slot; these can be used to determine market-clearing prices for the slots.

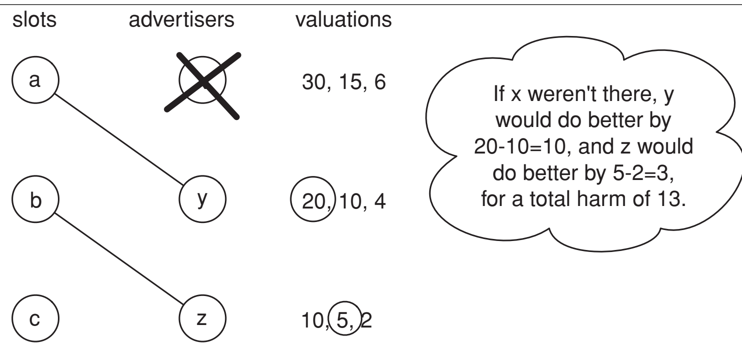

(a)

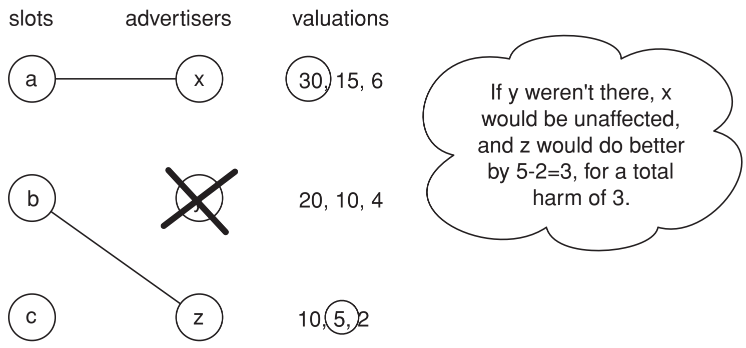

(b)

Figure 15.4. The VCG price an individual buyer pays for an item can be determined by working out how much better off all other buyers would be if this individual buyer were not present.

P1: SBT
cuus984-net CUUS984-Easley 0 521 19533 1 November 30, 2009 16:2

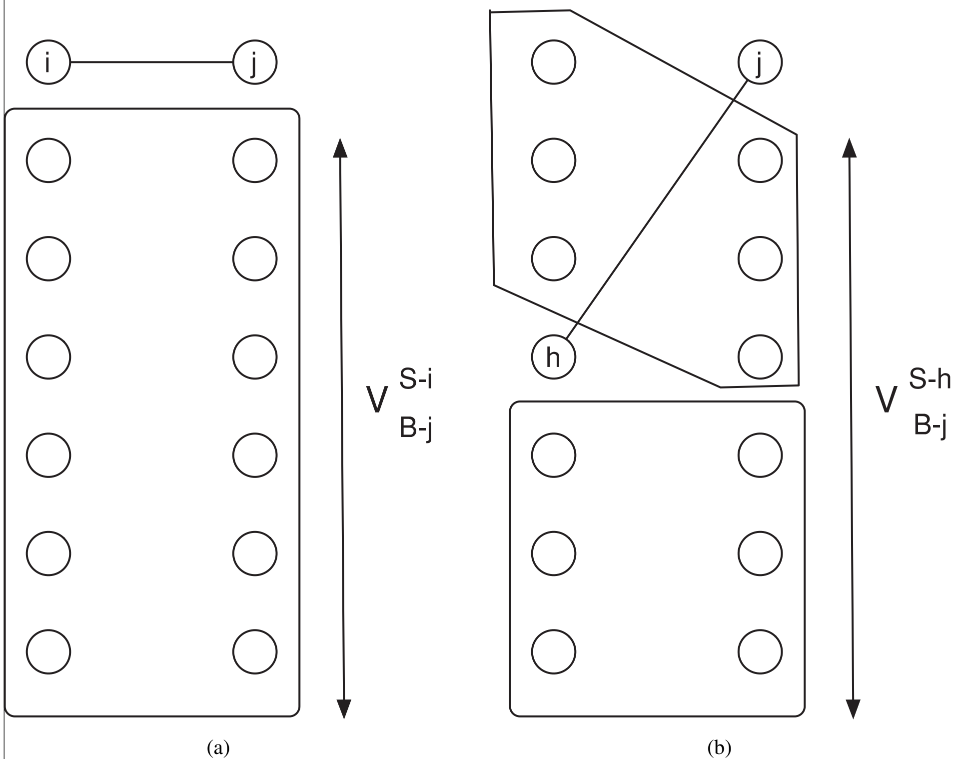

Figure 15.5. The heart of the proof that the VCG procedure encourages truthful bidding comes down to a comparison of the value of two matchings.

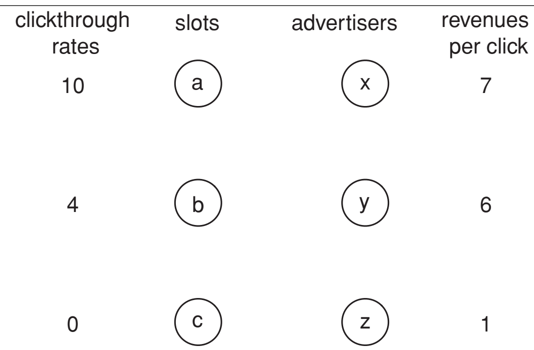

Figure 15.6. An example of a set of advertisers and slots for which truthful bidding is not an equilibrium in the Generalized Second Price auction. Moreover, this example possesses multiple equilibria, some of which are not socially optimal.

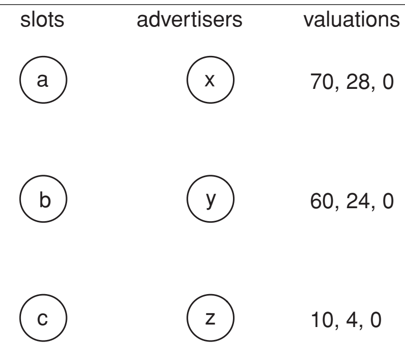

Figure 15.7. Representing the example in Figure 15.6 as a matching market, with advertiser valuations for the full set of clicks associated with each slot.

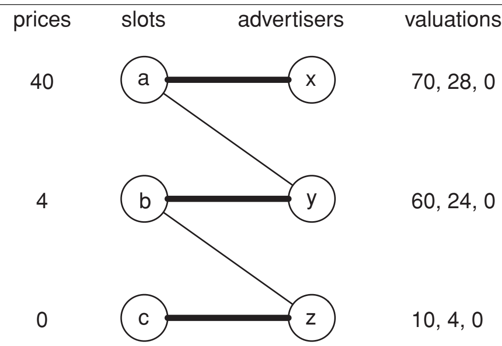

Figure 15.8. Determining market-clearing prices for the example in Figure 15.6, starting with its representation as a matching market.

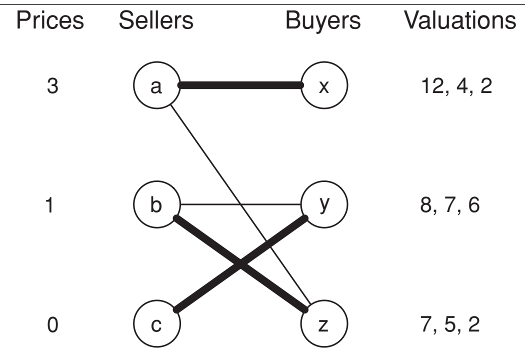

Figure 15.9. A matching market, with valuations and market-clearing prices specified, and a perfect matching in the preferred-seller graph indicated by the bold edges.

P1: SBT
cuus984-net CUUS984-Easley 0 521 19533 1 November 30, 2009 16:2

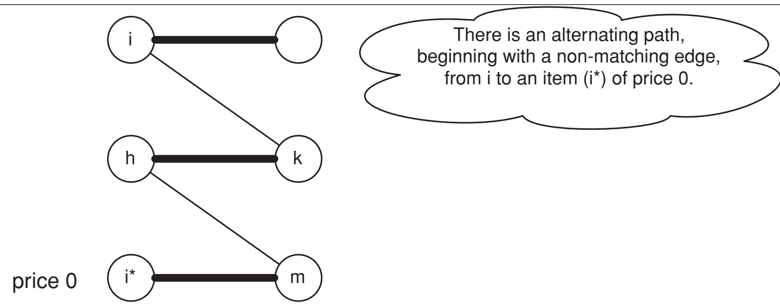

Figure 15.10. The key property of the preferred-seller graph for minimum market-clearing prices: for each item of price greater than 0, there is an alternating path, beginning with a non-matching edge, to an item of price 0.

P1: SBT
cuus984-net CUUS984-Easley 0 521 19533 1 November 30, 2009 16:2

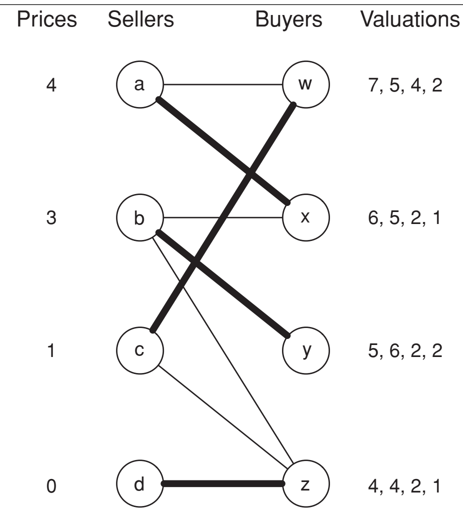

Figure 15.11. A matching market with market-clearing prices of minimum total sum. Note how from each item, there is an alternating path, beginning with a non-matching edge, that leads to the item of zero price.

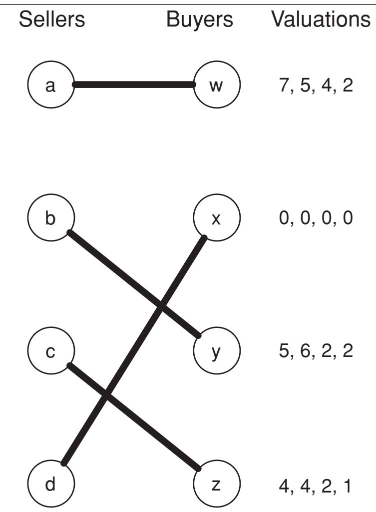

Figure 15.12. If we start with the example in Figure 15.11 and zero out buyer x, the structure of the optimal matching changes significantly.

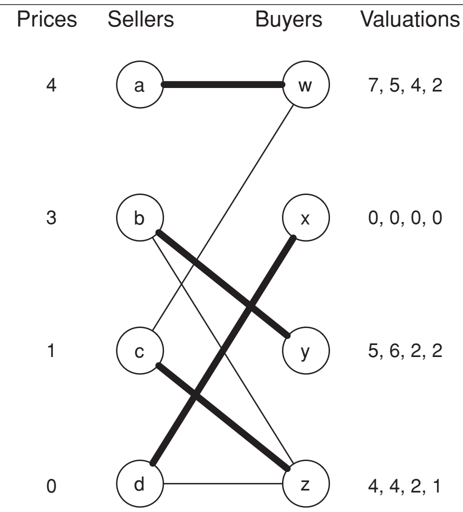

Figure 15.13. However, even after we zero out buyer x, the same set of prices remain market-clearing. This principle is true not just for this example, but in general.

P1: SBT
cuus984-net CUUS984-Easley 0 521 19533 1 November 30, 2009 16:2

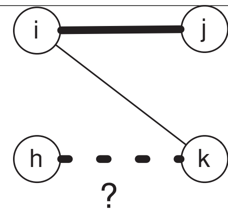

Figure 15.14. In order for a matching edge from a buyer k to an item h to leave the preferred-seller graph when the price of i is reduced by 1, it must be that k now strictly prefers i. In this case, k must have previously viewed i as comparable in payoff to h, resulting in a non-matching edge to i.

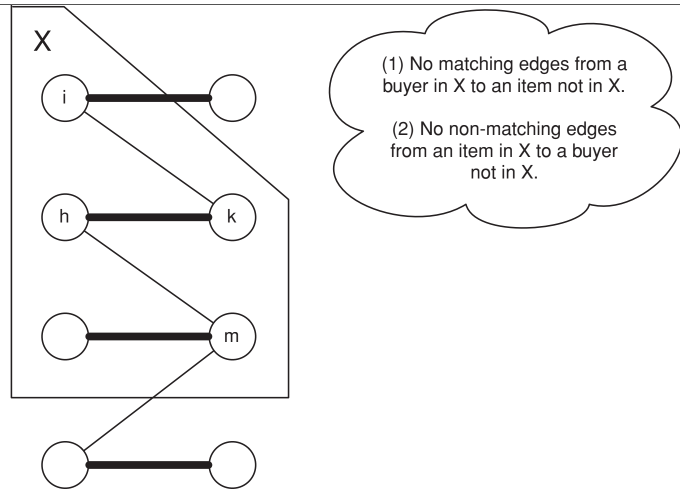

Figure 15.15. Consider the set X of all nodes that can be reached from i using an alternating path that begins with a non-matching edge. As we argue in the text, if k is buyer in X, then the item to which she is matched must also be in X. Also, if h is an item in X, then any buyer to which h is connected by a non-matching edge must also be in X. Here is an equivalent way to phrase this: there cannot be a matching edge connecting a buyer in X to an item not in X, or a non-matching edge connecting an item in X to a buyer not in X,

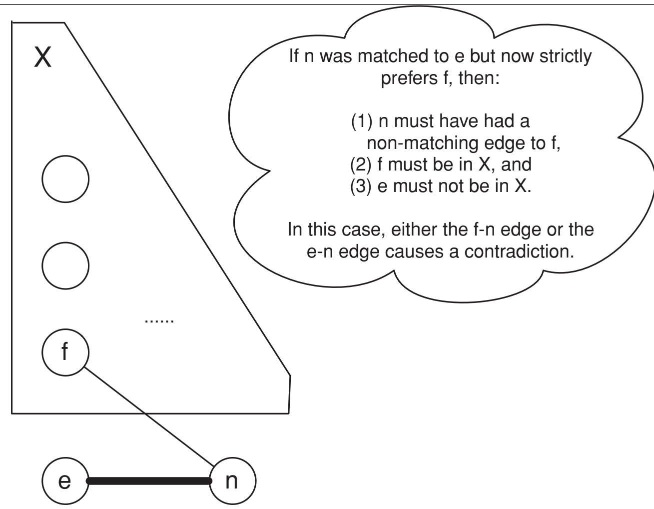

Figure 15.16. We can reduce the prices of all items in X by 1 and still retain the market-clearing property: as we argue in the text, the only way this can fail is if some matching edge connects a buyer in X to an item not in X, or some non-matching edge connects an item in X to a buyer not in X. Either of these possibilities would contradict the facts in Figure 15.15.

P1: SBT
cuus984-net CUUS984-Easley 0 521 19533 1 November 30, 2009 16:2

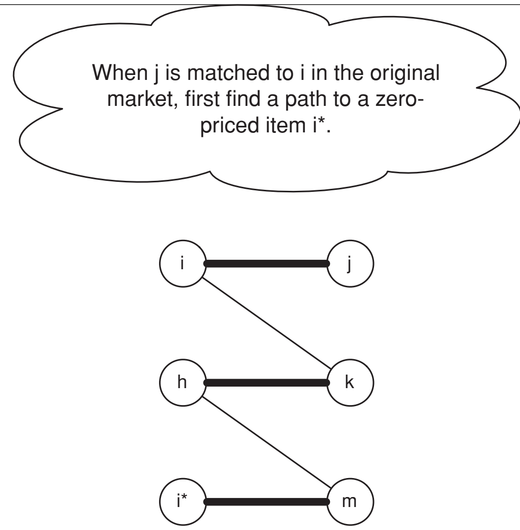

Figure 15.17. The first step in analyzing the market with j zeroed out: find an alternating path from item i — to which buyer j was matched in the original market — to a zero-priced item i^*.

P1: SBT
cuus984-net CUUS984-Easley 0 521 19533 1 November 30, 2009 16:2

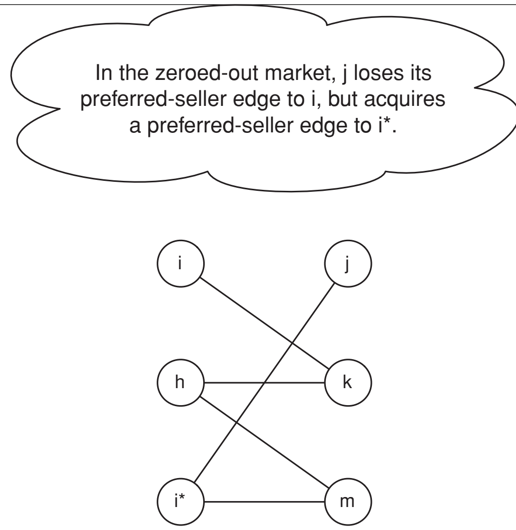

Figure 15.18. The second step in analyzing the market with j zeroed out: build the new preferred-seller graph by rewiring j's preferred-seller edges to point to the zero-priced items.

P1: SBT
cuus984-net CUUS984-Easley 0 521 19533 1 November 30, 2009 16:2

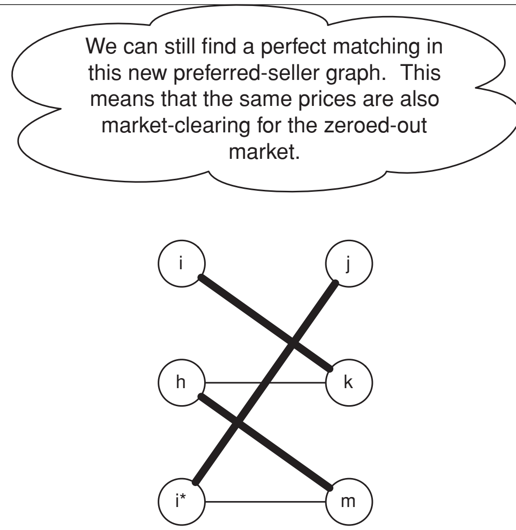

Figure 15.19. The third and final step in analyzing the market with j zeroed out: observe that the rewired preferred-seller graph still contains a perfect matching, in which j is now paired with i^*.

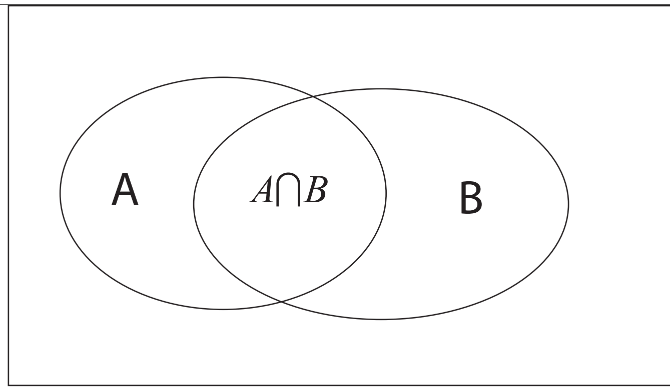

Figure 16.1. Two events A and B in a sample space, and the joint event $A \cap B$.

P1: SBT
cuus984-net CUUS984-Easley 0 521 19533 1 November 30, 2009 16:2

		States	
		B	G
Signals	L	q	$1-q$
	H	$1-q$	q

Figure 16.2. The probability of receiving a low or high signal, as a function of the two possible states of the world (G or B).

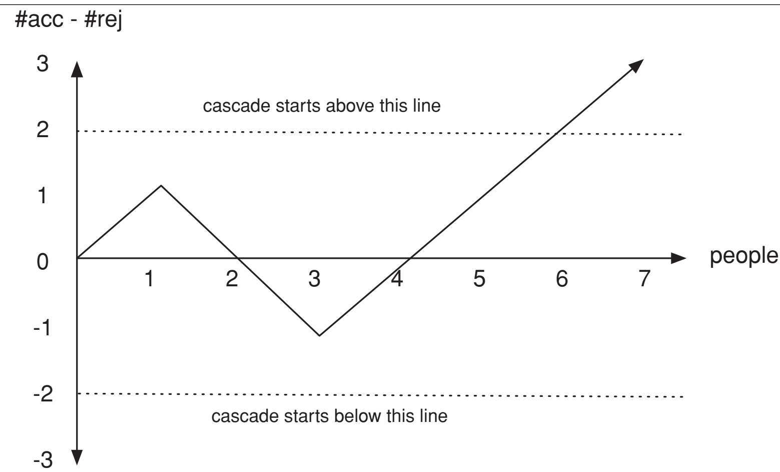
#acc - #rej
3
2
1
0
-1
-2
-3
cascade starts above this line
cascade starts below this line
1
2
3
4
5
6
7
people

Figure 16.3. .

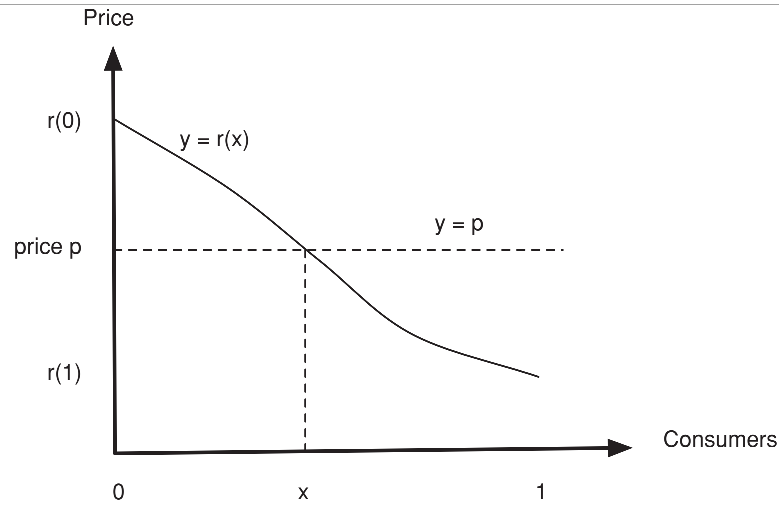

Figure 17.1. When there are no network efforts, the demand for a product at a fixed market price p can be found by locating the point where the curve $y = r(x)$ intersects the horizontal line $y = p$.

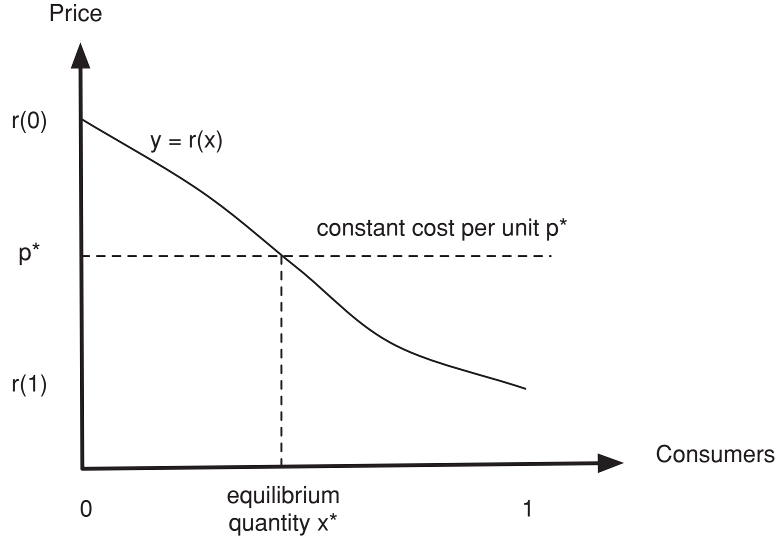

Figure 17.2. When copies of a good can be produced at a constant cost p^* per unit, the equilibrium quantity consumed will be the number x^* for which $r(x^*) = p^*$.

P1: SBT
cuus984-net CUUS984-Easley 0 521 19533 1 November 30, 2009 16:2

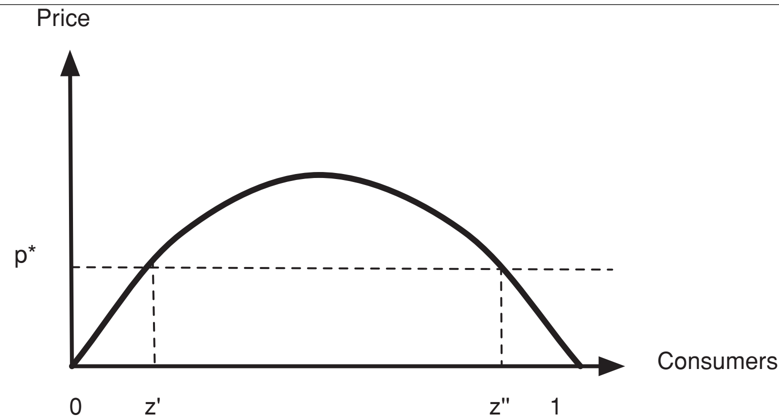

Figure 17.3. Suppose there are network effects and $f(0) = 0$, so that the good has no value to people when no one is using it. In this case, there can be multiple self-fulfilling expectations equilibria: at $z = 0$, and also at the points where the curve $r(z) f(z)$ crosses the horizontal line at height p^*.

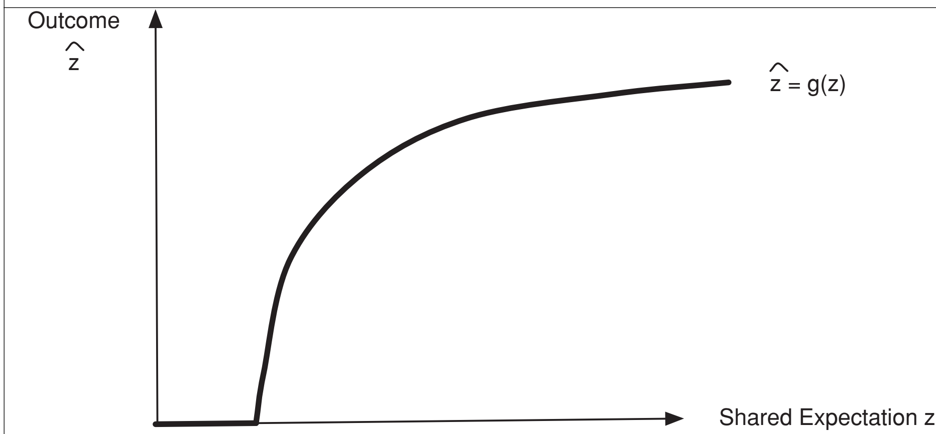

Figure 17.4. From a model with network effects, we can define a function $\hat{z} = g(z)$: if everyone expects a z fraction of the population to purchase the good, then in fact a $g(z)$ fraction will do so.

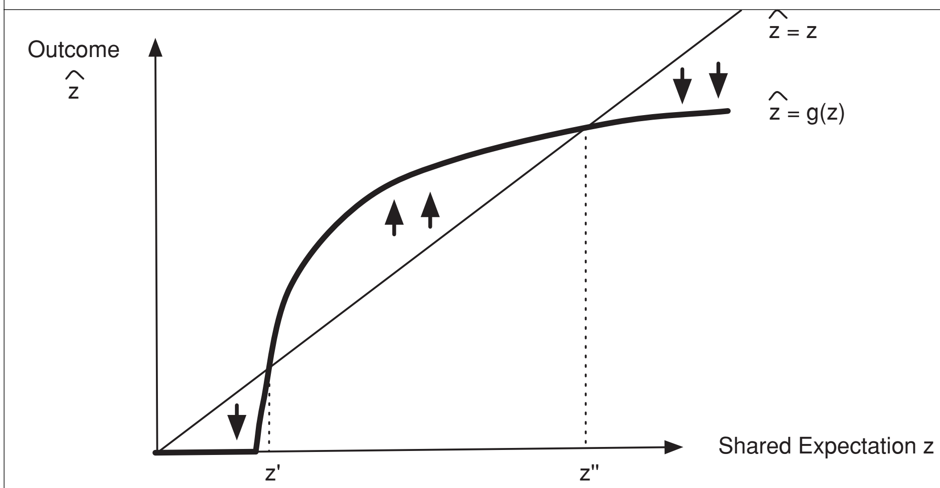

Figure 17.5. When $r(x) = 1 - x$ and $f(z) = z$, we get the curve for $g(z)$ shown in the plot: $g(z) = 1 - p^*/z$ if $z \geq p^*$ and $g(z) = 0$ if $z < p^*$. Where the curve $\hat{z} = g(z)$ crosses the line $\hat{z} = z$, we have self-fulfilling expectations equilibria. When $\hat{z} = g(z)$ lies below the line $\hat{z} = z$, we have downward pressure on the consumption of the good (indicated by the downward arrows); when $\hat{z} = g(z)$ lies above the line $\hat{z} = z$, we have upward pressure on the consumption of the good (indicated by the upward arrows). This indicates visually why the equilibrium at z' is unstable while the equilibrium at z'' is stable.

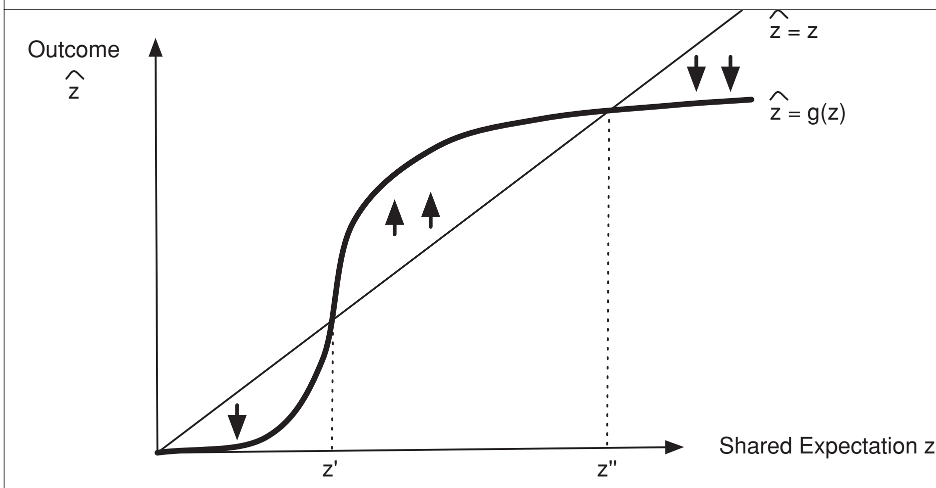

Figure 17.6. This curve $g(z)$, and its relation to the line $\hat{z} = z$, illustrates a pattern that we expect to see in settings more general than just the example used for Figure 17.5.

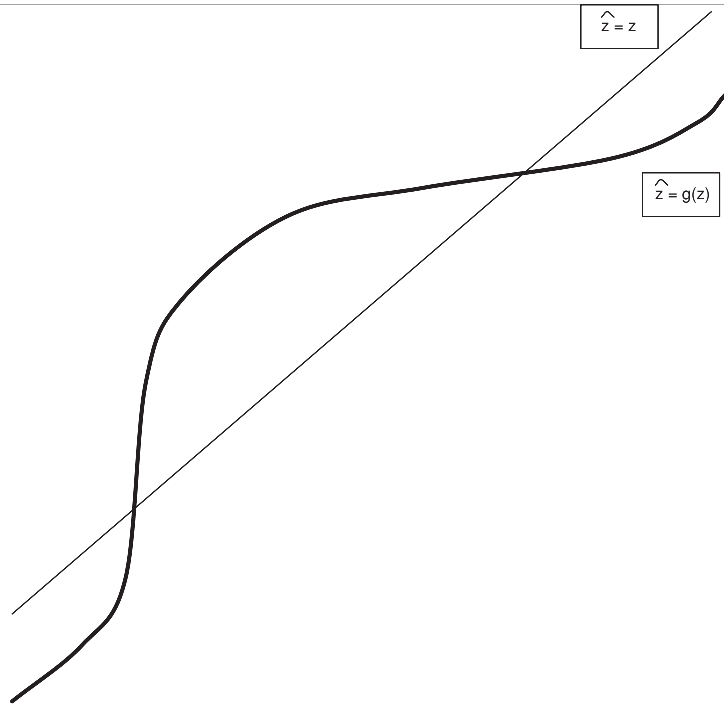

Figure 17.7. A "zoomed-in" region of a curve $\hat{z} = g(z)$ and its relation to the line $\hat{z} = z$.

P1: SBT
cuus984-net CUUS984-Easley 0 521 19533 1 November 30, 2009 16:2

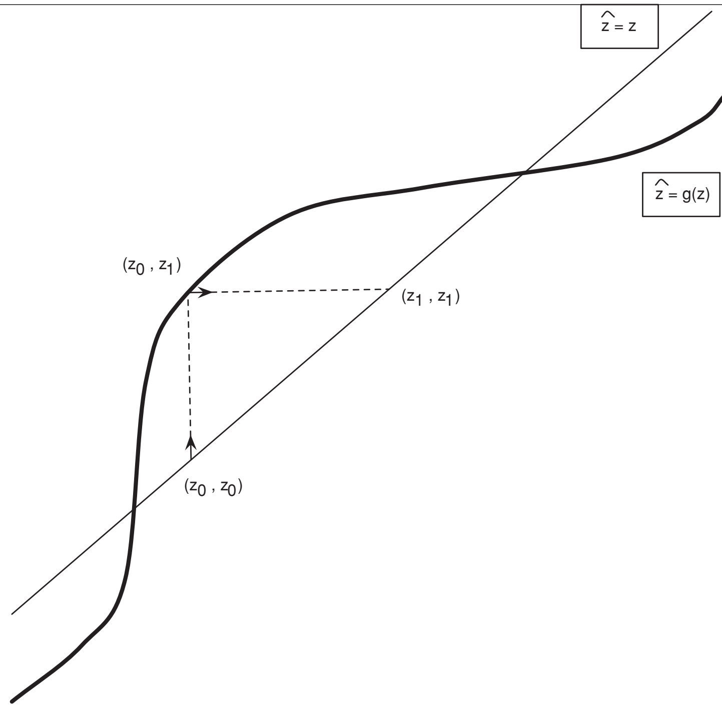

Figure 17.8. The audience size changes dynamically as people react to the current audience size. This effect can be tracked using the curve $\hat{z} = g(z)$ and the line $\hat{z} = z$.

P1: SBT
cuus984-net CUUS984-Easley 0 521 19533 1 November 30, 2009 16:2

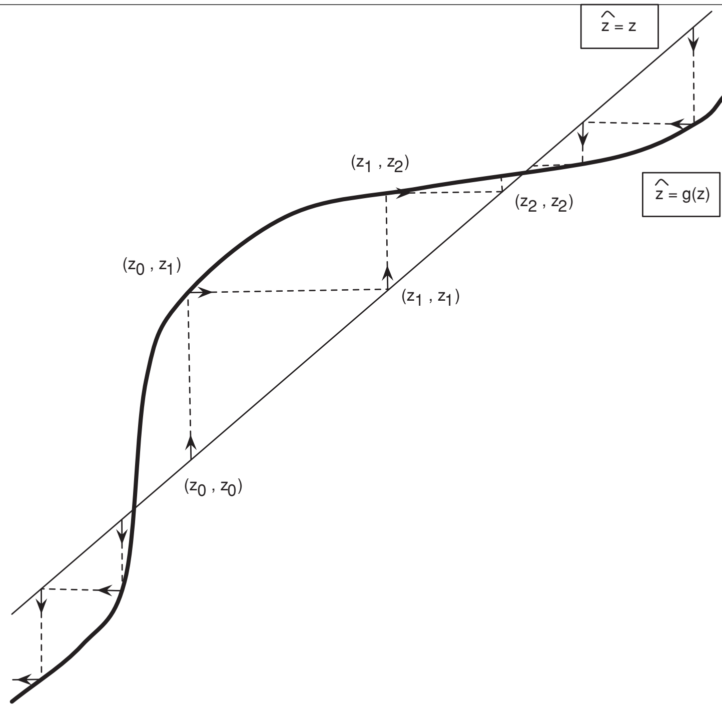

Figure 17.9. Successive updates cause the audience size to converge to a stable equilibrium point (and to move away from the vicinities of unstable ones).

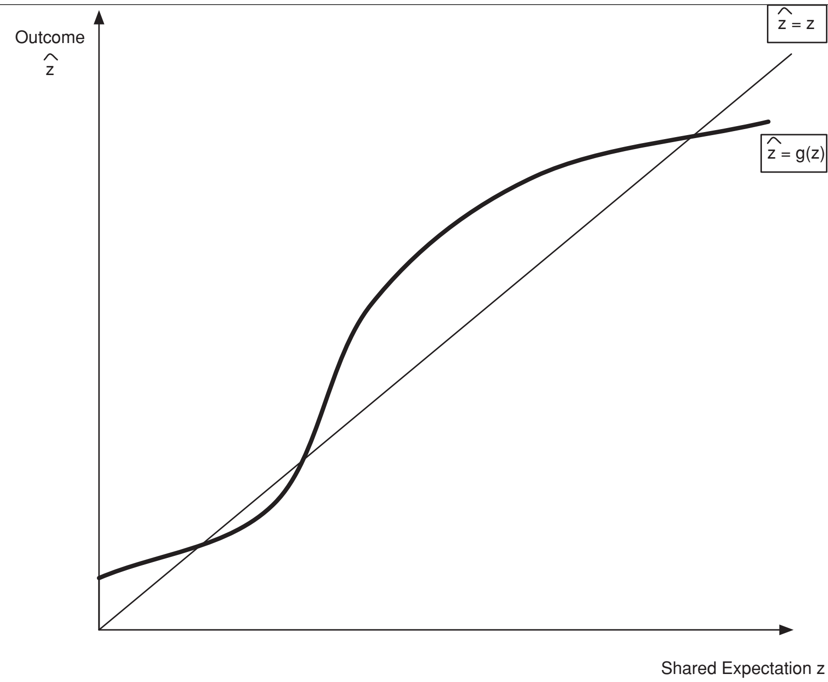

Figure 17.10. When $f(0) > 0$, so that people have value for the product even when they are the only user, the curve $\hat{z} = g(z)$ no longer passes through the point $(0, 0)$, and so an audience size of 0 is no longer an equilibrium.

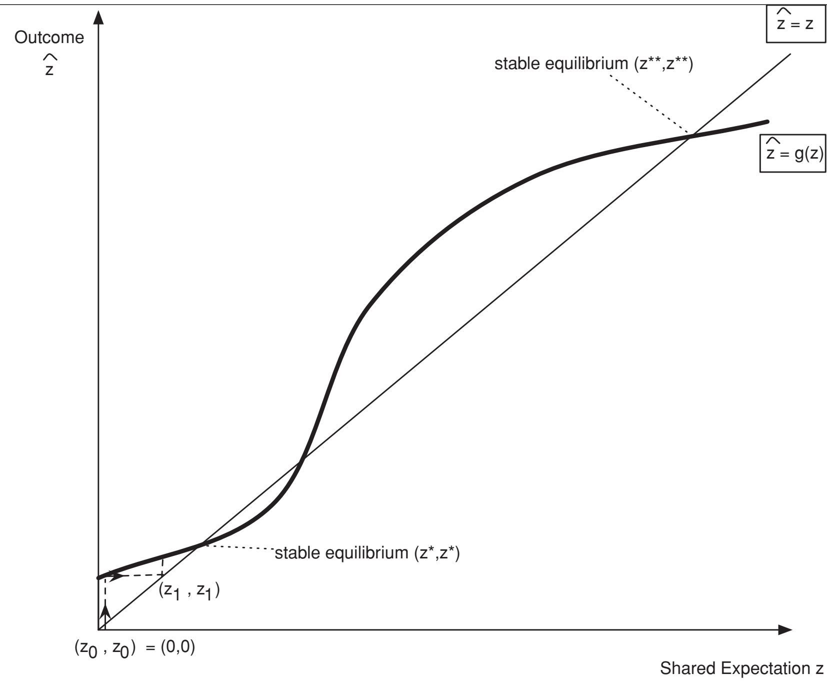

Figure 17.11. The audience grows dynamically from an initial size of zero to a relatively small stable equilibrium size of z^*.

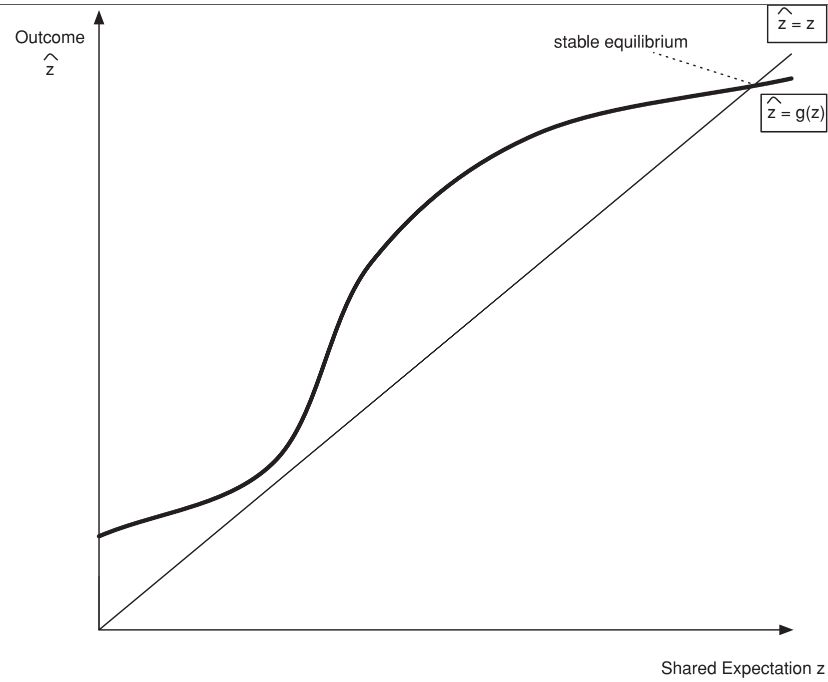

Figure 17.12. If the price is reduced slightly, the curve $\hat{z} = g(z)$ shifts upward so that it no longer crosses the line $\hat{z} = z$ in the vicinity of the point (z^*, z^*).

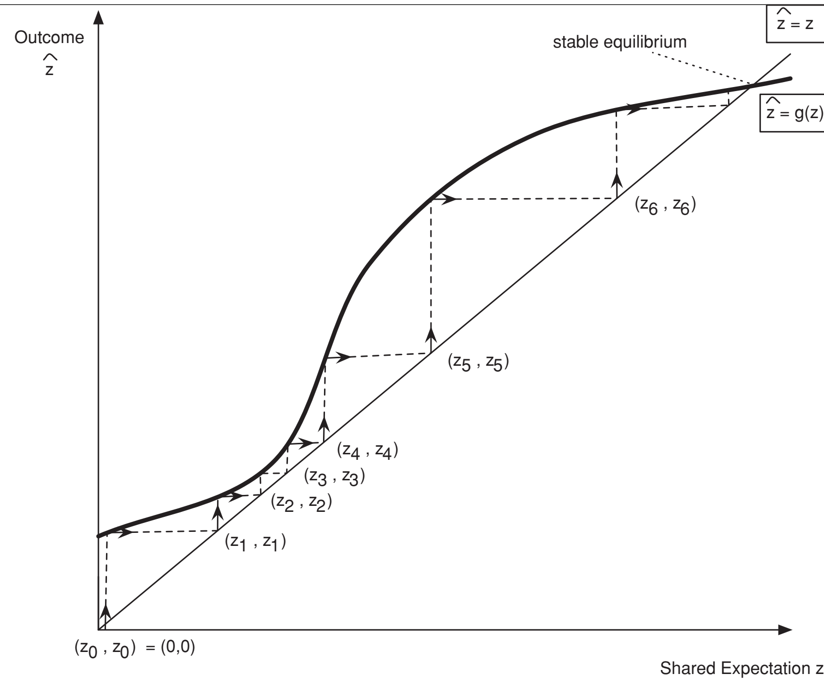

Figure 17.13. The small reduction in price that shifted the curve $\hat{z} = g(z)$ has a huge effect on the equilibrium audience size that is reached starting from zero.

P1: SBT
cuus984-net CUUS984-Easley 0 521 19533 1 November 30, 2009 16:2

		Player 2	
		Stay	*Go*
Player 1	*Stay*	$0, 0$	$0, x$
	Go	$x, 0$	$-y, -y$

Figure 17.14. Two-Player El Farol Problem

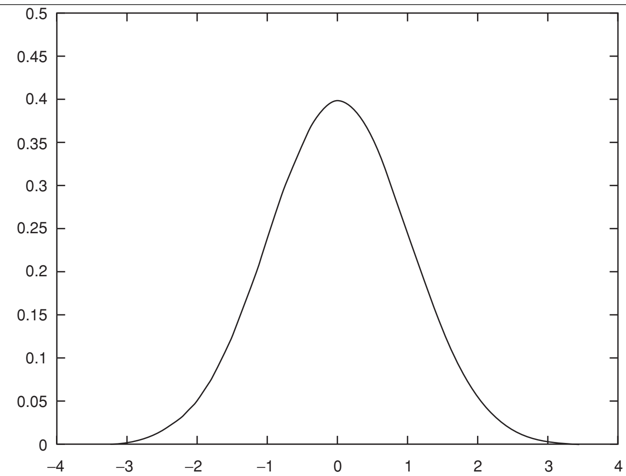

Figure 18.1. The density of values in the normal distribution.

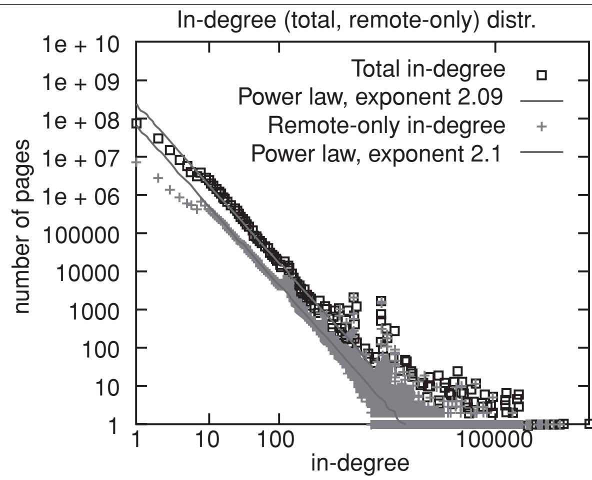

Figure 18.2. A power law distribution (such as this one for the number of Web page in-links, from Broder et al. [79]) shows up as a straight line on a log-log plot.

P1: SBT
cuus984-net CUUS984-Easley 0 521 19533 1 November 30, 2009 16:2

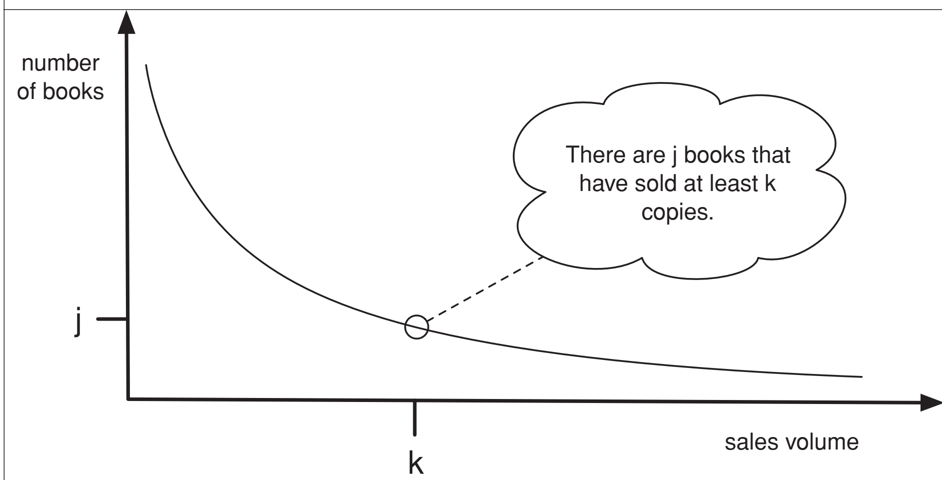

Figure 18.3. The distribution of popularity.

P1: SBT
cuus984-net CUUS984-Easley 0 521 19533 1 November 30, 2009 16:2

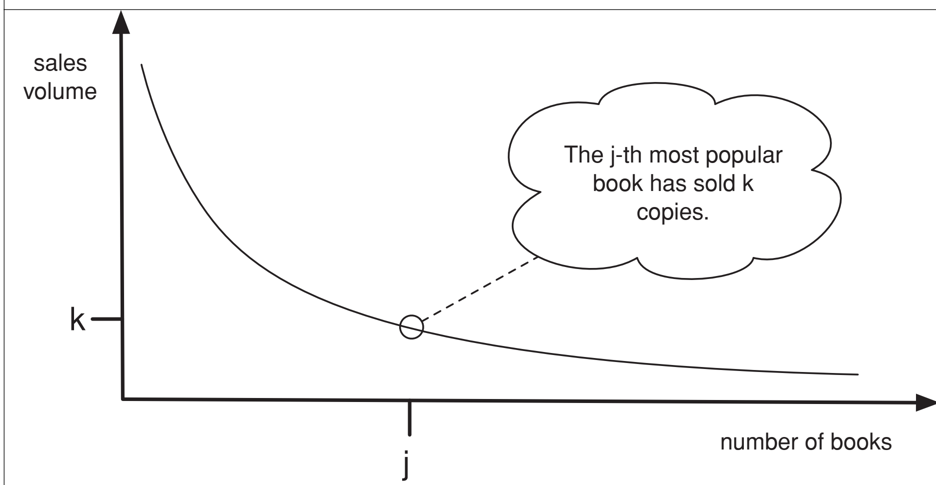

Figure 18.4. The distribution of popularity.

P1: SBT
cuus984-net CUUS984-Easley 0 521 19533 1 November 30, 2009 16:2

		w	
		A	B
v	A	a, a	$0, 0$
	B	$0, 0$	b, b

Figure 19.1. *A*-*B* Coordination Game

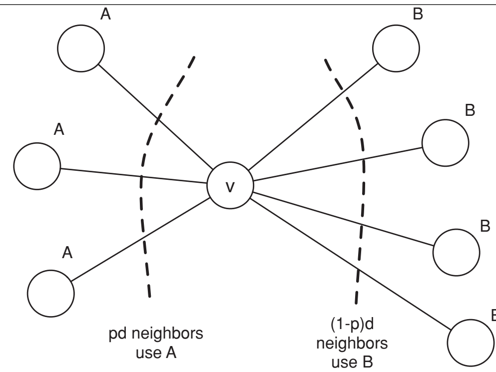

Figure 19.2. v must choose between behavior A and behavior B, based on what its neighbors are doing.

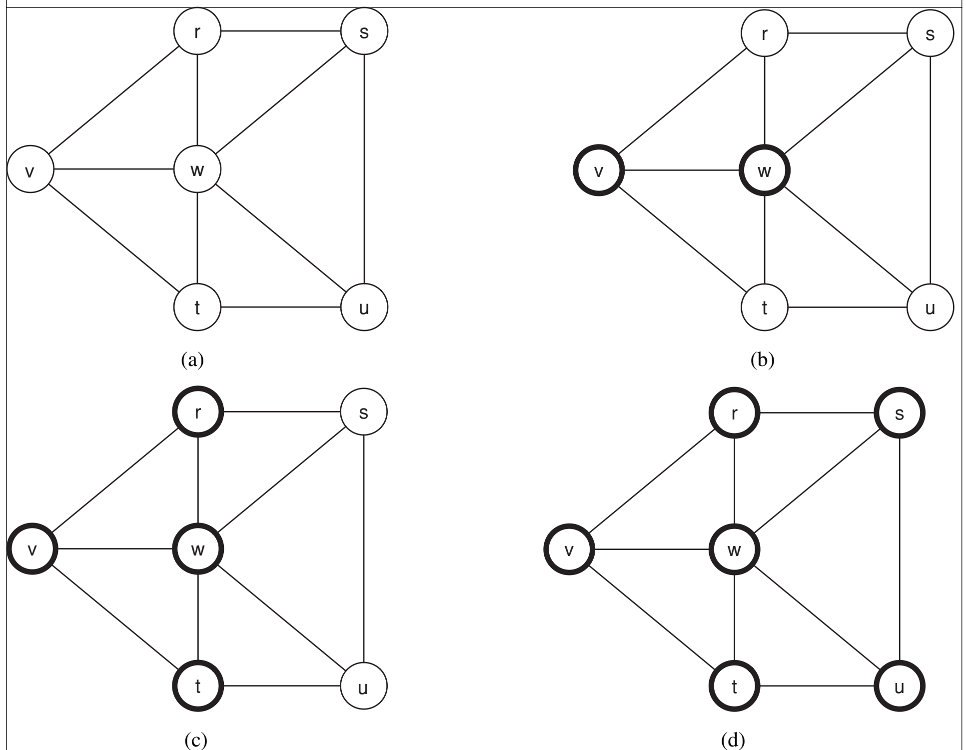

Figure 19.3. Starting with v and w as the initial adopters, and payoffs $a = 3$ and $b = 2$, the new behavior A spreads to all nodes in two steps. Nodes adopting A in a given step are drawn with dark borders; nodes adopting B are drawn with light borders.

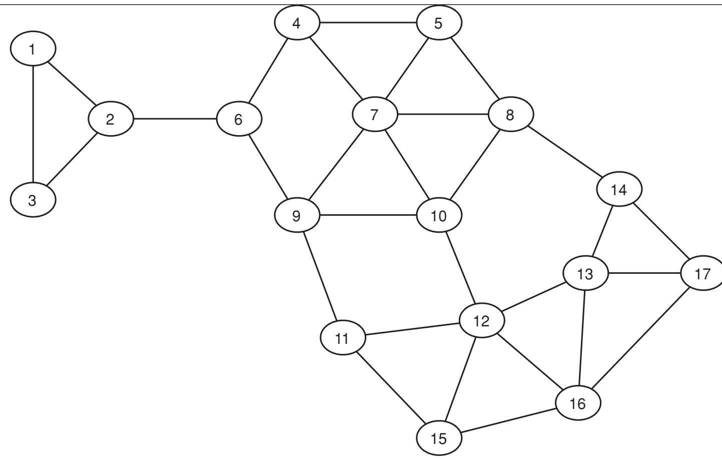

Figure 19.4. A larger example.

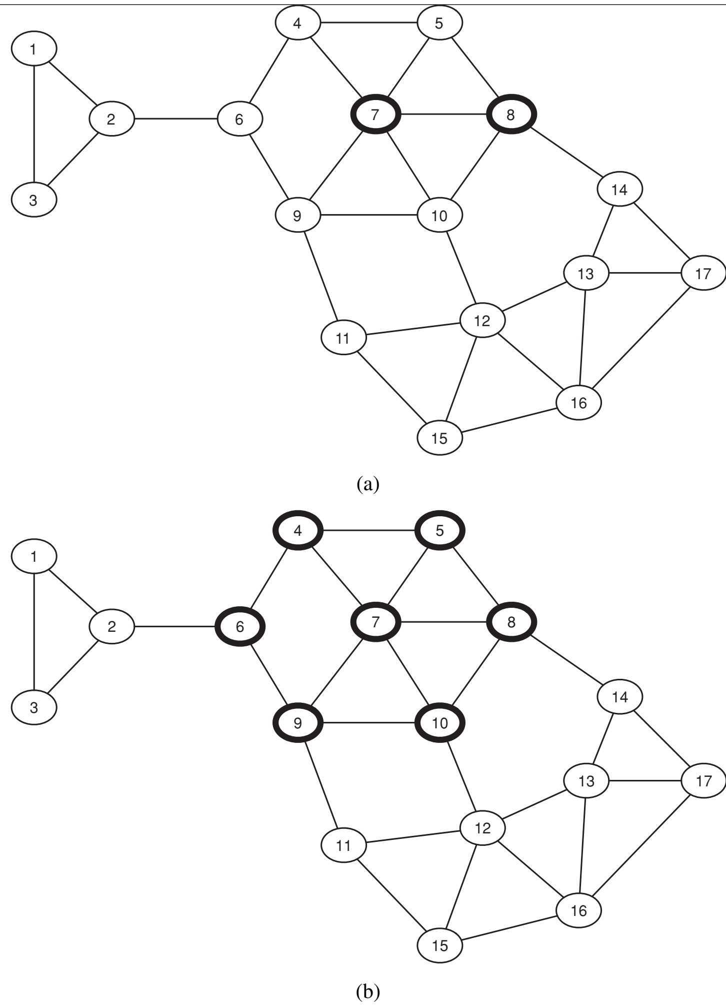

Figure 19.5. Starting with nodes 7 and 8 as the initial adopters, the new behavior *A* spreads to some but not all of the remaining nodes.

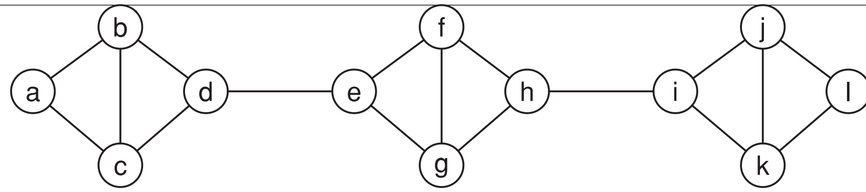

Figure 19.6. A collection of four-node clusters, each of density $2/3$.

P1: SBT
cuus984-net CUUS984-Easley 0 521 19533 1 November 30, 2009 16:2

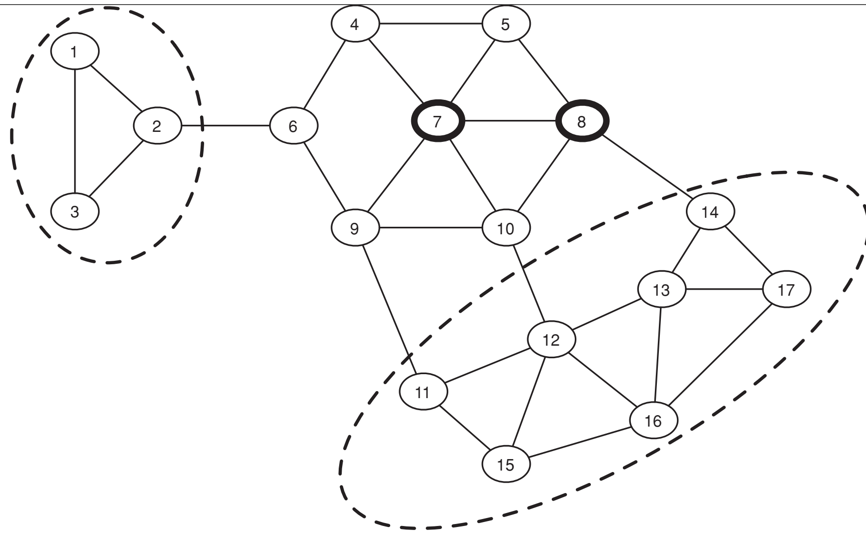

Figure 19.7. Two clusters of density 2/3 in the network from Figure 19.4.

P1: SBT
cuus984-net CUUS984-Easley 0 521 19533 1 November 30, 2009 16:2

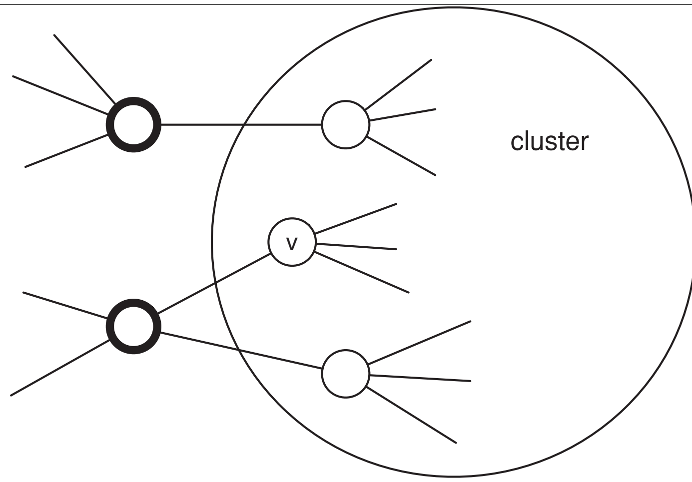

Figure 19.8. The spread of a new behavior, when nodes have threshold q, stops when it reaches a cluster of density greater than $(1 - q)$.

P1: SBT
cuus984-net CUUS984-Easley 0 521 19533 1 November 30, 2009 16:2

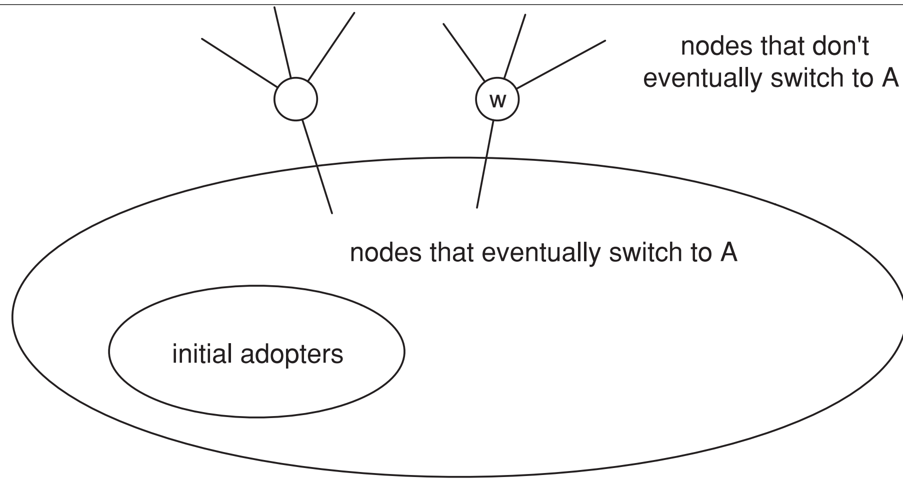

Figure 19.9. If the spread of A stops before filling out the whole network, the set of nodes that remain with B form a cluster of density greater than $1 - q$.

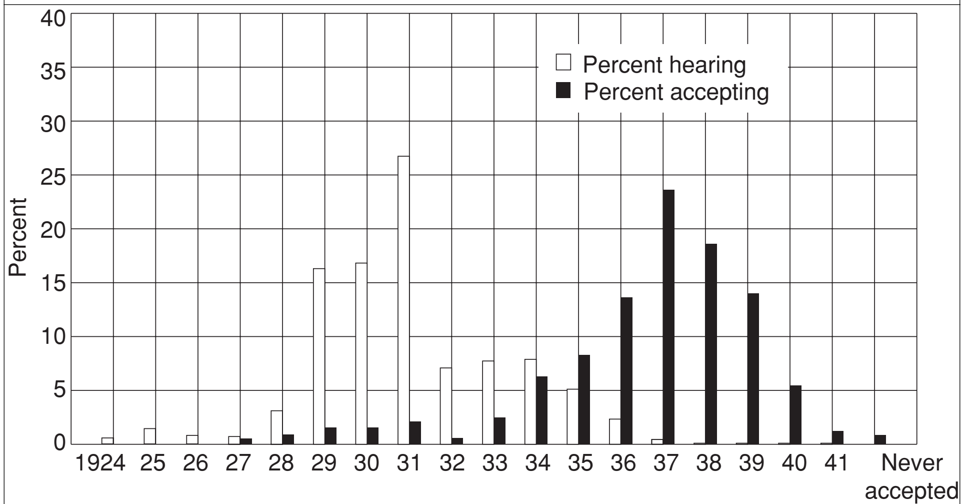

Figure 19.10. The years of first awareness and first adoption for hybrid seed corn in the Ryan-Gross study. (Image from [352].)

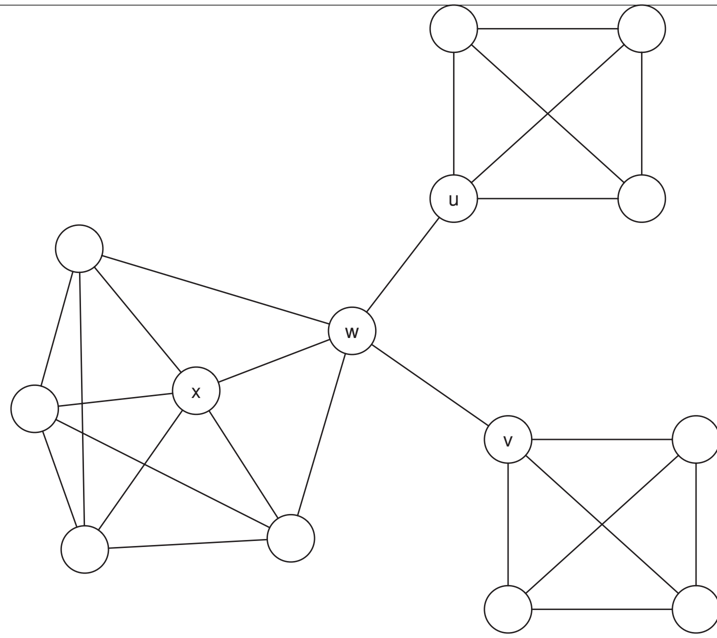

Figure 19.11. The u-w and v-w edges are more likely to act as conduits for information than for high-threshold innovations.

		w A	w B
v	A	a_v, a_w	$0, 0$
	B	$0, 0$	b_v, b_w

Figure 19.12. *A*-*B* Coordination Game

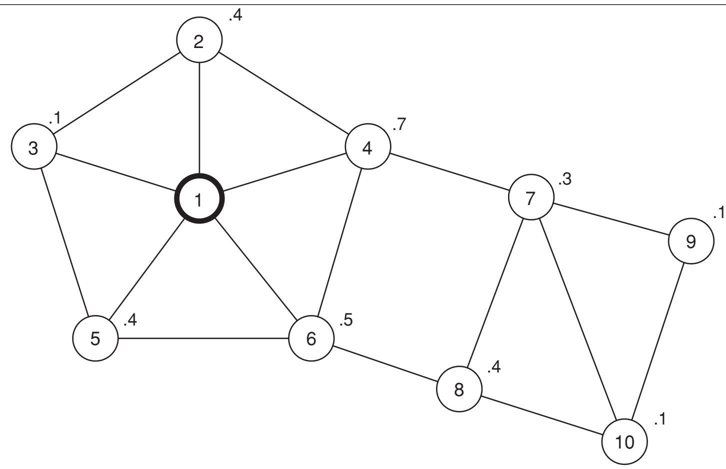

(a)

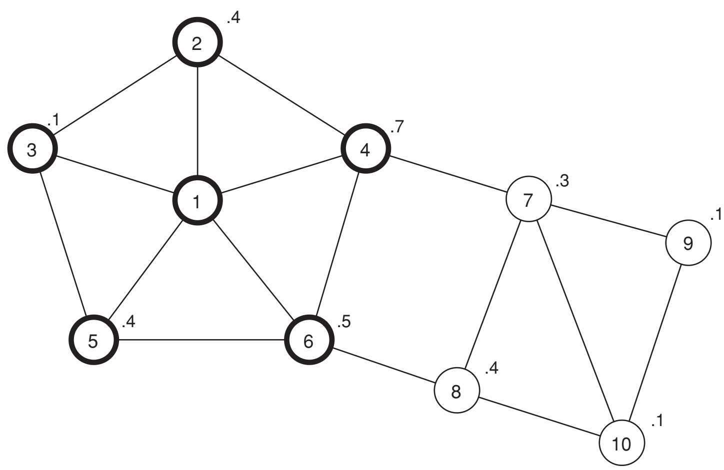

(b)

Figure 19.13. Starting with node 1 as the unique initial adopter, the new behavior *A* spreads to some but not all of the remaining nodes.

P1: SBT
cuus984-net CUUS984-Easley 0 521 19533 1 November 30, 2009 16:2

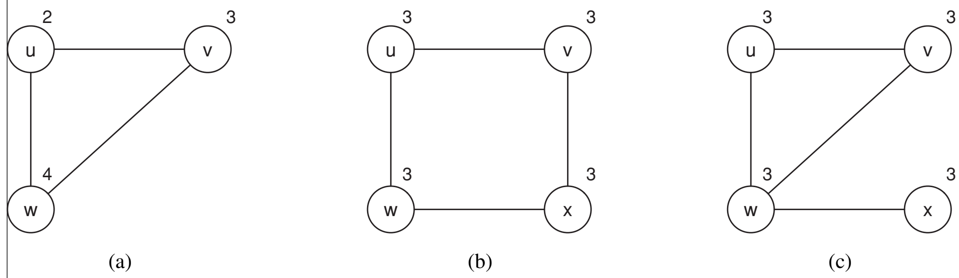

Figure 19.14. Each node in the network has a threshold for participation, but only knows the threshold of itself and its neighbors.

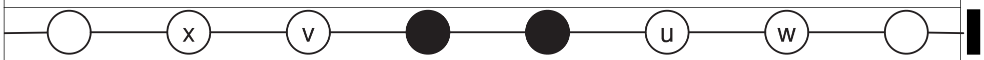

Figure 19.15. An infinite path with a set of early adopters of behavior *A* (shaded).

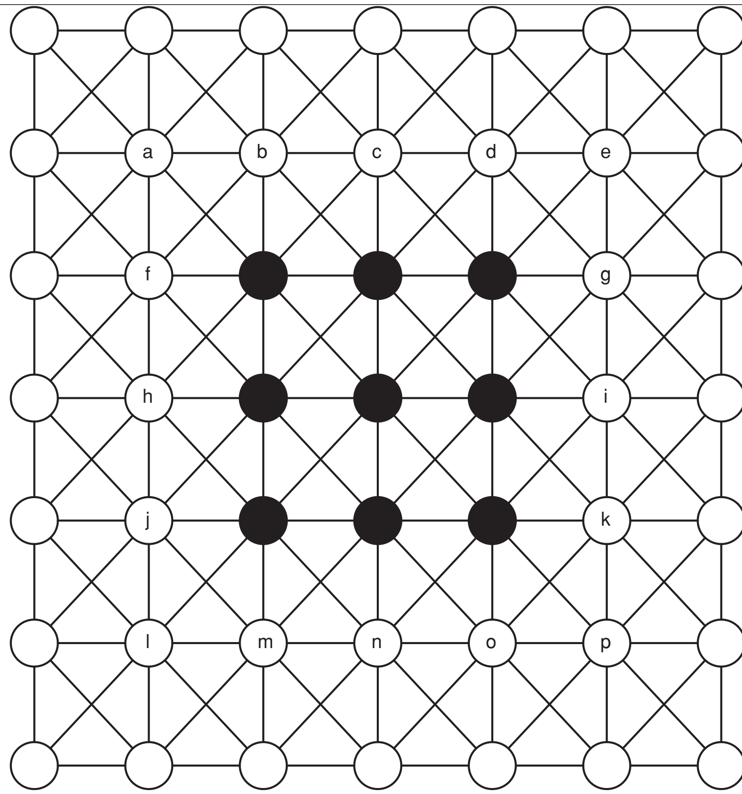

Figure 19.16. An infinite grid with a set of early adopters of behavior A (shaded).

P1: SBT
cuus984-net CUUS984-Easley 0 521 19533 1 November 30, 2009 16:2

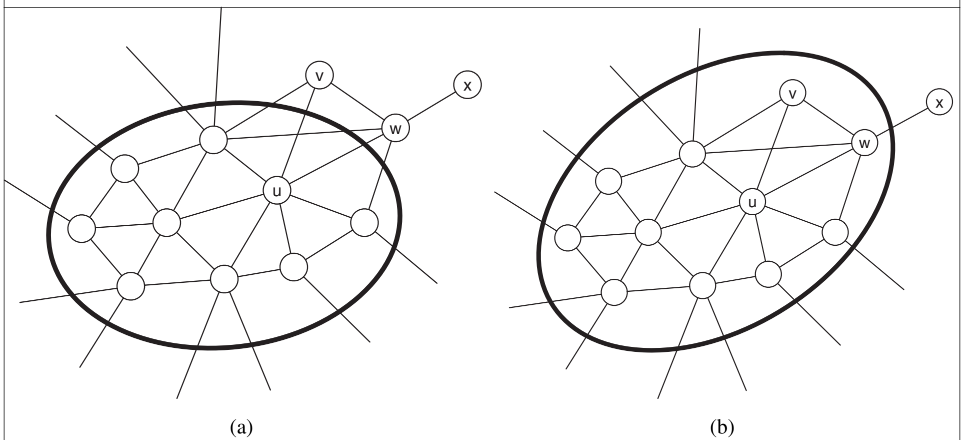

Figure 19.17. Let the nodes inside the dark oval be the adopters of A. One step of the process is shown, in which v and w adopt A: after they adopt, the size of the interface has strictly decreased. In general, the size of the interface strictly decreases with each step of the process when $q > \frac{1}{2}$.

			w	
		A	B	AB
	A	a, a	$0, 0$	a, a
v	B	$0, 0$	b, b	b, b
	AB	a, a	b, b	$(a, b)^+, (a, b)^+$

Figure 19.18. A Coordination Game with a bilingual option. Here the notation $(a, b)^+$ denotes the larger of a and b.

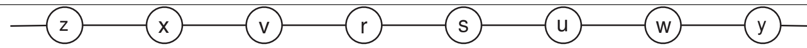

Figure 19.19. An infinite path, with nodes r and s as initial adopters of A.

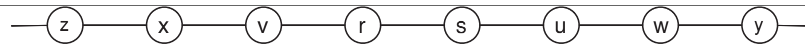

Start	B	B	B	A	A	B	B	B
Step 1	B	B	AB	A	A	AB	B	B
Step 2	B	AB	AB	A	A	AB	AB	B
Step 3	AB	AB	A	A	A	A	AB	AB
Step 4	AB	A	A	A	A	A	A	AB

Figure 19.20. With payoffs $a = 5$ and $b = 3$ for interaction using A and B respectively, and a cost $c = 1$ for being bilingual, the strategy A spreads outward from the initial adopters r and s through a two-phase structure. First, the strategy AB spreads, and then behind it, nodes switch permanently from AB to A.

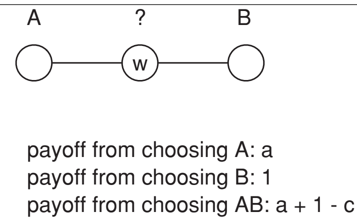

Figure 19.21. The payoffs to a node on the infinite path with two neighbors using A and B.

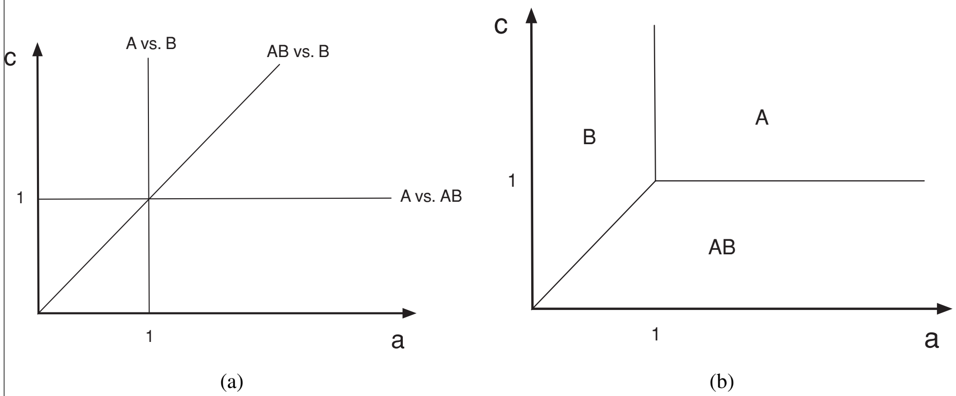

Figure 19.22. Given a node with neighbors using A and B, the values of a and c determine which of the strategies A, B, or AB it will choose. (Here, by re-scaling, we can assume $b = 1$.) We can represent the choice of strategy as a function of a and c by dividing up the (a, c)-plane into regions corresponding to different choices.

P1: SBT
cuus984-net CUUS984-Easley 0 521 19533 1 November 30, 2009 16:2

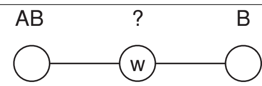

payoff from choosing A: a
payoff from choosing B: 2
payoff from choosing AB: a + 1 - c (if A is better)

Figure 19.23. The payoffs to a node on the infinite path with two neighbors using AB and B.

P1: SBT
cuus984-net CUUS984-Easley 0 521 19533 1 November 30, 2009 16:2

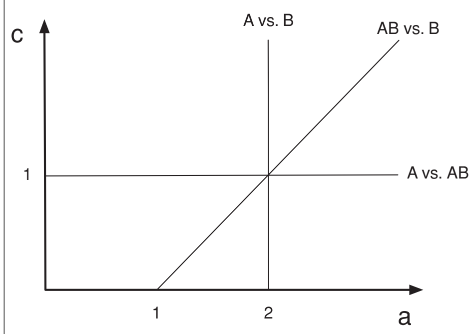

(a) *Lines showing break-even points between strategies.*

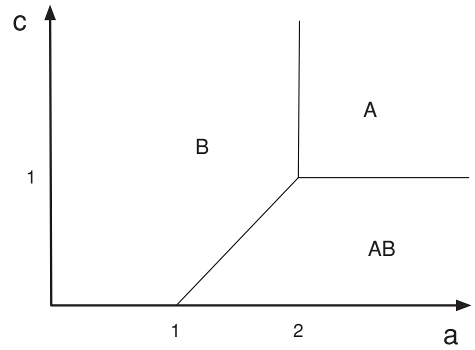

(b) *Regions defining the best choice of strategy.*

Figure 19.24. Given a node with neighbors using AB and B, the values of a and c determine which of the strategies A, B, or AB it will choose, as shown by this division of the (a, c)-plane into regions.

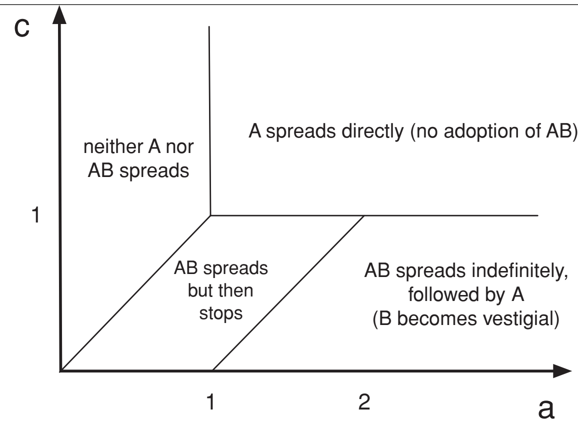

Figure 19.25. There are four possible outcomes for how *A* spreads or fails to spread on the infinite path, indicated by this division of the (a, c)-plane into four regions.

P1: SBT
cuus984-net CUUS984-Easley 0 521 19533 1 November 30, 2009 16:2

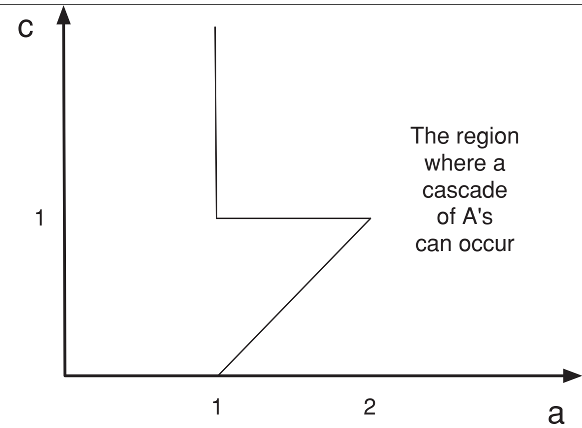

Figure 19.26. The set of values for which a cascade of A's can occur defines a region in the (a, c)-plane consisting of a vertical line with a triangular "cut-out."

P1: SBT
cuus984-net CUUS984-Easley 0 521 19533 1 November 30, 2009 16:2

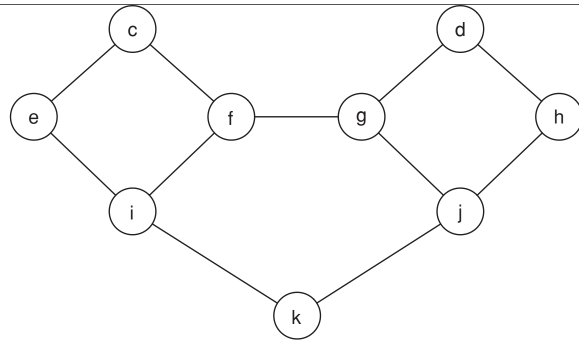

Figure 19.27.

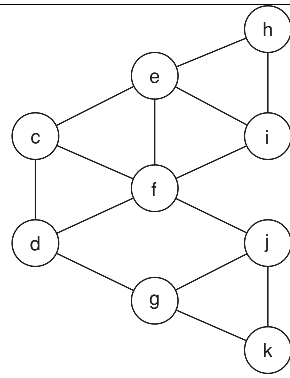

Figure 19.28.

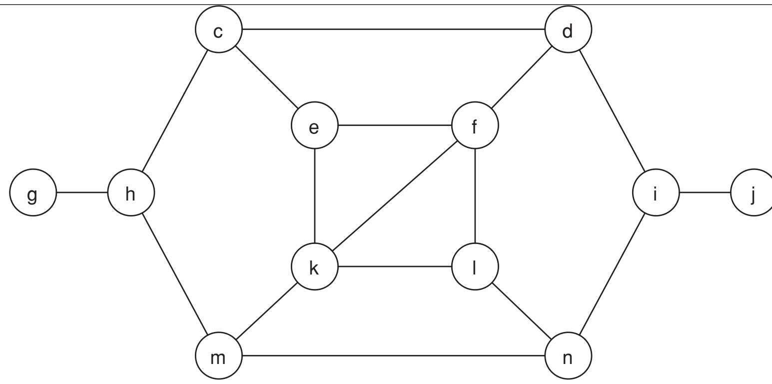

Figure 19.29. A social network in which a new behavior is spreading.

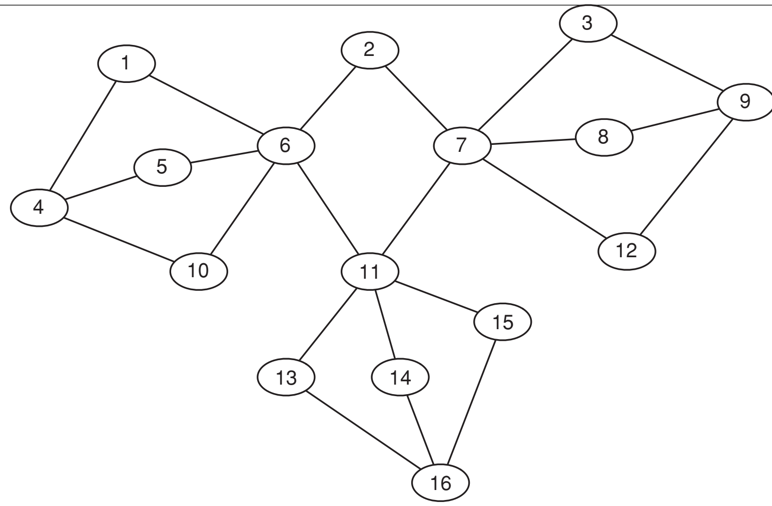

Figure 19.30. A social network on which a new behavior diffuses.

P1: SBT
cuus984-net CUUS984-Easley 0 521 19533 1 November 30, 2009 16:2

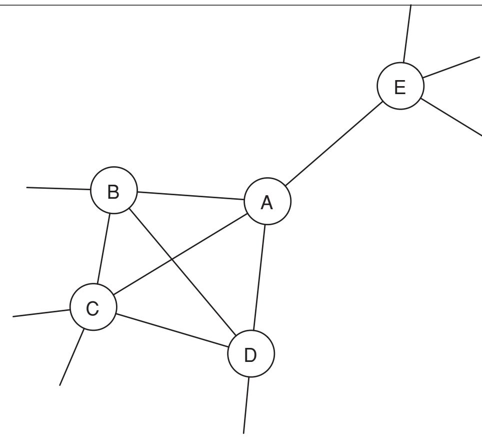

Figure 19.31.

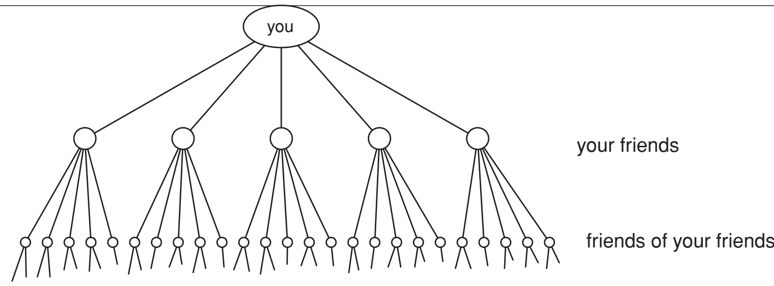

(a)

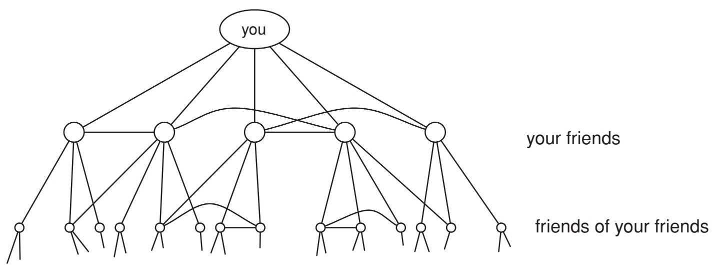

(b)

Figure 20.1. Social networks expand to reach many people in only a few steps.

P1: SBT
cuus984-net CUUS984-Easley 0 521 19533 1 November 30, 2009 16:2

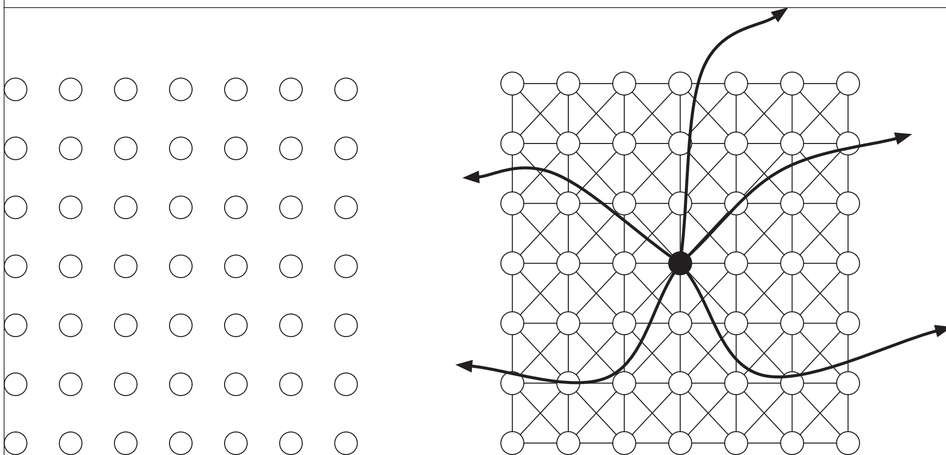

(a) (b)

Figure 20.2. The Watts-Strogatz model arises from a highly clustered network (such as the grid), with a small number of random links added in.

P1: SBT
cuus984-net CUUS984-Easley 0 521 19533 1 November 30, 2009 16:2

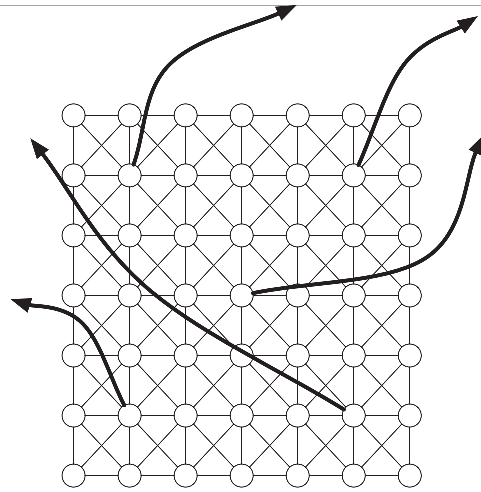

Figure 20.3. The general conclusions of the Watts-Strogatz model still follow even if only a small fraction of the nodes on the grid each have a *single* random link.

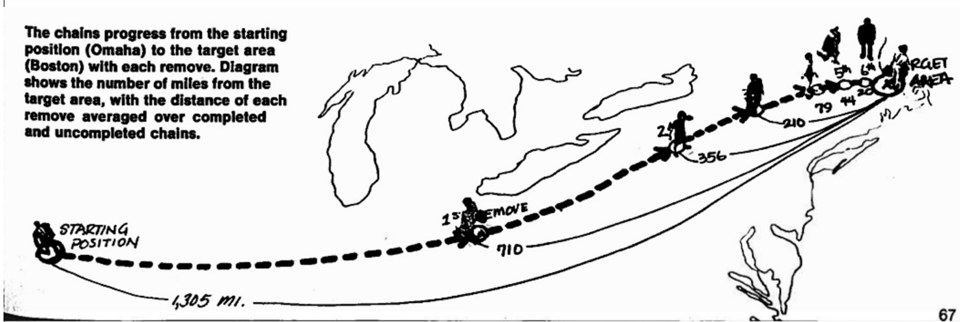

Figure 20.4. A drawing of one of the successful paths converging on the target person, from Milgram's original article in *Psychology Today*. (Image from [292].)

P1: SBT
cuus984-net CUUS984-Easley 0 521 19533 1 November 30, 2009 16:2

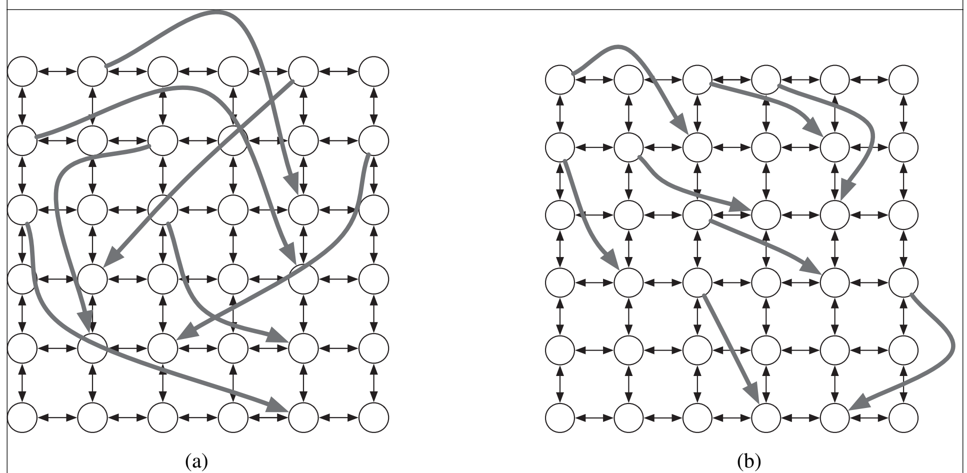

Figure 20.5. With a small clustering exponent, the random edges tend to span long distances on the grid; as the clustering exponent increases, the random edges become shorter.

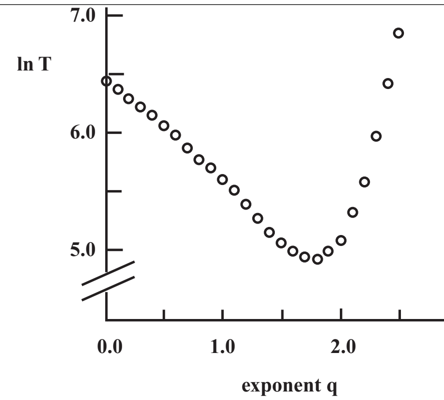

Figure 20.6. Simulation of decentralized search in the grid-based model with clustering exponent q. Each point is the average of 1000 runs on (a slight variant of) a grid with 400 million nodes. The delivery time is best in the vicinity of exponent $q = 2$, as expected; but even with this number of nodes, the delivery time is comparable over the range between 1.5 and 2 [244].

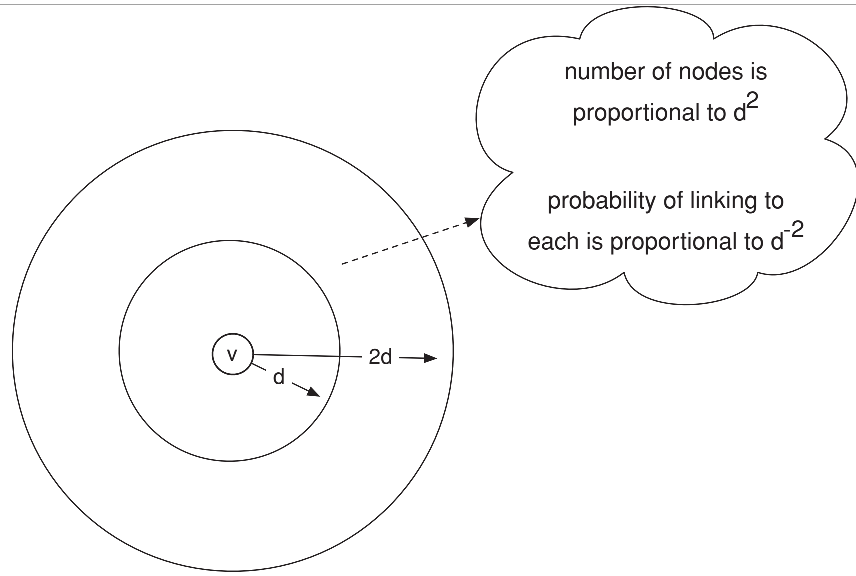

Figure 20.7. The concentric scales of resolution around a particular node.

P1: SBT
cuus984-net CUUS984-Easley 0 521 19533 1 November 30, 2009 16:2

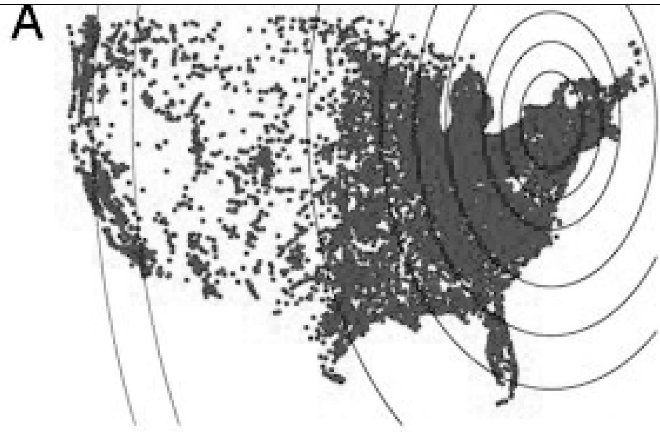

Figure 20.8. The population of the LiveJournal network studied by Liben-Nowell et al. (Image from [272].)

P1: SBT
cuus984-net CUUS984-Easley 0 521 19533 1 November 30, 2009 16:2

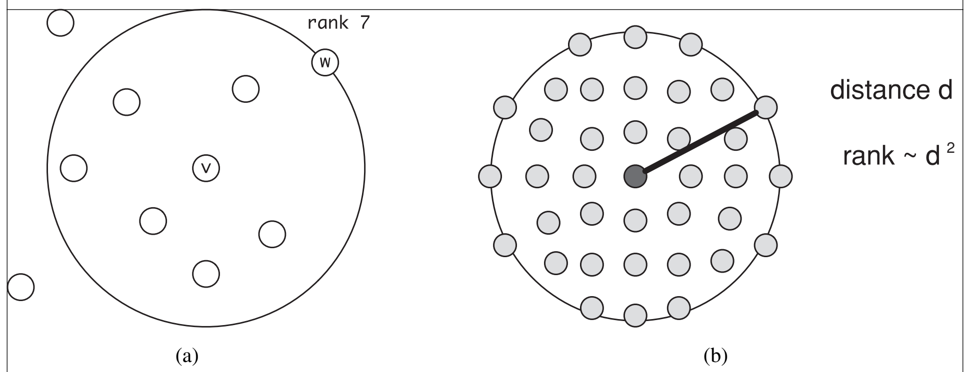

Figure 20.9. When the population density is non-uniform, it can be useful to understand how far w is from v in terms of its *rank* rather than its physical distance. In (a), we say that w has rank 7 with respect to v because it is the 7th closest node to v, counting outward in order of distance. In (b), we see that for the original case in which the nodes have a uniform population density, a node w at distance d from v will have a rank that is proportional to d^2, since all the nodes inside the circle of radius d will be closer to v than w is.

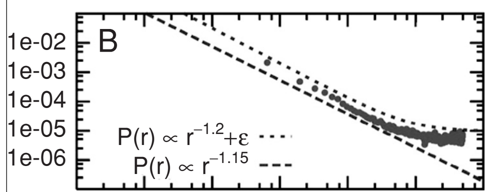

(a)

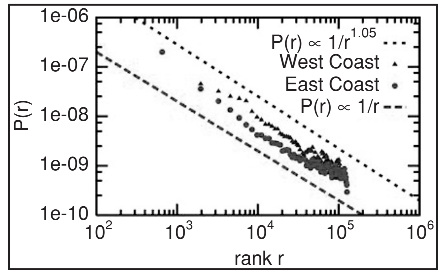

(b)

Figure 20.10. The probability of a friendship as a function of geographic rank on the blogging site LiveJournal. (Image from [272].)

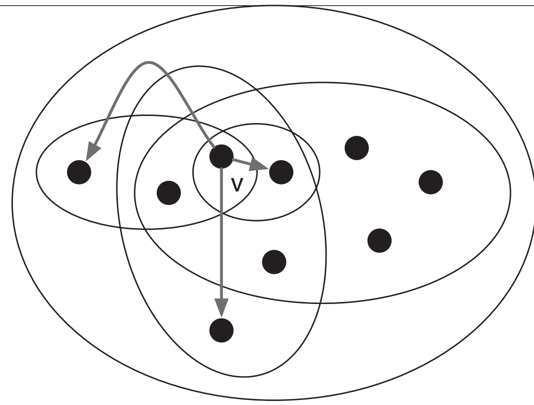

Figure 20.11. When nodes belong to multiple foci, we can define the social distance between two nodes to be the smallest focus that contains both of them. In the figure, the foci are represented by ovals; the node labeled v belongs to five foci of sizes 2, 3, 5, 7, and 9 (with the largest focus containing all the nodes shown).

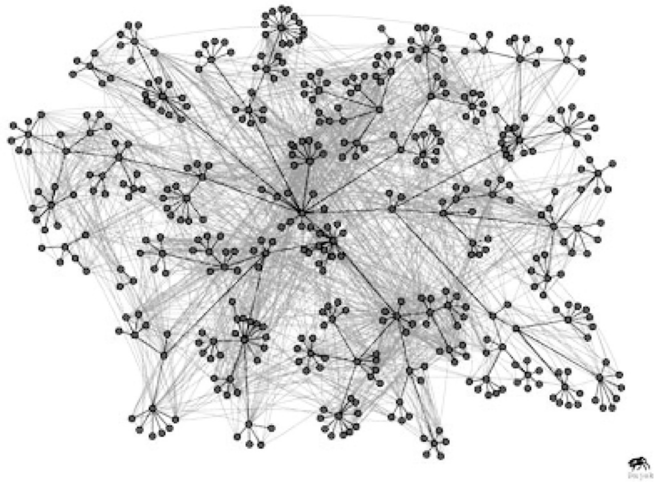

Figure 20.12. The pattern of e-mail communication among 436 employees of Hewlett Packard Research Lab is superimposed on the official organizational hierarchy, showing how network links span different social foci [6]. (Image from http://www-personal.umich.edu/ ladamic/img/hplabsemailhierarchy.jpg)

P1: SBT
cuus984-net CUUS984-Easley 0 521 19533 1 November 30, 2009 16:2

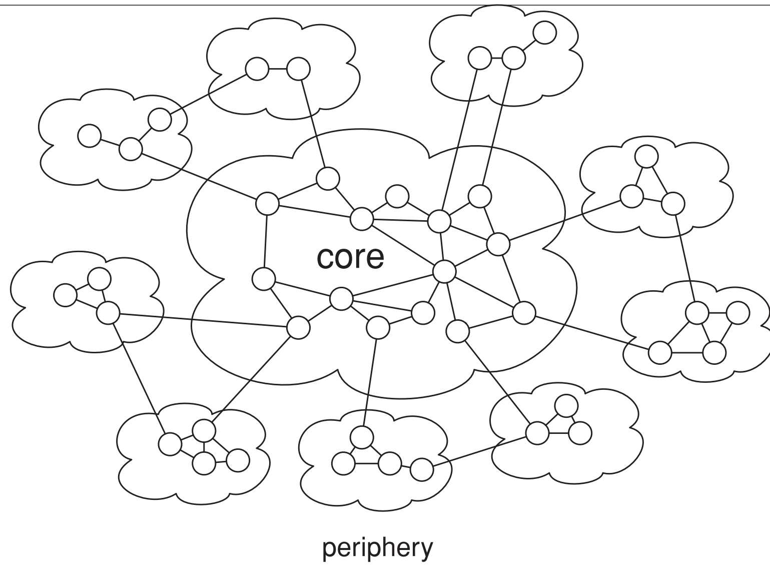

Figure 20.13. The core-periphery structure of social networks.

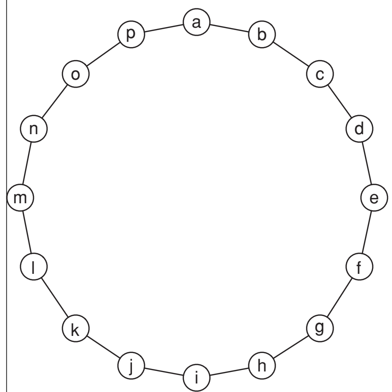

(a)

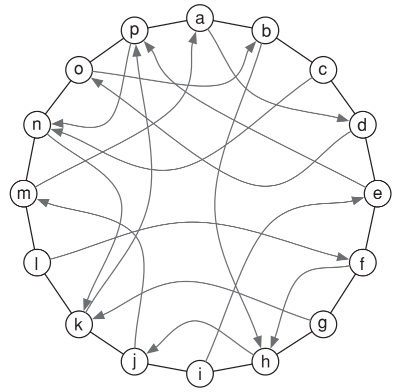

(b)

Figure 20.14. The analysis of decentralized search is a bit cleaner in one dimension than in two, although it is conceptually easy to adapt the arguments to two dimensions. As a result, we focus most of the discussion on a one-dimensional ring augmented with random long-range links.

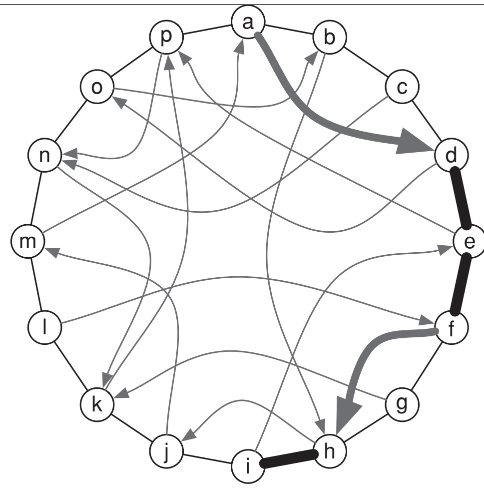

Figure 20.15. In myopic search, the current message-holder chooses the contact the lies closest to the target (as measured on the ring), and it forwards the message to this contact.

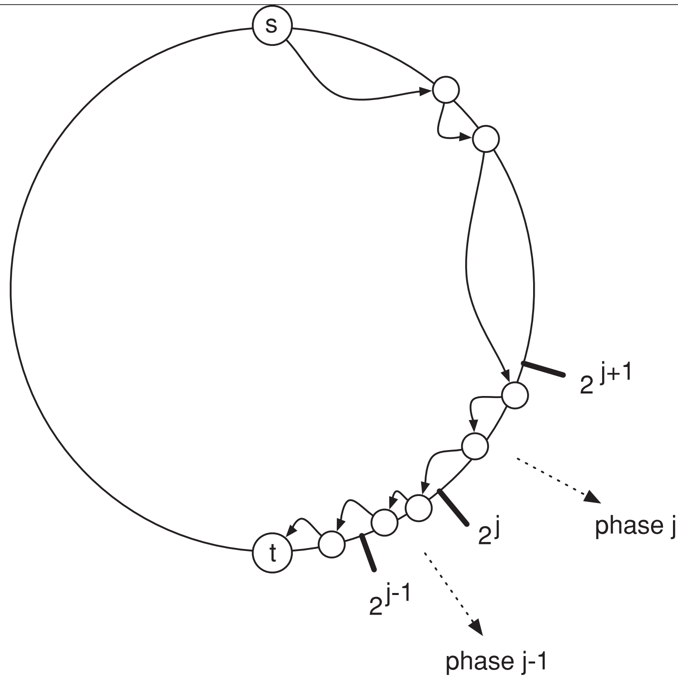

Figure 20.16. We analyze the progress of myopic search in *phases*. Phase j consists of the portion of the search in which the message's distance from the target is between 2^j and 2^{j+1}.

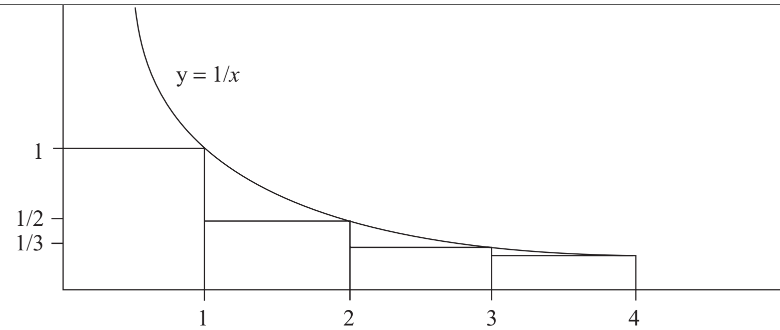

Figure 20.17. Determining the normalizing constant for the probability of links involves evaluating the sum of the first $n/2$ reciprocals. An upper bound on the value of this sum can be determined from the area under the curve $y = 1/x$.

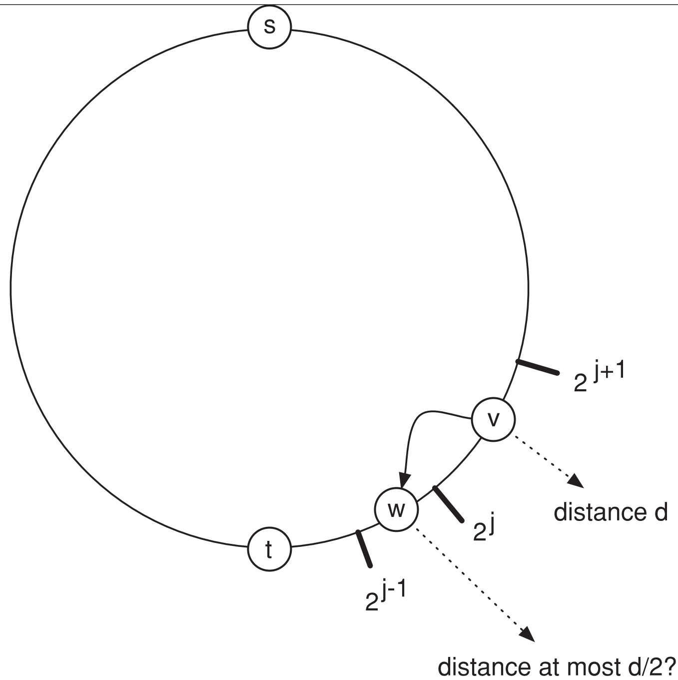

Figure 20.18. At any given point in time, the search is in some phase j, with the message residing at a node v at distance d from the target. The phase will come to an end if v's long-range contact lies at distance $\leq d/2$ from the target t, and so arguing that the probability of this event is large provides a way to show that the phase will not last too long.

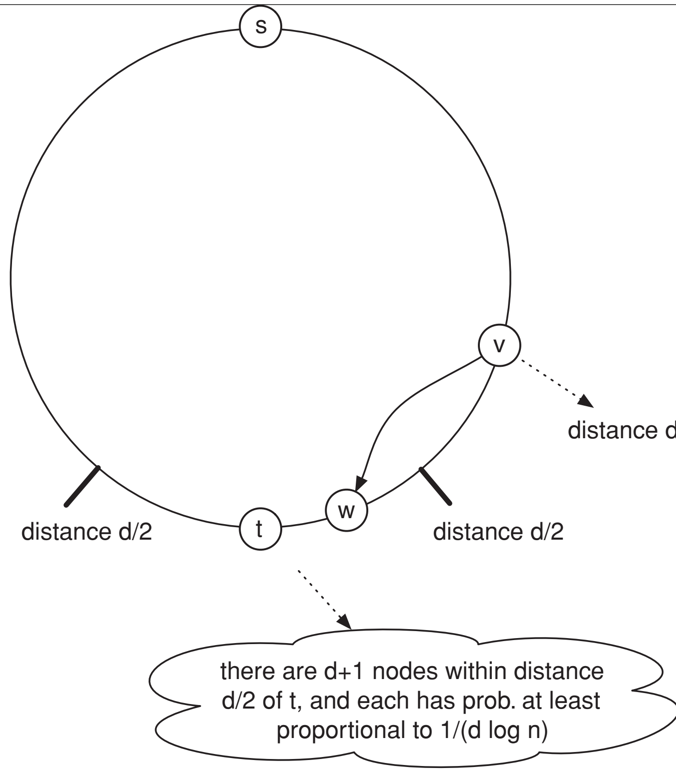

Figure 20.19. Showing that, with reasonable probability, v's long-range contact lies within half the distance to the target.

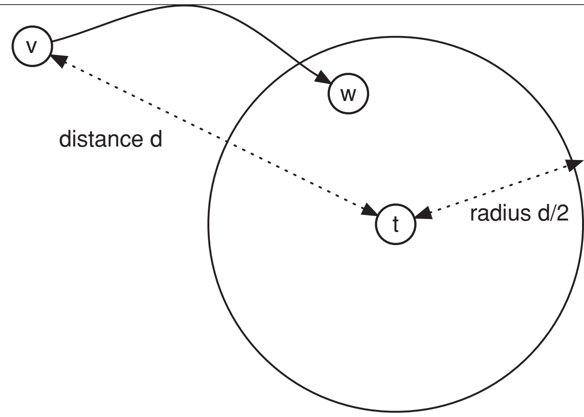

Figure 20.20. The analysis for the one-dimensional ring can be carried over almost directly to the two-dimensional grid. In two dimensions, with the message at a current distance d from the target t, we again look at the set of nodes within distance $d/2$ of t, and argue that the probability of entering this set in a single step is reasonably large.

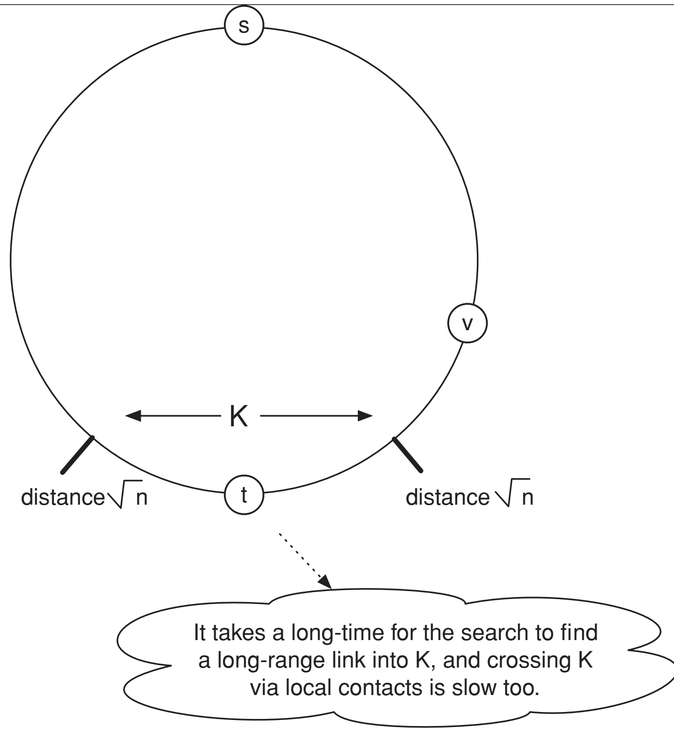

Figure 20.21. To show that decentralized search strategies require large amounts of time with exponent $q = 0$, we argue that it is difficult for the search to cross the set of $\sqrt{n}$ nodes closest to the target. Similar arguments hold for other exponents $q < 1$.

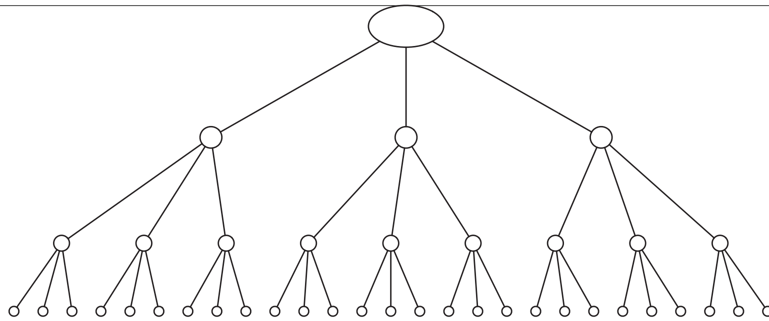

(a)

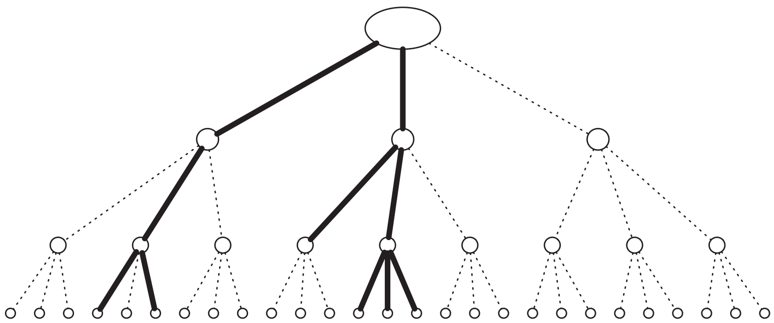

(b)

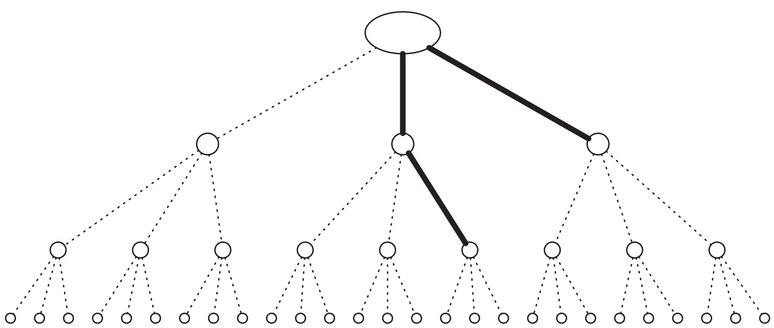

(c)

Figure 21.1. The branching process model is a simple framework for reasoning about the spread of an epidemic as one varies both the amount of contact among individuals and the level of contagion.

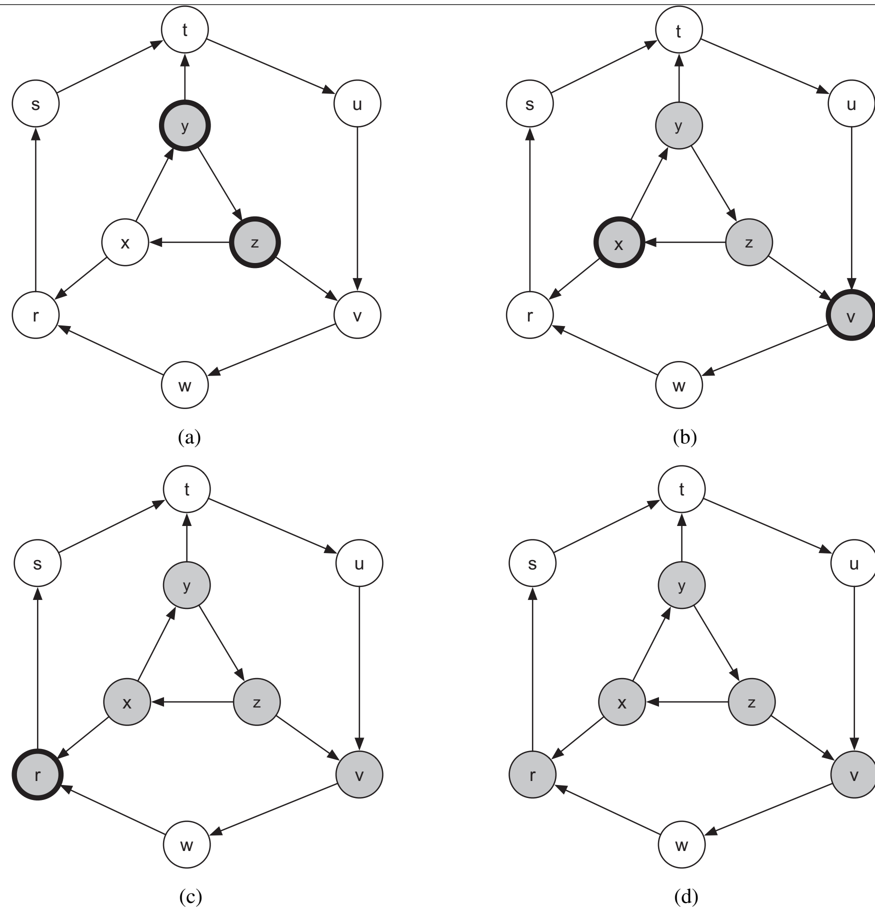

Figure 21.2. The course of an SIR epidemic in which each node remains infectious for a number of steps equal to $t_I = 1$. Starting with nodes y and z initially infected, the epidemic spreads to some but not all of the remaining nodes. In each step, shaded nodes with dark borders are in the Infectious (I) state and shaded nodes with thin borders are in the Removed (R) state.

P1: SBT
cuus984-net CUUS984-Easley 0 521 19533 1 November 30, 2009 16:2

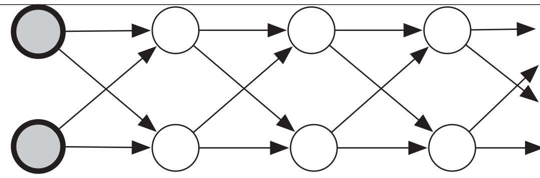

Figure 21.3. In this network, the epidemic is forced to pass through a narrow "channel" of nodes. In such a structure, even a highly contagious disease will tend to die out relatively quickly.

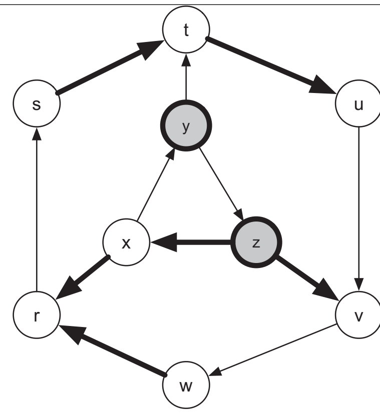

Figure 21.4. An equivalent way to view an SIR epidemic is in terms of *percolation*, where we decide in advance which edges will transmit infection (should the opportunity arise) and which will not.

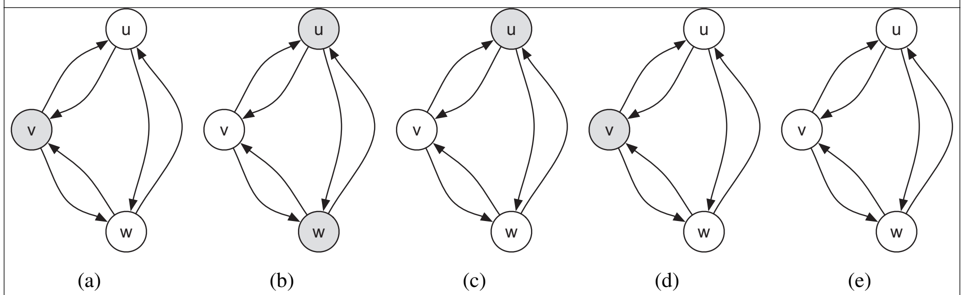

Figure 21.5. In an SIS epidemic, nodes can be infected, recover, and then be infected again. In each step, the nodes in the Infectious state are shaded.

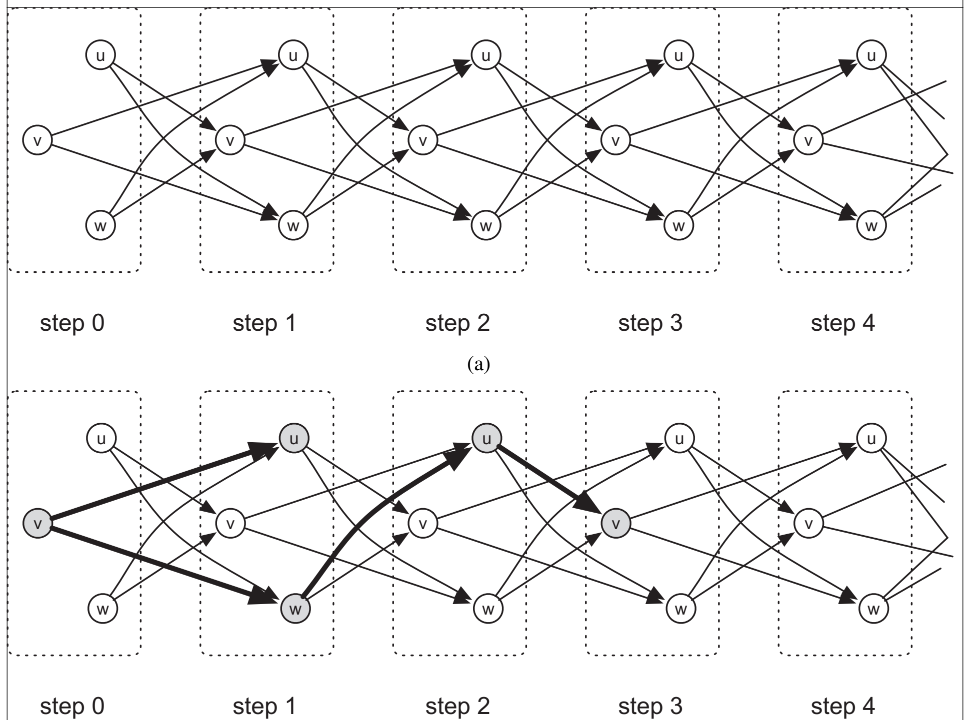

(a)

(b)

Figure 21.6. An SIS epidemic can be represented in the SIR model by creating a separate copy of the contact network for each time step: a node at time t can infect its contact neighbors at time $t + 1$.

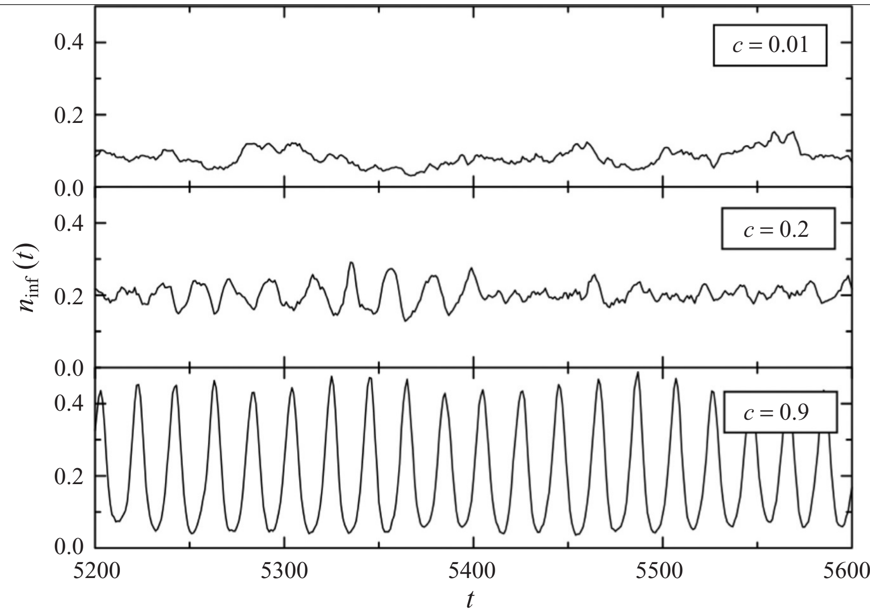

Figure 21.7. These plots depict the number of infected people over time (the quantity $n_{\mathrm{inf}}(t)$ on the y-axis) by SIRS epidemics in networks with different proportions of long-range links. With c representing the fraction of long-range links, we see an abscence of oscillations for small c ($c = 0.01$), wide oscillations for large c ($c = 0.9$), and a transitional region ($c = 0.2$) where oscillations intermittently appear and then disappear. (Results and image from [263].)

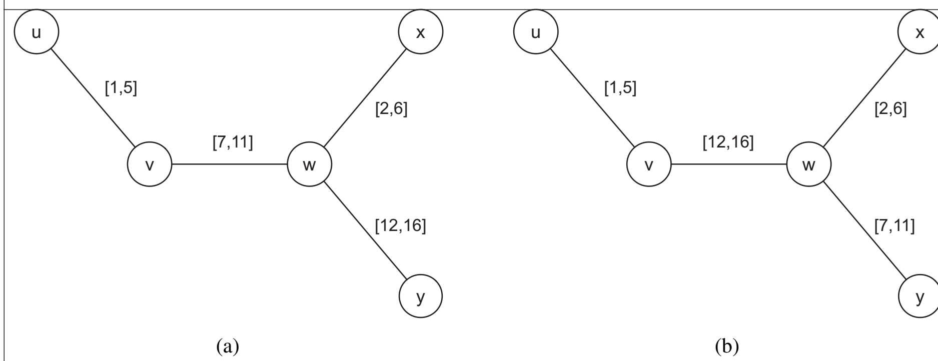

Figure 21.8. Different timings for the edges in a contact network can affect the potential for a disease to spread among individuals. For example, in (a) the disease can potentially pass all the way from u to y, while in (b) it cannot.

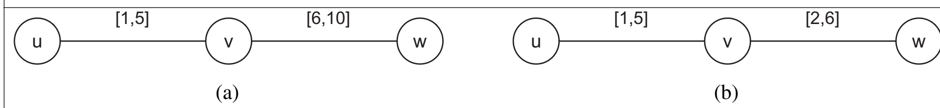

Figure 21.9. A disease tends to be able to spread more widely with concurrent partnerships (b) than with serial partnerships (a).

P1: SBT
cuus984-net CUUS984-Easley 0 521 19533 1 November 30, 2009 16:2

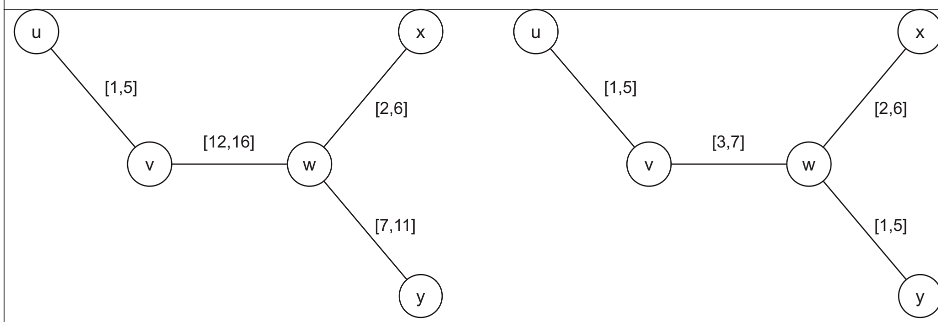

(a) (b)

Figure 21.10. In larger networks, the effects of concurrency on disease spreading can become particularly pronounced.

P1: SBT
cuus984-net CUUS984-Easley 0 521 19533 1 November 30, 2009 16:2

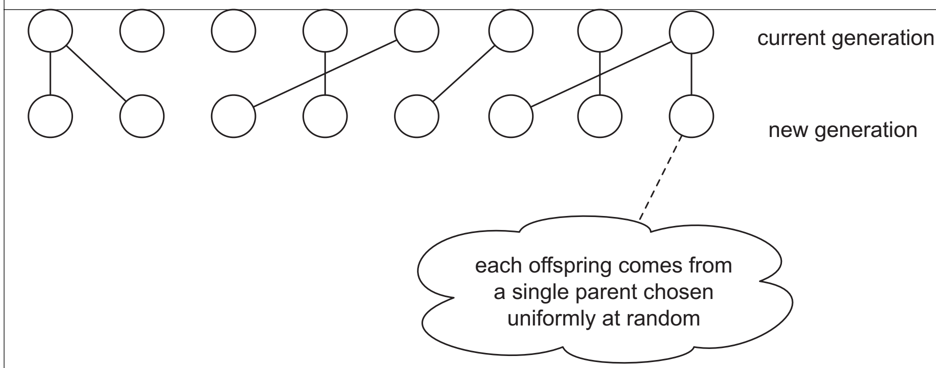

Figure 21.11. In the basic Wright-Fisher model of single-parent ancestry, time moves step-by-step in generations; there are a fixed number of individuals in each generation; and each offspring in a new generation comes from a single parent in the current generation.

P1: SBT
cuus984-net CUUS984-Easley 0 521 19533 1 November 30, 2009 16:2

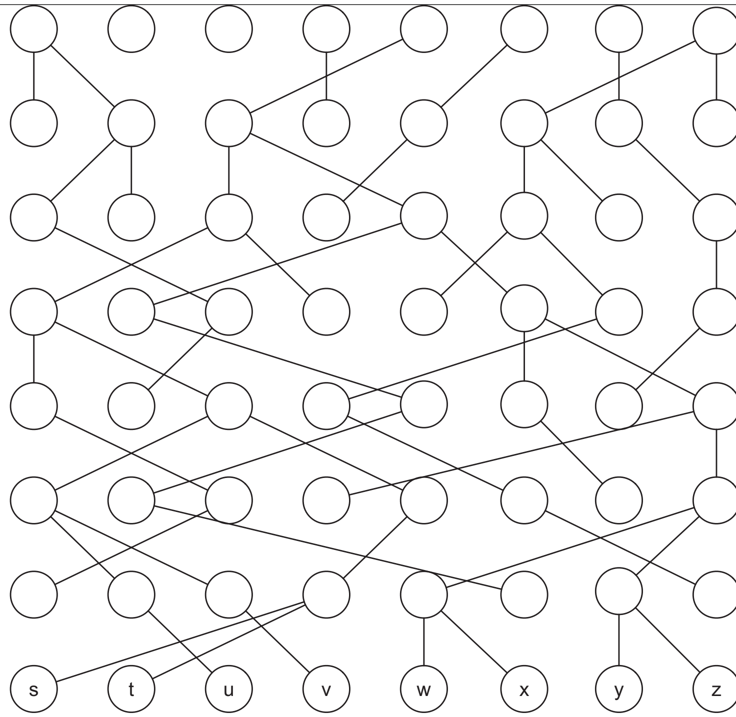

Figure 21.12. We can run the model forward in time through a sequence of generations, ending in a set of present-day individuals. Each present-day individual can then follow its single-parent lineage by following edges leading upward through the network.

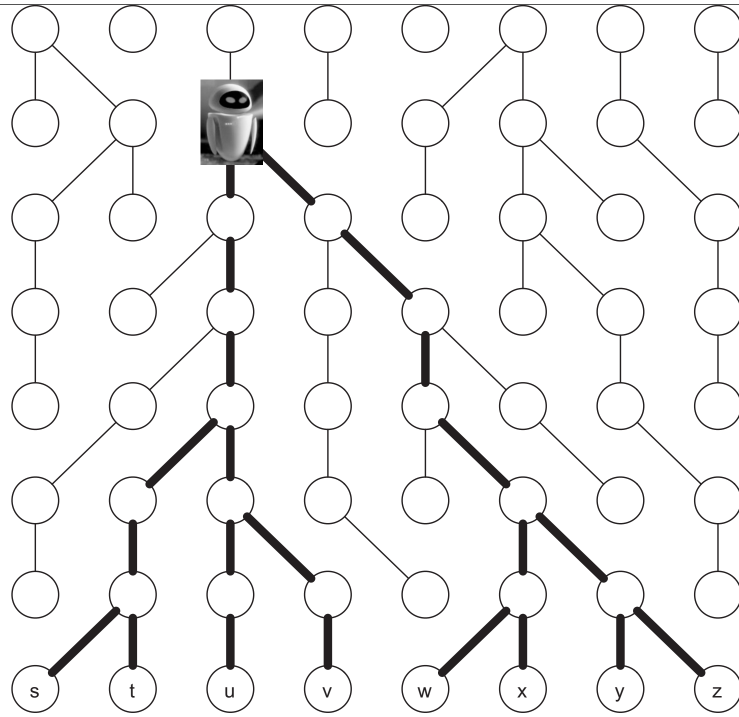

Figure 21.13. A re-drawing of the single-parent network fom Figure 21.12. As we move back in time, lineages of different present-day individuals coalesce until they have all converged at the most recent common ancestor.

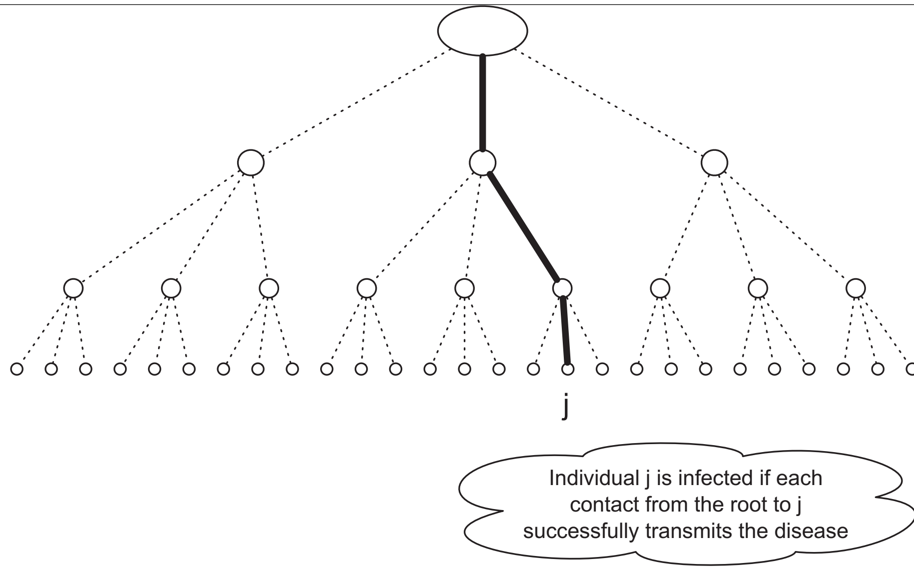

Figure 21.14. To determine the probability that a particular node is infected, we multiply the (independent) probabilities of infection on each edge leading from the root to the node.

P1: SBT
cuus984-net CUUS984-Easley 0 521 19533 1 November 30, 2009 16:2

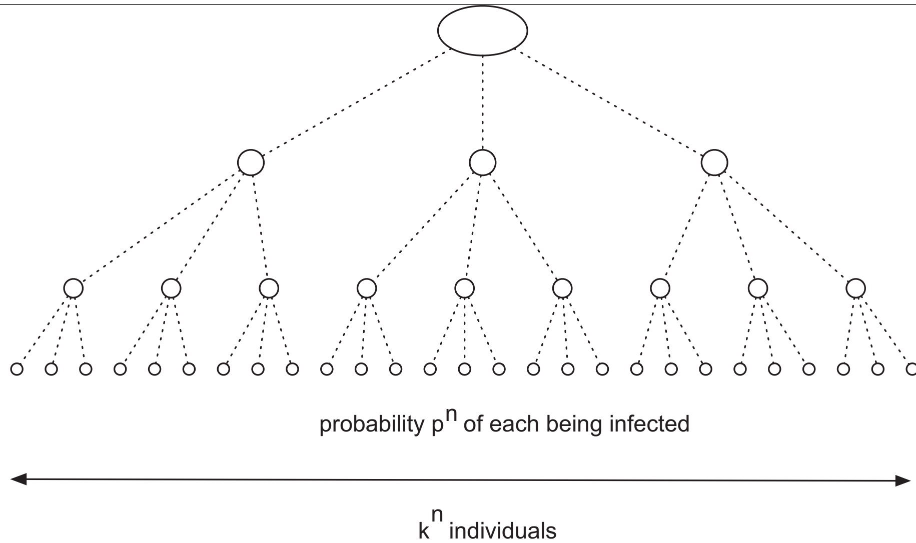

Figure 21.15. The expected number of individuals infected at level n is the product of the number of individuals at that level (k^n) and the probability that each is infected (p^n).

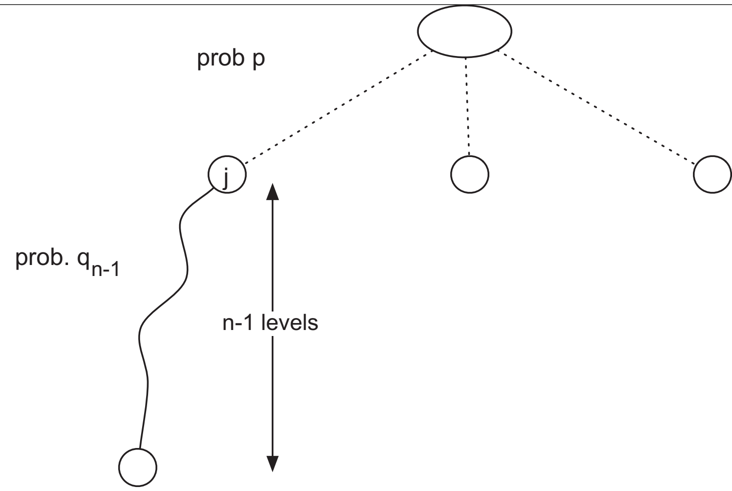

Figure 21.16. In order for there to be an infection at level n, the root must infect one of its immediate descendents, and then this descendent must, recursively, produce an infection at level $n-1$.

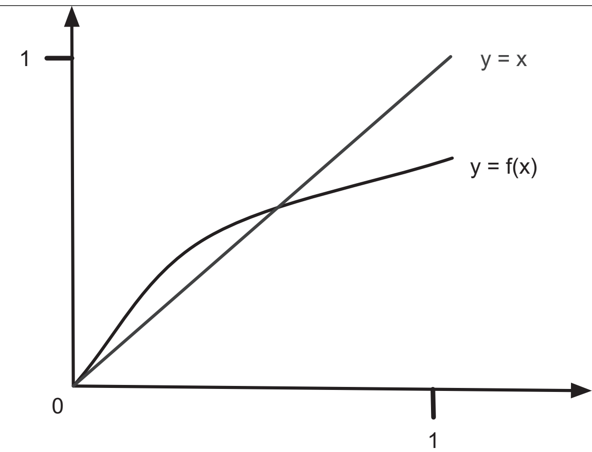

Figure 21.17. To determine the limiting probability of an infection at depth n, as n goes to infinity, we need to repeatedly apply the function $f(x) = 1 - (1 - px)^k$, which is the basis for the recurrence $q_n = f(q_{n-1})$.

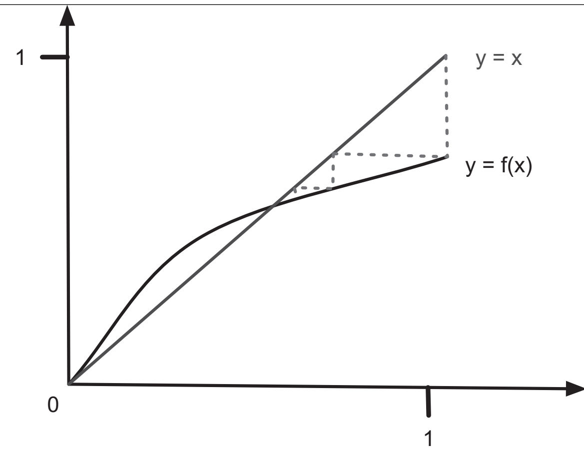

Figure 21.18. When we repeatedly apply the function $f(x)$, starting at $x = 1$, we can follow its trajectory by tracing out the sequence of steps between the curves $y = f(x)$ and $y = x$.

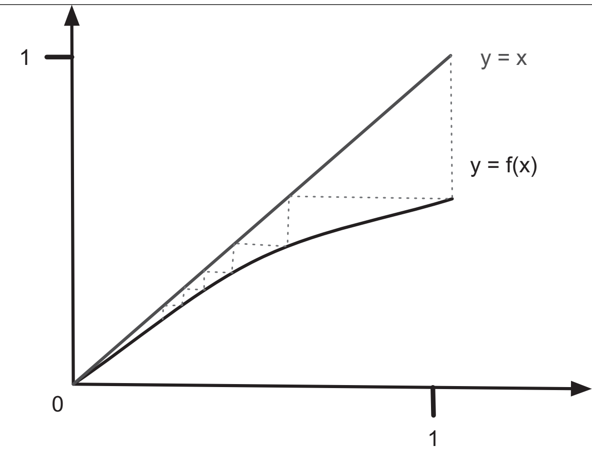

Figure 21.19. When $y = f(x)$ only intersects $y = x$ at zero, the repeated application of $f(x)$ starting at $x = 1$ converges to 0.

P1: SBT
cuus984-net CUUS984-Easley 0 521 19533 1 November 30, 2009 16:2

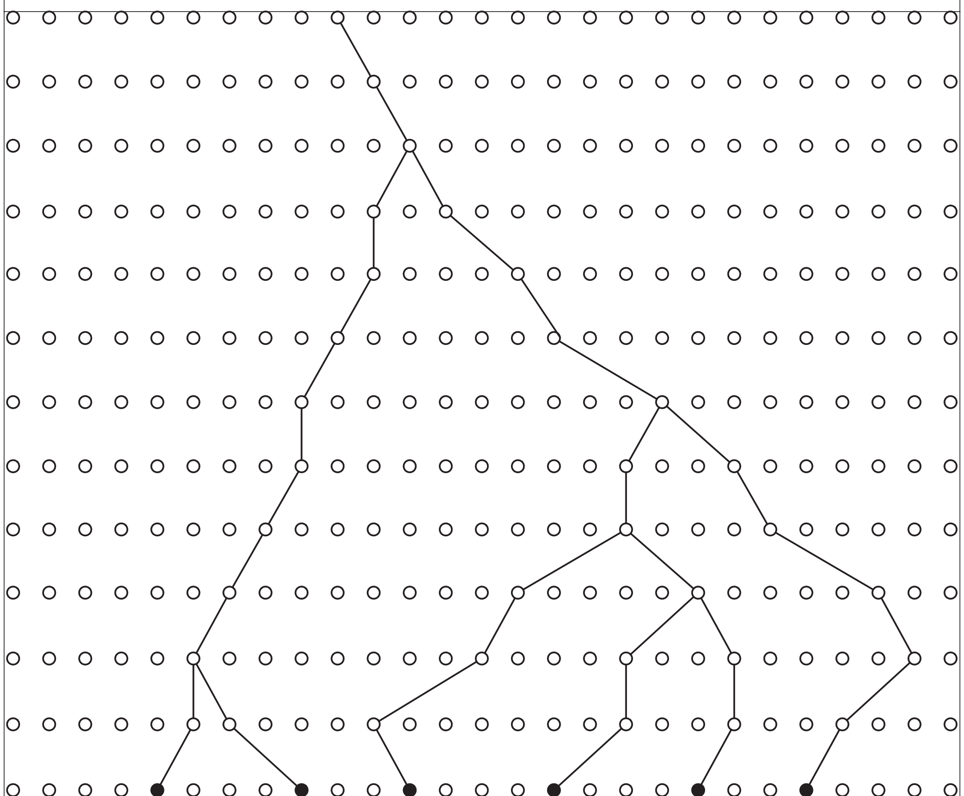

Figure 21.20. We can view the search for coalescence as a backward walk through a sequence of earlier generations, following lineages as they collide with each other.

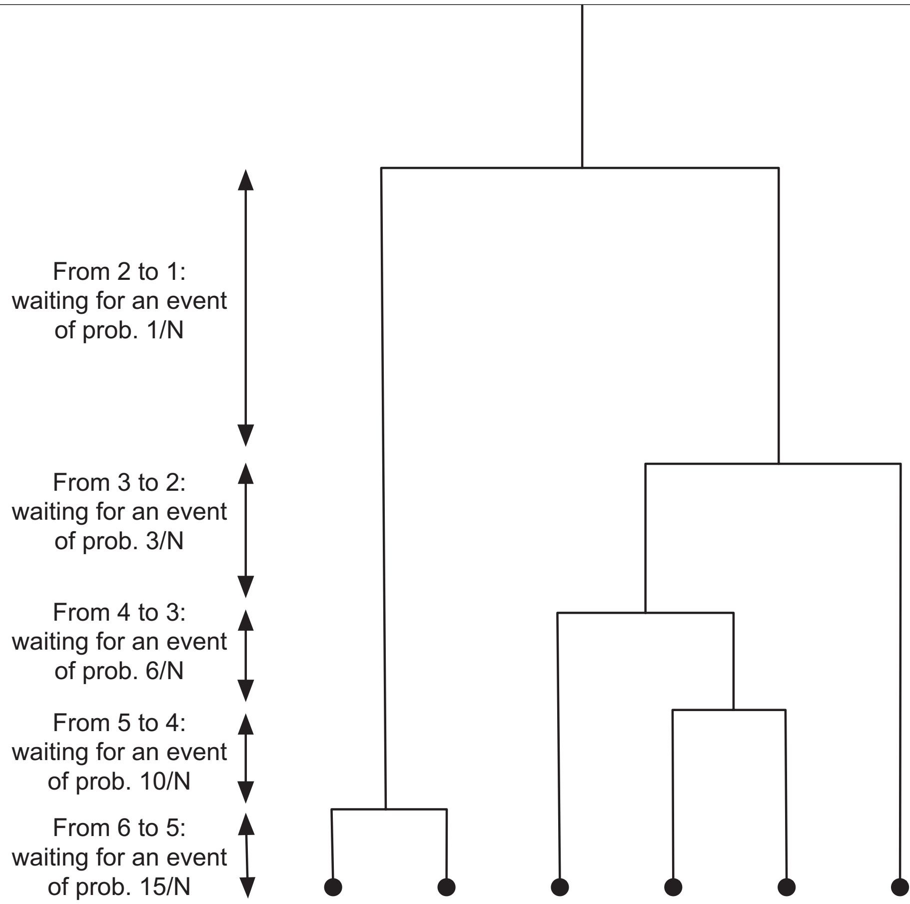

Figure 21.21. Assuming that no three lineages ever collide simultaneously, the time to coalescence can be computed as the time for a sequence of distinct collision events to occur.

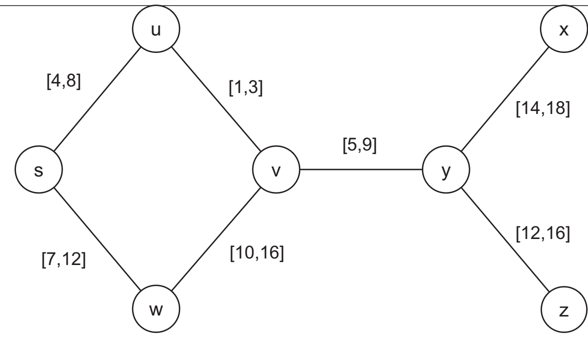

Figure 21.22. Contacts among a set of people, with time intervals showing when the contacts occurred.

P1: SBT
cuus984-net CUUS984-Easley 0 521 19533 1 November 30, 2009 16:2

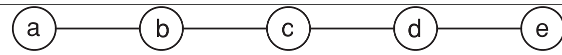

Figure 21.23. A contact graph on five people.

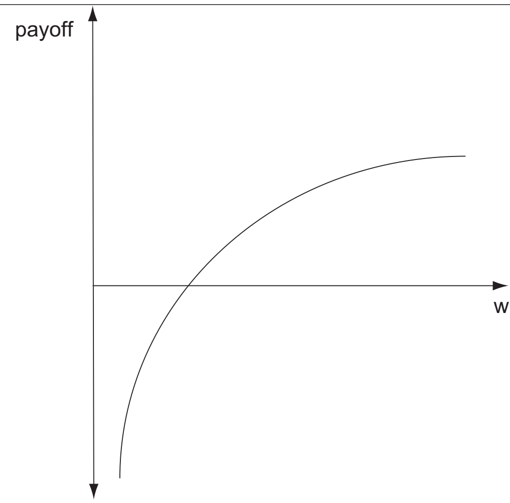

Figure 22.1. When we assume that an individual's utility is logarithmic in his wealth, this means that utility grows at a decreasing rate as wealth increases.

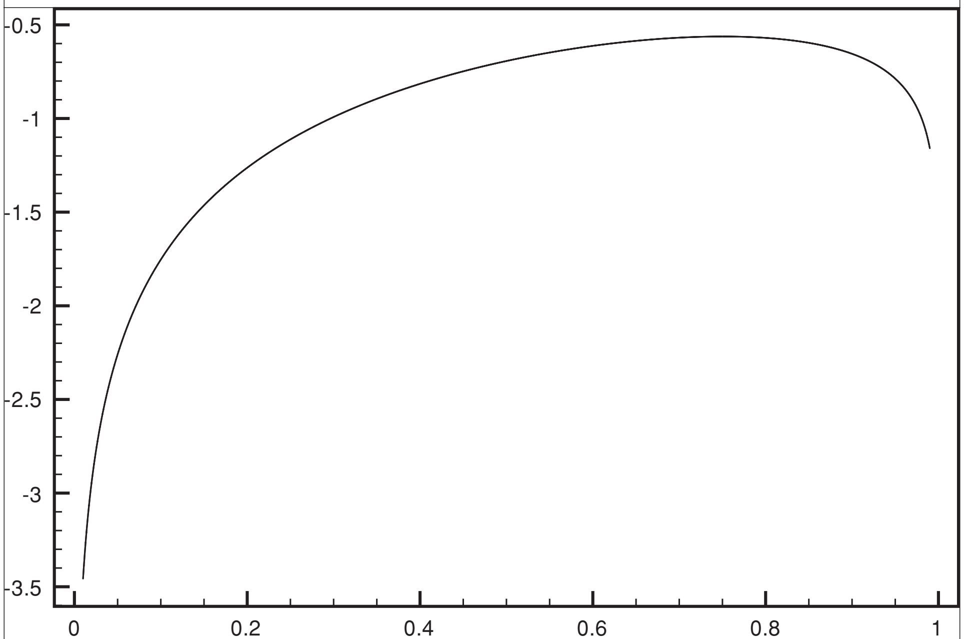

Figure 22.2. A plot of $a \ln(r) + b \ln(1 - r)$ as a function of r, when $a = 0.75$. The maximum is achieved when $r = a$.

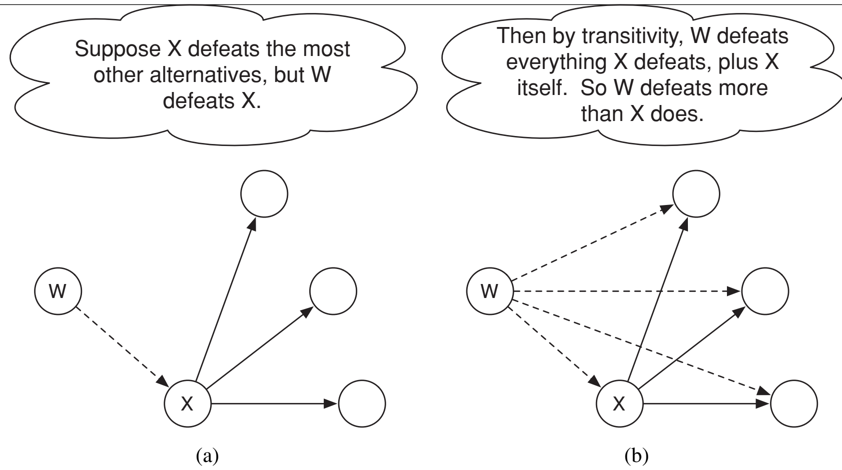

Figure 23.1. With complete and transitive preferences, the alternative X that defeats the most others in fact defeats all of them. If not, some other alternative W would defeat X (as in (a)), but then by transitivity W would alternatives than X does (as in (b)).

P1: SBT
cuus984-net CUUS984-Easley 0 521 19533 1 November 30, 2009 16:2

College	National Ranking	Average Class Size	Scholarship Money Offered
X	4	40	$3000
Y	8	18	$1000
Z	12	24	$8000

Figure 23.2. When a single individual is making decisions based on multiple criteria, the Condorcet Paradox can lead to non-transitive preferences. Here, if a college applicants wants a school with a high ranking, small average class size, and a large scholarship offer, it is possible for each option to be defeated by one of the others on a majority of the criteria.

P1: SBT
cuus984-net CUUS984-Easley 0 521 19533 1 November 30, 2009 16:2

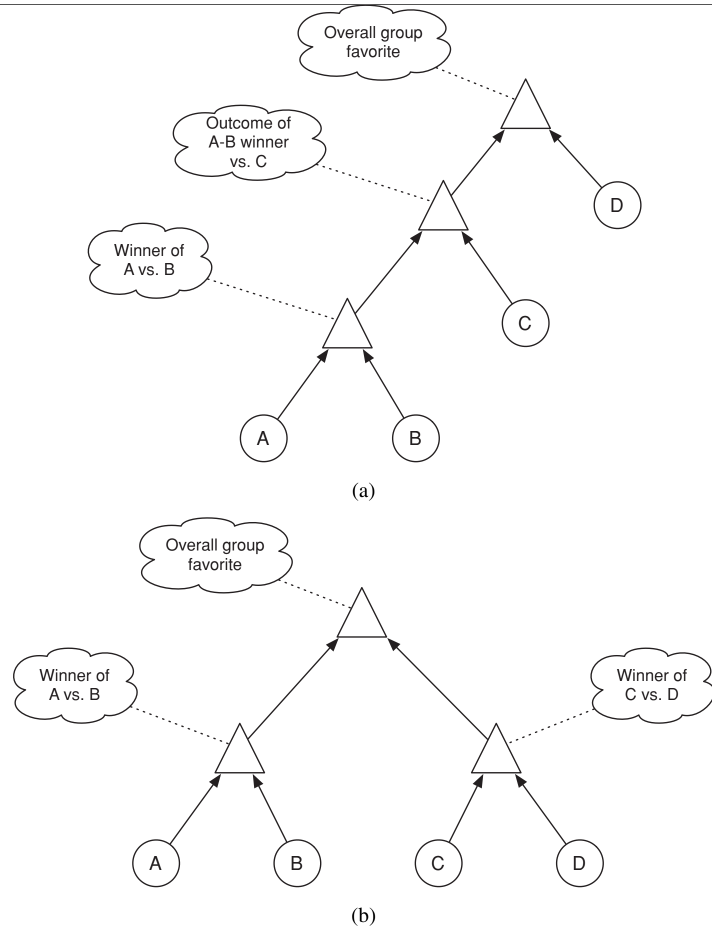

Figure 23.3. One can use majority rule for pairs to build voting systems on three of more alternatives. The alternatives are considered according to a particular "agenda" (in the form of an elimination tournament), and they are eliminated by pairwise majority vote according to this agenda. This produces an eventual winner that serves as the overall group favorite.

P1: SBT
cuus984-net CUUS984-Easley 0 521 19533 1 November 30, 2009 16:2

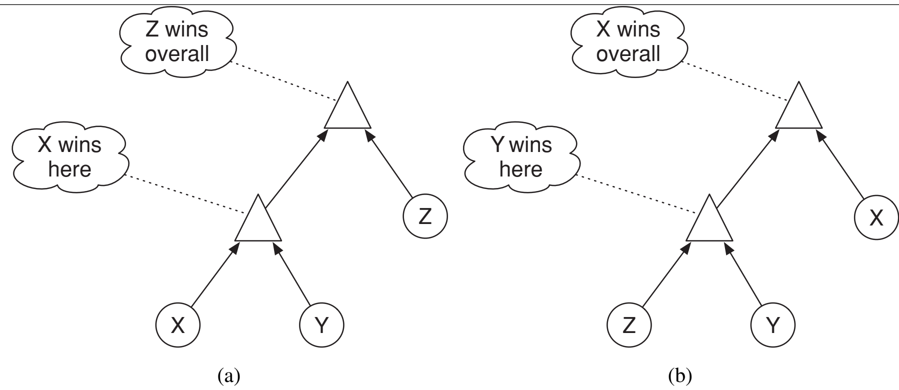

Figure 23.4. With individual rankings as in the Condorcet Paradox, the winner of the elimination tournament depends entirely on how the agenda is set.

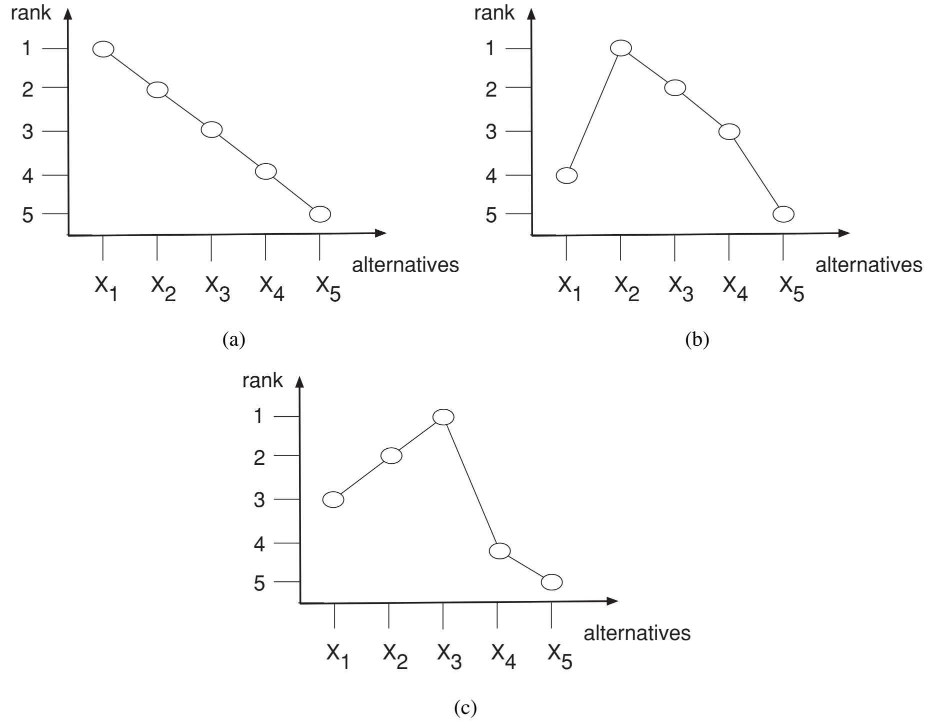

Figure 23.5. With single-peaked preferences, each voter's ranking of alternatives decreases on both sides of a "peak" corresponding to her favorite choice.

P1: SBT
cuus984-net CUUS984-Easley 0 521 19533 1 November 30, 2009 16:2

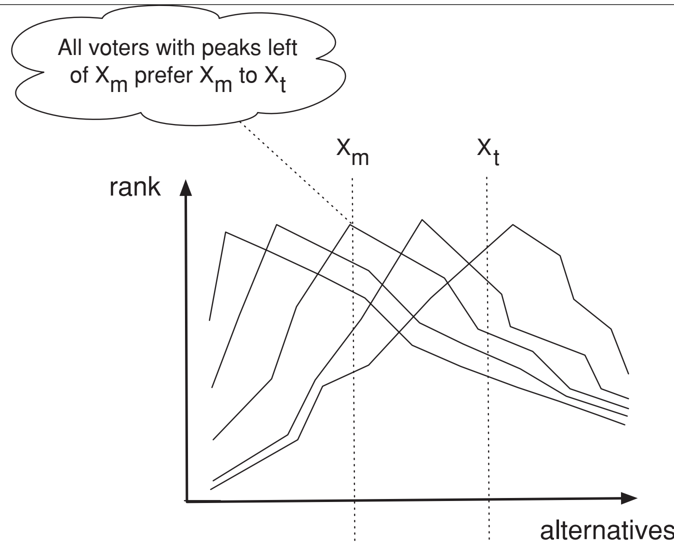

Figure 23.6. The proof that the median individual favorite X_m defeats every other alternative X_t in a pairwise majority vote: if X_t is to the right of X_m, then X_m is preferred by all voters whose peak is on X_m or to its left. (The symmetric argument applies when X_t is to the left of X_m.)

Profile 1:

Individual	Ranking	Ranking restricted to X and Y
1	$W \succ X \succ Y \succ Z$	$X \succ Y$
2	$W \succ Z \succ Y \succ X$	$Y \succ X$
3	$X \succ W \succ Z \succ Y$	$X \succ Y$

Profile 2:

Individual	Ranking	Ranking restricted to X and Y
1	$X \succ Y \succ W \succ Z$	$X \succ Y$
2	$Z \succ Y \succ X \succ W$	$Y \succ X$
3	$W \succ X \succ Y \succ Z$	$X \succ Y$

Figure 23.7. The two profiles above involve quite different rankings, but for each individual, her ranking restricted to X and Y in the first profile is the same as her ranking restricted to X and Y in the second profile. If the voting system satisfies IIA, then it must produce the same ordering of X and Y in the group ranking for both profiles.

P1: SBT
cuus984-net CUUS984-Easley 0 521 19533 1 November 30, 2009 16:2

Profile P:

Individual	Ranking
1	$X \succ \cdots \succ Y \succ \cdots \succ Z \succ \cdots$
2	$X \succ \cdots \succ Z \succ \cdots \succ Y \succ \cdots$
3	$\cdots \succ Y \succ \cdots \succ Z \succ \cdots \succ X$

Profile P':

Individual	Ranking
1	$X \succ \cdots \succ Z \succ Y \succ \cdots$
2	$X \succ \cdots \succ Z \succ \cdots \succ Y \succ \cdots$
3	$\cdots \succ Z \succ Y \succ \cdots \succ X$

Figure 23.8. A polarizing alternative is one that appears at the beginning or end of every individual ranking. A voting system that satisfies IIA must put such an alternative at the beginning or end of the group ranking as well. The figure shows the key step in the proof of this fact, based on rearranging individual rankings while keeping the polarizing alternative in its original position.

Profile P_0:

Individual	Ranking
1	$\cdots \succ Y \succ \cdots \succ Z \succ \cdots \succ X$
2	$\cdots \succ Z \succ \cdots \succ Y \succ \cdots \succ X$
3	$\cdots \succ Y \succ \cdots \succ Z \succ \cdots \succ X$

Profile P_1:

Individual	Ranking
1	$X \succ \cdots \succ Y \succ \cdots \succ Z \succ \cdots$
2	$\cdots \succ Z \succ \cdots \succ Y \succ \cdots \succ X$
3	$\cdots \succ Y \succ \cdots \succ Z \succ \cdots \succ X$

Profile P_2:

Individual	Ranking
1	$X \succ \cdots \succ Y \succ \cdots \succ Z \succ \cdots$
2	$X \succ \cdots \succ Z \succ \cdots \succ Y \succ \cdots$
3	$\cdots \succ Y \succ \cdots \succ Z \succ \cdots \succ X$

Profile P_3:

Individual	Ranking
1	$X \succ \cdots \succ Y \succ \cdots \succ Z \succ \cdots$
2	$X \succ \cdots \succ Z \succ \cdots \succ Y \succ \cdots$
3	$X \succ \cdots \succ Y \succ \cdots \succ Z \succ \cdots$

Figure 23.9. To find a potential dictator, one can study how a voting system behaves when we start with an alternative at the end of each individual ranking, and then gradually (one person at a time) move it to the front of people's rankings.

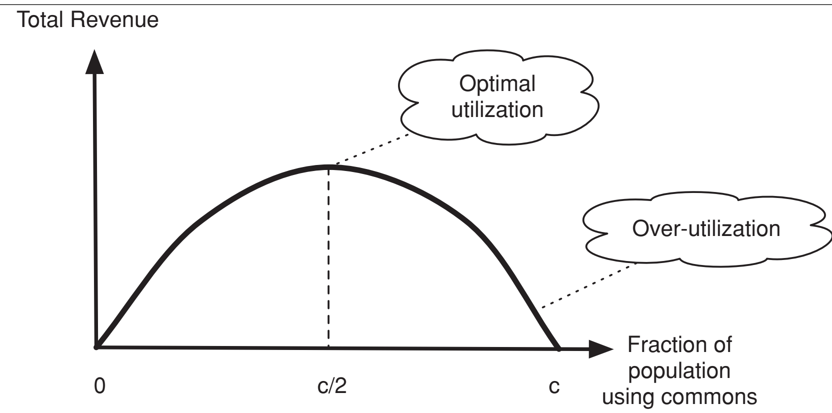

Figure 24.1. In the Tragedy of the Commons, a freely shared resource can easily be overused unless some form of property rights are established.